School of Molecular and Life Sciences

Pathogen Interactions in Co-infected Wheat Determine Disease Ontogeny and Severity

Araz Sedqi Abdullah

ORCID: 0000-0003-1880-9070

This thesis is presented for the Degree of

Doctor of Philosophy

of

Curtin University

October 2019

Declaration

To the best of my knowledge and belief, this thesis contains no material previously published by any other person except where due acknowledgement has been made. This thesis contains published work and work prepared for publication. The thesis contains no material that has been accepted for the award of any other degree or diploma in any university.

Signature: Araz Abdullah

Date: 10/07/202

Acknowledgements

I would like to express my appreciation to Dr Caroline Moffat and Dr Fran Lopez for their invaluable scientific input. Special thanks to Professor Mark Gibberd for his support and mentorship – your input has been great particularly in hardship events. My special thanks extend to Professor John Hamblin for serving as my mentor as well as an advisor on the thesis committee – thank you very much, John, for your guidance and support, without you, I would not have been able to reach this stage. Special thanks also to Dr Amir Abadi for his input in my PhD and life guidance.

Thanks to all CCDM members, staff and students, for their collaboration and help. I enjoyed working with you and thank you for your continuous support and encouragement. Special thanks to Leon Hodgson, Kasia Clark, Steven Chan, Julie Lawrence, Belinda Cox, Jordi Muria and Cynthia Ge. Thanks so much for your assistance in field sampling and guidance in molecular work. I would like to acknowledge and thank Evan John and Johannes Debler for their help in fungal transformation, and Connie Jackaman for technical assistance in fluorescent microscopy. I am grateful for the Australian government for the Research Training Program scholarship opportunity. I also like to express my gratitude for the financial assistance obtained from the Centre for Crop and Disease Management, Curtin University

During times when I had been exhausted, I have had friends that I could always count on for support. Special thanks for Leila Heidarvand, Hugh and Kate Beggs, Kristi Uusaed, Haylee D'Agui and Vicki Sharp for your continuous support and encouragement. I am grateful to have known you and thank you very much for being lifelong friends. Thank you also for your stimulating scientific discussions and conversation about life and future directions.

Thesis summary

Research into plant-pathogen interactions has historically taken a simplified approach involving a single host and a single disease. However, in natural and agroecosystems, plants frequently interact with several pathogen species or genotypes, exhibiting complexities not captured by the widely used single disease approach. The interaction between multiple pathogens and a host, known as co-infection, has long been recognised for its significance on disease development and severity but has rarely been studied empirically.

This thesis addresses the complex dynamics of plant co-infection by using a tripartite pathosystem consisting of wheat as the host and two major fungal pathogens: *Pyrenophora tritici-repentis* (Died.) Drechs. (Ptr) and *Parastagonospora nodorum* (Berk.) (Pan). These fungi commonly infect wheat leaves, causing yield loss by reducing leaf area available for photosynthesis. Symptoms caused by these fungi are very similar and often difficult to distinguish visually. Symptoms can also be misdiagnosed when unrelated wheat pathogens challenge conventional disease diagnosis. The development of disease symptoms in response to these fungi is mainly mediated by the secretion of necrotrophic effectors (host-selective toxins). These facilitate *in planta* growth by triggering cell death in wheat cultivars carrying matching sensitivity genes. Ptr possesses a toxin known as ToxA; the gene encoding ToxA is thought to have been acquired from Pan. Sharing a pathogenicity gene suggests that co-infection of wheat leaves by these two fungi is likely. However, direct evidence for the occurrence scale of this co-infection is lacking.

The first chapter of this thesis reviews the literature on pathosystems in which disease is caused by more than one pathogen species or genotype. The review covers insights into dynamics of co-infection and considers possible mechanisms through which pathogens co-exist, compete or cooperate. Examples of co-infection from a range of pathogen types are drawn upon, where these provide useful insight for future research. The second chapter addresses a technical challenge associated with studying co-infection and reports on the development of a duplex quantitative polymerase chain reaction (qPCR) assay. The assay uses a set of uniquely assigned and differentially tagged hydrolysis probes allowing quantification of Ptr and Pan simultaneously. This assay provides accurate detection of both pathogens, even at low levels of disease development allowing the determination of fungal abundance as a function of disease severity throughout the season.

In the third chapter, the qPCR assay was deployed to survey the prevalence of Ptr and Pan across three geographically spread sites in the main wheat-growing area of Western Australia. The survey examined Ptr and Pan prevalence on three cultivars varying in resistance. Results showed that co-infection by Ptr and Pan was frequent, occurring in 94% of the surveyed samples. Pan was only detected in association with Ptr in the co-infected leaves. Site and cultivar resistance drove most of the variability in the relative abundance of Ptr and Pan, but the frequency of co-infection was independent of the resistance of the host cultivar. These results highlight the importance of considering Ptr and Pan as a complex, and accounting for this complex will be central for successful disease management efforts.

The fourth chapter reports on a series of controlled-environment experiments conducted utilising molecular, histological, and cytological techniques. The main objective of these experiments was to investigate disease development and pathogen interactions in co-inoculated wheat plants. Results showed that Ptr and Pan can complement their infection processes of co-inoculated wheat leaves, causing accelerated and extensive disease damage. Molecular evidence showed that, while Ptr and Pan co-existed, Ptr often suppressed, but did not exclude Pan. The success of Ptr and Pan in causing significant disease was influenced by the timing of their access to host tissues. Prior inoculation, up to 48 h, by Pan can exacerbate Ptr aggressiveness leading to rapid disease development mostly associated with Ptr. This chapter presents cytological observations demonstrating an anatomical separation in leaf tissue occupied by Ptr and Pan that is likely to enable their co-infection. Such anatomical separation has not been reported previously for fungal pathogens, to the best of my knowledge.

Table of Contents

List of Figures

List of Tables

General Introduction

Until recently, plant-pathogen interactions have been studied in simplified experimental systems that generally involve a single host species and a single pathogen. In such systems, artificial inoculations of a single pathotype are undertaken or assumed to naturally occur. Although many plant diseases are considered as being caused by a dominant pathotype, evidence is increasing that plants in-field and natural conditions are co-infected by several pathogen species or pathotypes. Such co-infections may occur synchronously or asynchronously and may affect the severity of damage a plant experiences (Alizon et al., 2013; Susi et al. 2015; Tollenaere et al., 2016). Despite their common occurrence and significance, studies targeting co-infections in plants are rare.

This thesis investigates pathogen-pathogen interactions and their consequences for disease severity in co-infected plants. Throughout the research chapters, the host plant wheat (*Triticum aestivum*) is used. Wheat is a small-grain cereal broadly cultivated throughout the world. Several pathogenic organisms attack wheat; nematodes, viruses, bacteria and fungi can all cause disease. Much of the past wheat research focused on biotrophic fungal diseases such as rusts and mildews (Dean et al., 2012; Oliver et al., 2016). However, necrotrophic diseases of wheat can devastate a crop and are often difficult to control with existing disease management strategies (Oliver et al., 2016; Vleeshouwers and Oliver 2014). Among the necrotrophic diseases of wheat, the foliar fungi *Pyrenophora tritici-repentis* (Ptr) and *Parastagonospora nodorum* (Pan) are the most common (Bhathal et al., 2003; Blixt et al., 2010). Separately, Ptr and Pan cause tan (yellow) spot and septoria nodorum blotch of wheat, respectively. Jointly, Ptr and Pan have recently been associated with a leaf spot complex in wheat (Abdullah et al., 2018; Blixt et al., 2010). Both pathogens frequently infect plant leaves, reducing the photosynthetically active leaf area (Bhathal et al., 2003; Johnson 1987; Salam et al., 2013). Annual losses to these pathogens is estimated to cost Western Australian wheat growers about $220 million (Murray and Brennan 2009; Salam et al., 2013).

Symptoms caused by Ptr and Pan manifest as necrosis (browning), chlorosis (yellowing) or both. Symptoms can be similar and often difficult to distinguish visually (Abdullah et al., 2018). Symptoms can also be confounded when other diseases challenge conventional

diagnosis (Blixt et al., 2010). The development of symptoms in response to Ptr and Pan is mostly attributed to the secretion of necrotrophic effectors. These confer virulence on wheat cultivars carrying matching sensitivity genes (Rybak et al., 2017). Ptr possesses an effector known as ToxA. The gene encoding ToxA is thought to have been acquired from Pan before 1941 when Ptr was first reported as a serious disease of cultivated wheat (Friesen et al., 2006). Sharing an effector gene suggests that co-infection of wheat leaves by these two species is likely. Direct evidence examining the extent of this co-infection under agricultural conditions is lacking.

This thesis investigates Ptr-Pan interactions and their consequences for disease severity in co-infected wheat plants. The thesis is organised into five main chapters (Table 0.1). The first chapter provides an overview of the literature where the disease was caused by more than one pathogen species or genotype. The review covers insights into the dynamics of co-infection and describes a theoretical framework based on mechanisms through which pathogens co-exist, compete or cooperate (Abdullah et al., 2017). The second chapter reports on the development of a molecular method that simultaneously detects and quantifies the presence of Ptr and Pan in a sample. The method uses a duplex quantitative polymerase chain reaction (qPCR) approach taking advantage of pathogen-specific primers and probes (Abdullah et al., 2018). The third chapter reports on a field survey of three geographically spread sites in the main wheat-growing region of Western Australia (Abdullah et al., 2020). The survey investigated the prevalence of co-infection by Ptr and Pan in naturally infected wheat fields. The fourth chapter reports on a series of controlled-environment experiments designed to examine the interactions between Ptr and Pan. These experiments combine molecular, histological and cytological techniques to investigate pathogen interactions and disease development in co-inoculated wheat leaves. The fifth chapter summarises the aims of the thesis and presents its major findings. The chapter also discusses the implications of the findings for the scientific community and broader wheat industry.

Table 0.1. Overview of the chapters implemented in this thesis.

	Question	Prior knowledge	Knowledge gap/Finding	Conclusion
Ch. 1	What evidence exists in the literature for co-infection by plant pathogens?	Co-infection thought to occur widely.	Methods for quantifying co-infecting pathogens are limited.	Better analytical tools and understanding of pathogen interactions may unlock new possibilities for disease management.
	What impacts do co-infection have on disease outcomes?	Theoretical advances of co-infection outpace empirical data.	Pathogen-pathogen interactions are poorly understood.	Detailed empirical work of co-infection is required.
Ch. 2	Can qPCR be used to detect and quantify Ptr and Pan in co-infected wheat leaves?	Independent qPCR assays exist for Ptr and Pan.	Simultaneous Ptr-Pan detection was developed and demonstrated for large-scale field studies.	New qPCR is suitable for field investigations by enabling high sensitivity, simultaneous assessment of Ptr-Pan co-infection.
Ch. 3	How prevalent is Ptr-Pan co-infection under agricultural conditions?	Ptr and Pan cause similar disease symptoms and most past studies have poorly differentiated their effects on wheat.	Ptr and Pan co-occur frequently. The method developed in Ch. 2 is tested and demonstrated for field-derived samples.	Ptr and Pan occur as a complex with overlapping symptoms in most circumstances.
	To what extent do host resistance and location influence Ptr-Pan co-infection?	Ptr and Pan might have exchanged genetic materials and hence are likely to co-occur.	The abundance of Ptr and Pan is dynamic during the season. Host genotype plays a role but this is secondary to time within the season and location.	Ptr and Pan should be studied and managed as a complex.
Ch. 4	How do Ptr and Pan infections progress in co-inoculated leaves?	Ptr and Pan co-infection is common and dynamic but poorly understood.	Ptr and Pan can complement their infection, speeding up disease development. Pan can modulate Ptr virulence towards the host.	Ptr and Pan can overlap and co-occur. Disease dynamics are potentially altered by their interactions.
	What are the outcomes of Ptr-Pan co-inoculation?	Ptr and Pan co-infection in the field may occur asynchronously.	Ptr overgrows Pan in co-inoculated leaves.	Their co-infection triggers Ptr aggressiveness towards wheat.
	What mechanisms may enable Ptr-Pan co-infection?	Symptoms of Ptr and Pan may overlap.	Ptr and Pan may occupy adjacent but different tissues of the same leaf.	Ptr and Pan are likely to have overlapping ecology and distribution.
Ch. 5	Discusses the implications of the findings for the scientific and agricultural community.			

References

Abdullah, A. S., Moffat, C. S., Lopez-Ruiz, F. J., Gibberd, M. R., Hamblin, J., and Zerihun, A. 2017. Host-multi-pathogen warfare: pathogen interactions in co-infected plants. *Frontiers in Plant Science* **8**,1806.

Abdullah, A. S., Turo, C., Moffat, C. S., Lopez Ruiz, F. J., Gibberd, M. R., Hamblin, J., and Zerihun, A. 2018. Real-time PCR enables diagnosis of co-infection by two globally distributed fungi of wheat. *Frontiers in Plant Science* **9**,1086.

Abdullah, A. S., Gibberd, M. R., Hamblin, J. 2020. Prevalence of co-infection of wheat by *Pyrenophora tritici-repentis* and *Parastagonospora nodorum* in the wheatbelt of Western Australia. *Crop and Pasture Science* **71**, 119-127.

Alizon, S., de Roode, J. C., and Michalakis, Y. 2013. Multiple infections and the evolution of virulence. *Ecology Letters* **16**, 556-567.

Bhathal, J., Loughman, R., and Speijers, J. 2003. Yield reduction in wheat in relation to leaf disease from yellow (tan) spot and septoria nodorum blotch. *European Journal of Plant Pathology* **109**, 435-443.

Blixt, E., Olson, A., Lindahl, B., Djurle, A., and Yuen, J. 2010. Spatiotemporal variation in the fungal community associated with wheat leaves showing symptoms similar to stagonospora nodorum blotch. *European Journal of Plant Pathology* **126**, 373-386.

Dean, R., Van Kan, J. A., Pretorius, Z. A., Hammond-Kosack, K. E., Di Pietro, A., Spanu, P. D., Rudd, J. J., Dickman, M., Kahmann, R., and Ellis, J. 2012. The top 10 fungal pathogens in molecular plant pathology. *Molecular Plant Pathology* **13**, 414-430.

Friesen, T. L., Stukenbrock, E. H., Liu, Z., Meinhardt, S., Ling, H., Faris, J. D., Rasmussen, J. B., Solomon, P. S., McDonald, B. A., and Oliver, R. P. 2006. Emergence of a new disease as a result of interspecific virulence gene transfer. *Nature Genetics* **38**, 953-959.

Johnson, K. 1987. Defoliation, disease, and growth: a reply. *Phytopathology* **77**, 393-398.

Murray, G. M., and Brennan, J. P. 2009. Estimating disease losses to the Australian wheat industry. *Australasian Plant Pathology* **38**, 558-570.

Oliver, R., Tan, K.-C., and Moffat, C. 2016. Necrotrophic pathogens of wheat. In: Wrigkey, C.W., Corke, H., Seetharaman, K. and Faubion, J., (eds) *Encyclopedia of Food Grains*, 2nd Edition, pp. 273-278. Oxford: Academic Press.

Rybak, K., See, P. T., Phan, H. T., Syme, R. A., Moffat, C. S., Oliver, R. P., and Tan, K. C. 2017. A functionally conserved Zn2Cys6 binuclear cluster transcription factor class regulates necrotrophic effector gene expression and host-specific virulence of two major Pleosporales fungal pathogens of wheat. *Molecular Plant Pathology* **18**, 420-434.

Salam, K. P., Thomas, G. J., Beard, C., Loughman, R., MacLeod, W. J., and Salam, M. U. 2013. Application of meta-analysis in plant pathology: a case study examining the impact of fungicides on wheat yield loss from the yellow spot—septoria nodorum blotch disease complex in Western Australia. *Food Security* **5**, 319-325.

Susi, H., Barres, B., Vale, P. F., and Laine, A.-L. 2015. Co-infection alters population dynamics of infectious disease. *Nature Communications* **6**, 5975.

Tollenaere, C., Susi, H., and Laine, A.-L. 2016. Evolutionary and epidemiological implications of multiple infection in plants. *Trends in Plant Science* **21**, 80-90.

Vleeshouwers, V. G., and Oliver, R. P. 2014. Effectors as tools in disease resistance breeding against biotrophic, hemibiotrophic, and necrotrophic plant pathogens. *Molecular Plant-microbe Interactions* **27**, 196-206.

1 Literature Review[I]

Abstract

This chapter reviews insights into co-infections focusing on the dynamics of host-multi-pathogen interactions and their consequences for plant disease. In co-infection systems, pathogen interactions include: (i) Competition, in which competing pathogens develop physical barriers or utilise toxins to exclude competitors from resource-dense niches; (ii) Cooperation, whereby pathogens beneficially interact, by providing mutual biochemical signals essential for pathogenesis, or through functional complementation via exchange of resources necessary for survival; (iii) Coexistence, whereby pathogens can stably coexist through niche specialisation. Furthermore, hosts are also able to, actively or passively, modulate niche interactions through defence responses targeting at least one pathogen. Typically, however, virulent pathogens subvert host defences to facilitate infection, and responses elicited by one pathogen may be modified in the presence of another pathogen. Evidence exists, albeit rare, of pathogens incorporating foreign genes that broaden niche adaptation and improve virulence. Throughout this review, examples of co-infection from a range of pathogen types are drawn upon, where these provide useful insight for future research.

[I]This chapter was published in October 2017: Abdullah, A. S., Moffat, C. S., Lopez-Ruiz, F. J., Gibberd, M. R., Hamblin, J. and Zerihun, A. Host-multi-pathogen warfare: pathogen interactions in co-infected plants. Frontiers in Plant Science., | doi.org/10.3389/fpls.2017.01806.

Authors' contribution: Araz Abdullah conceived the idea, revised the literature and drafted the manuscript. Caroline Moffat, Fran Lopez, Ayalsew Zerihun, Mark Gibberd, and John Hamblin supervised the work and provided critical suggestions on the article. All authors read and approved the final version of the article.

1.1 Introduction

Plant pathology has focused predominantly on single host and single disease interactions. Whilst this simplification has proved useful, plants in nature interact with multiple pathogen species/pathotypes (Kozanitas et al., 2017; Tollenaere et al., 2017). This interaction, known as co-infection, is of particular interest since it tends to alter the course of the disease and the severity of expression (i.e., overall virulence). How heterogeneity of diseases influence overall virulence has been the subject of a recent review in plant epidemiology (Tollenaere et al., 2016).

Three key interactions can cause damage in co-infected plants: host-pathogen, pathogen-pathogen, and host-multiple-pathogen complexes. Host-pathogen interactions are well studied and are generally detrimental to the plant resulting in reduced fitness (Brown, 2015). In contrast, pathogen-pathogen and host-multiple-pathogen interactions are less studied. These interactions can lead to various results: antagonism, synergism, coexistence, mutualism or cooperation (Table 1.1). The level of disease damage the plant experiences varies depending on the outcome of the interactions and the corresponding host responses. For example, several strains of *Pseudomonas* bacteria secrete antimicrobial compounds that are antagonistic to sensitive pathogens within the host (Walsh et al., 2001). Many such compounds are also phytotoxic and may exacerbate the level of disease damage (Maurhofer et al., 1992). Furthermore, some pathogens, such as the biotroph *Blumeria graminis* f. sp. *tritici* and the necrotroph *Zymoseptoria tritici* of wheat, do not interact directly to cause damage to the host as one pathogen can inhibit the development of the other (Orton and Brown, 2016). Such inhibition can be so profound that the plant plays an active role in promoting the growth of disease suppressive pathogens (Smith et al., 1999). Therefore, moving beyond how heterogeneity of infection influences overall virulence requires a holistic understanding of how a host responds to co-infection and how pathogens interact and coexist.

Table 1.1. Examples of pathogen-pathogen interactions in various pathosystems.

Pathogen species	Host	Co-infection	Interaction	Reference
Pseudomonas syringae/ Alternaria brassicicola	Arabidopsis	Synchronous	Synergistic	Spoel et al., 2007
Fusarium oxysporum/ Pseudomonas fluorescens	Wheat	Synchronous	Synergistic	Notz et al., 2002
Fusarium oxysporum(Fo47)/ Fusarium oxysporum(Fol8)	Tomato	Asynchronous	Antagonistic	Aime et al., 2013
Pseudomonas putida/ Botrytis cinerea	Field bean	Synchronous	Antagonistic	Ongena et al., 2005
Leptosphaeria maculans/ Leptosphaeria biglobosa	Oilseed rape	Asynchronous	Coexistence	Toscano-Underwood et al., 2003
Zymoseptoria tritici/ Blumeria graminis tritici	Wheat	Synchronous/ Asynchronous	Antagonistic	Orton and Brown, 2016
Fusarium verticillioides/ Ustilago maydis	Maize	Synchronous	Antagonistic	Jonkers et al., 2012
Fusarium graminearum/ Phoma sp	Finger millet	Synchronous	Antagonistic	Mousa et al., 2015
Fusarium oxysporum/ Pseudomonas fluorescens	Tomato	Synchronous	Synergistic	Kamilova et al., 2008
Rhizopus microspores/ Burkholderia sp	Rice	Synchronous	Symbiosis	Partida-Martinez and Hertweck, 2005
Rice yellow mottle virus/ *Xanthomonas oryzae*	Rice	Synchronous/ Asynchronous	Synergistic	Tollenaere et al., 2017

Recent advances in genomics and molecular techniques have led to new insights into host-multi-pathogen interactions. For example, metagenomics and microbial tag sequencing have created novel opportunities for studying the wide range of pathogens associated with a single host (Petrosino et al., 2009; Tollenaere et al., 2012). These tools have provided insights into the prevalence of multiple infections in the field, and current knowledge indicates that the extent of co-infection can be significant in some pathosystems (Susi et al., 2015; Tollenaere et al., 2017). Furthermore, co-infections can lead to several outcomes: (i) competitive exclusion, where over time one pathogen excludes the other (Al-Naimi et al., 2005); (ii) mutualistic coexistence, in which all co-infecting pathogens receive benefits from the interaction (Mordecai et al., 2016); and (iii) emergence of new recombinant genomes where one pathogen incorporates a complementary gene set from another pathogen, leading to large-scale epidemics (Friesen et al., 2006). Indeed, populations of one pathogen may modify host environments to the advantage/disadvantage of other pathogens, affecting their frequencies and persistence within a pathogenic population (Perefarres et al.,

2014). Hence, understanding within-host pathogen interactions is crucial for the prediction of long-term dynamics of multiple disease outcomes.

This review discusses recent insights into within-host disease diversity and dynamics of pathogen interactions. The review focuses on current understanding of pathogen competition and cooperation, and the mechanisms that allow long-term coexistence to occur. Examples from a range of necrotrophic and biotrophic pathogens are drawn upon, where these provide useful insights for understanding of pathogen interactions and coexistence.

1.2 Plant defence responses to co-infection

The overwhelming majority of studies on plant defence responses to pathogenic infections have been conducted on single-pathotype systems. However, under conducive conditions, plants frequently encounter multiple pathogens, often with differing levels and mechanisms of virulence. Hence, a successful plant defence system will incorporate several resistance (*R*) genes that coordinate a response to multiple attacks. The genomes of plants encode a coordinated array of *R*-genes that permit recognition of the pathogen and rapid defence responses (Dangl and Jones, 2001). Prioritisation of defence may occur, leading to larger investments in defence metabolites against certain pathogens depending on virulence (Castrillo et al., 2017; Hacquard et al., 2016). This raises the question: does infection by one pathogen influence a host defence to subsequent infection by other pathogens?

1.2.1 Pathogen-triggered host susceptibility

Some pathogenic infections can be detrimental to the defence systems predisposing the plant to subsequent secondary infections. For example, infection of Arabidopsis by the foliar bacterium *Pseudomonas syringae* renders plants vulnerable to invasion by the necrotrophic ascomycete *Alternaria brassicicola* (Spoel et al., 2007). Infection by the biotrophic oomycete *Albugo candida* suppresses Arabidopsis defences, permitting subsequent infections by several otherwise avirulent pathogens (Cooper et al., 2008). Similarly, infection of maize by the phytopathogenic fungi *Fusarium verticillioides* facilitates infection by several related fungi, through the suppression of production of major secondary defence metabolites in the plant host (Saunders and Kohn, 2008). The mechanisms that lead to the suppression of defence have been defined in some cases. For

example, the natriuretic peptide receptor NPA expressed by *P. syringae* permits subsequent infection by virulent *A. brassicicola* in Arabidopsis through downregulating a large range of defence-related genes (Cooper et al., 2008; Spoel et al., 2003). Similarly, fusaric acid secreted by *F. oxysporum* suppresses expression of genes that regulate the antimicrobial activity of 2,4-diacetylphloroglucinol and predisposes wheat to *P. fluorescens* infection (Notz et al., 2002).

1.2.2 Pathogen-triggered host immunity

Some pathogenic infections can enhance the defensive capacity of their hosts and activate responses against subsequent attacks. For example, infection by the foliar bacterium *P. fluorescens* suppresses flagellin-triggered defence in *Arabidopsis thaliana* via apoplastic secretion of low-molecular-weight defence metabolites (Millet et al., 2010). Upon exposure to the bacterium, the defence system of the plant is locally suppressed; although a defence-signalling cascade develops systematically and spreads across infected plant parts conferring resistance to subsequent attacks (Van der Ent et al., 2009). Some root infections can confer resistance by forming rhizosphere networks that connect infected plants and signal-induced resistance to neighbouring plants (Song et al., 2010). Similarly, induced resistance has been reported for co-infections by pathotypes of the same species, where non-pathogenic *F. oxysporum* primed tomato plants against pathogenic *F. oxysporum* in a vaccine-like fashion (Aime et al., 2013). The molecular mechanisms involved in this priming have not been fully elucidated, although direct antagonism, detoxification of pathogen effectors and elevated expressions of plant defense-related genes have been recorded (Aime et al., 2013; Conrath et al., 2015; Ravensdale et al., 2014).

1.2.3 Crosstalk among jasmonate, ethylene, and salicylate

Recently, there has been growing interest in plant defence responses to co-infection at the hormonal level. This involves a comparative pathway analysis following infections by several pathogenic organisms. Expression levels of genes responsive to jasmonic acid (JA), ethylene (Et) and salicylic acid (SA) are commonly measured in such analyses. Generally, JA and Et are considered to be mutual pathways and linked to defence against necrotrophic pathogens such as *Botrytis cinerea* (Grant and Jones, 2009). SA, on the other hand, is often linked to defence against biotrophic pathogens such as *P. syringae* (Glazebrook, 2005). Antagonistic crosstalk between JA/ET and SA is well-documented (Pieterse et al., 2009;

Robert-Seilaniantz et al., 2011), permitting the plant to mount the appropriate defence responses to the attacking pathogen. In Arabidopsis, elevated expression of JA/Et-responsive genes resulted in antagonistic effects on SA-responsive genes and increased plant resistance to *B. cinerea* (Moffat et al., 2012). Similarly, exogenously applied SA revealed antagonist effects on expressions of JA-responsive genes but simultaneously increased Arabidopsis resistance to *P. syringae* (Gazzarrini and Mccourt, 2003). Pathogens have evolved sophisticated mechanisms to exploit this antagonism and counter host defence responses. For example, the polyketide phytotoxin coronatine secreted by *P. syringae* is structurally analogous to jasmonoyl-isoleucine and can bind to JA receptors, hijacking the JA mediated defence and causing disease susceptibility to *P. syringae* (Katsir et al., 2008). Similarly, the avirulent effector AvrPtoB produced by *P. syringae* disrupts hormonal signalling components in Arabidopsis creating a potential for vulnerability to subsequent infections (de Torres-Zabala et al., 2007).

Although SA and JA signalling can be activated separately, recent studies have shown varying degrees of involvement of both pathways depending on plant-pathogen combinations. An elegant comparative transcriptomic study revealed significant overlap in Arabidopsis responses to a set of biotrophic and necrotrophic attackers (De Vos et al., 2005). Global gene expression analyses revealed that all Arabidopsis-attackers stimulated JA biosynthesis (De Vos et al., 2005). Similarly, infection by the non-necrotrophic *P. syringae* induced a JA-mediated defence in Arabidopsis localised to infected regions (Cui et al., 2005). These results suggest the model of SA-mediated defence against biotrophs, and JA/Et-mediated defence against necrotrophs is too simplistic. The defence responses are likely to be fine-tuned to particular plant-pathogen combinations. There is much yet to be learned about mechanisms that allow for these differences, and this is an active area of research.

1.3 Multi-pathogen competition

Recent advances in metagenomics have highlighted the vast diversity of the community in which plant pathogens reside (Schenk et al., 2012). Due to the complex nature of these communities and the limited host resources, pathogens often enter into fierce competition. Fundamentally, competition between coexisting pathogens occurs for growth- and fitness-

limiting resources. Resource competition involves utilisation of limited host nutrients by one pathogen that then restricts supply to other pathogens sharing the same host. Monod (1949) was the first to point out the relationship between nutrients and pathogen growth: within a defined space in which all nutrients are provided, pathogens may stably coexist. Suboptimal nutrition leads to competition whereby some species may dominate. The severity and type of competition is determined by the consumption of nutrients over time, and this principle has been applied to plant and animal populations as an explanation of the dynamics of competing individuals (Adee et al., 1990; Chesson, 2000).

In nutritionally defined niches, such as plant leaves, pathogens with similar nutritional requirements compete for finite resources (West et al., 2006). Competition in such conditions may lead to selection for the more virulent species, or conversely, all associated pathogens may suffer (Rankin et al., 2007). For example, when maize was co-inoculated by *Ustilago maydis* and *F. verticillioides*, initially both fungal species had increased growth followed by decreased growth over time due to the depletion of nutrient resources (Jonkers et al., 2012). Pathogen traits such as cell-wall adhesion can support greater nutrient acquisition and provide competitive advantage (Hibbing et al., 2010). Adherent cell walls can enable greater resource capture efficiency even when growth substrates are present at low concentrations (Figure 1.1A). Similarly, pathogens that can halt certain metabolic processes, such as toxin production, when the necessary nutrients are exhausted, may show a greater competitive advantage (Glenn et al., 2008). Improved nutrient acquisition can also be achieved by the release of cell-wall degrading enzymes or toxins to sequester host nutrients (Greenberg and Yao, 2004; Rohmer et al., 2011). However, these compounds may also provide a competitive advantage to other opportunistic pathogens that do not have to bear the energetic costs for their production (Cornelis and Dingemans, 2013; Ghoul et al., 2014; Hentzer et al., 2003).

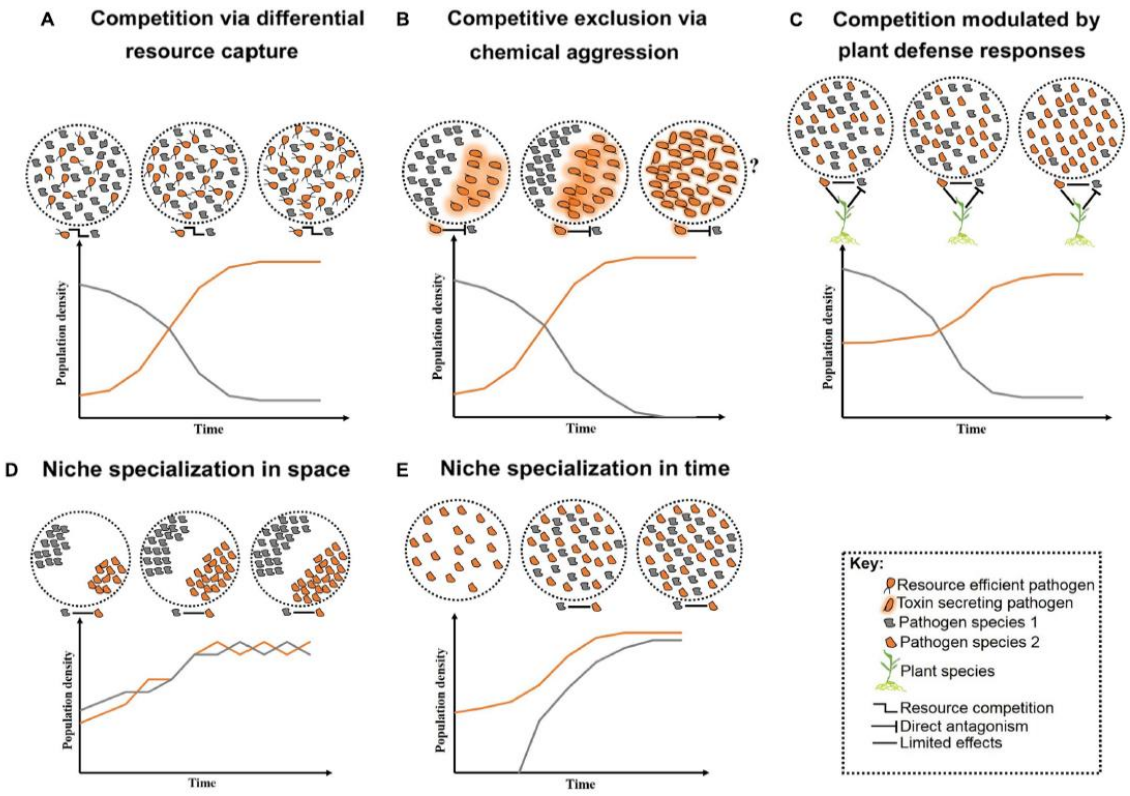

Figure 1.1. Schematic representation of long-term pathogen-pathogen interactions. Competition over growth-limiting resources and/or host niches can initially create high diversity, but low stability. Overtime, competition restricts diversity and allows competitive species to outgrow less competitive ones (A-C). Alternatively, neutral interactions occur when pathogens co-reside distinct niches within their host (D) or arrive at various time intervals (E). Question mark represents less studied cases where toxin production may lead to reduced fitness in the absence of competitors.

More aggressive forms of competition between pathogens include direct chemical exclusion (Figure 1.1B). A classic example of chemical aggression includes tenuazonic acid secreted by the finger millet colonising endophyte *Phoma* sp. which prevents growth of several pathogens including the toxigenic fungus *F. graminearum* (Mousa et al., 2015; Mousa et al., 2016a). Mechanical aggression also occurs through the disruption of cell membranes and the formation of multilayer physical barriers limiting growth and infection success of competitors. For example, the root-inhabiting bacteria *Enterobacter* sp. forms specialised root-pathogen structures to prevent infection by *F. graminearum* in finger millet (Mousa et al., 2016b). A molecular mechanism involved in pathogen competition has been identified. The N–alkylated benzylamine secreted by the nonpathogenic bacterium *P.*

putida acts as a lytic enzyme that inhibits fungal growth of *B. cinerea* in field bean (Ongena et al., 2005). Competition can also occur indirectly, mediated by the host through targeted defence responses against at least one pathogen (Figure 1.1C). However, the targeted defence can also provide a competitive advantage to pathogens that can counteract the recognition process of the host or that are capable of evading the plant defence system (Ren and Gijzen, 2016).

An expected outcome of competition is a localised reduction in diversity and concurrent specialisation of pathogens to various tissues and/or host species –i.e., niche specialisation. An individual plant may contain several niches in which pathogens can exist (Figure 1.1D), and heterogeneity in the biology and epidemiology of pathogens may permit niche specialisation (Figure 1.1E). For example, differences in disease onset resulted in temporal separation and stable coexistence between two related fungal pathogens of canola, *Leptosphaeria maculans* and *L. biglobosa* (Toscano-Underwood et al., 2003). Niche specialisation reduces the severity of competition, permitting coexistence (Fitt et al., 2006), although pathogens occupying various niches within a plant may interact indirectly by stimulating a common host defence response (Aghnoum and Niks, 2012). Nevertheless, on an evolutionary timescale, competition may result in exclusion, enabling species to coexist when arriving at various times (Fitt et al., 2006; Perefarres et al., 2014; Pfennig and Pfennig, 2009). However, when competition leads to the exclusion of the less competitive pathogen, the newly evolved highly competitive species may compete with other pathogens for their optimal niches (Perefarres et al., 2014). This situation may arise if a species integrates foreign genes allowing the invasion of novel niches (Friesen et al., 2006). Individuals of other species would then have fewer unoccupied niches in which to gain footholds, resulting in potentially large scale epidemics (Perefarres et al., 2014). Although the role of the integration of foreign genes in niche specialisation and expansion is less clear, interspecies acquisition of the *ToxA* gene has allowed *Pyrenophora tritici-repentis* to infect ToxA-sensitive wheat varieties (Friesen et al., 2006).

1.4 Opportunistic resource exploitation

Virulence of many plant pathogens depends on the secretion of growth-promoting factors that subvert host defences and improve their own nutrient uptake. These growth-promoting factors are often deployed into the extracellular matrix of the host and may hence be indirectly accessible by other pathogens in a local community (Harrison et al., 2006). In such cases, producing species can be vulnerable to exploitation by opportunists that can utilise virulence factors of their neighbours without contributing to the production of these factors. *P. syringae* provides a good example where common virulence factors give rise to opportunistic exploitation. Virulence in this pathogen is facilitated by the type III secretion system (T3SS), a needle-like apparatus that enables injection of toxins into host leaf mesophyll (Hauck et al., 2003). Virulence factors required for host manipulation by this pathogen are expressed in a bistable fashion, leading to a slow-growing toxin-secreting (T3SS+) strain and a fast-growing toxin-lacking (T3SS–) strain (Barrett et al., 2011). Co-infection experiments initiated with wild-type Arabidopsis revealed a growth advantage to the less virulent T3SS– strain resulting from the opportunistic exploitation of the toxins secreted by T3SS+ (Barrett et al., 2011). Iron-scavenging siderophores provide an additional example whereby co-infection gives rise to opportunistic exploitation. Many opportunistic bacteria can take up heterologous siderophores, diverting iron away from siderophore producing strains and simultaneously passing the cost of production to co-infecting neighbours (Khan et al., 2006). Hence, siderophore-producing bacteria are vulnerable to opportunistic bacteria that are able to utilise heterologous iron-binding products (Khan et al., 2006). The bacteria are not subject to the energetic costs associated with siderophore production and can outgrow more virulent producing genotypes (Alizon and Lion, 2011). Indeed, during co-infection of Arabidopsis with several strains of *P. aeruginosa*, siderophore lacking bacteria evolved more rapidly and dominated siderophore producers in iron-limited conditions (Khan et al., 2006).

1.5 Multi–pathogen cooperation

Besides competition, pathogens may also cooperate in associations that are essential for pathogenesis. These associations can be facilitated by biophysical and/or biochemical means. For example, hyphae of the fungal ascomycete *Didymella bryoniae* physically transported four bacterial species that co-infect Styrian oil pumpkin (Grube et al., 2011;

Figure 1.2A). Samples including both the fungus and bacteria have been recovered from the field, indicating that mutualistic effects on pathogenesis may occur in nature (Grube et al., 2011). The association between *Rhizopus microsporus* and *Burkholderia* sp. is an example where a precise biochemical fungal-bacterial association has been identified. *R. microsporus* is a highly destructive zygomycetous fungus that causes blight in rice seedlings. The fungus is thought to secrete a phytotoxin known as rhizoxin; although no standard polyketide synthesis genes could be identified in the fungus genome (Partida-Martinez and Hertweck, 2005). The rhizoxin was, however, found to be secreted by the endosymbiotic bacteria that are harboured by the fungus. Thus, it appears that *R. microsporus* owes its pathogenicity to the presence of an endosymbiont bacteria belonging to the genus *Burkholderia* (Partida-Martinez and Hertweck, 2005). Intimate biochemical fungal-bacterial symbiosis occurs when both a recognition system and a molecular dialogue bind the two. For instance, recognition of fusaric acid secreted by certain isolates of the fungus *F. oxysporum* stimulates growth in the bacterial pathogen *P. fluorescens* in tomato (de Weert et al., 2004; Kamilova et al., 2008).

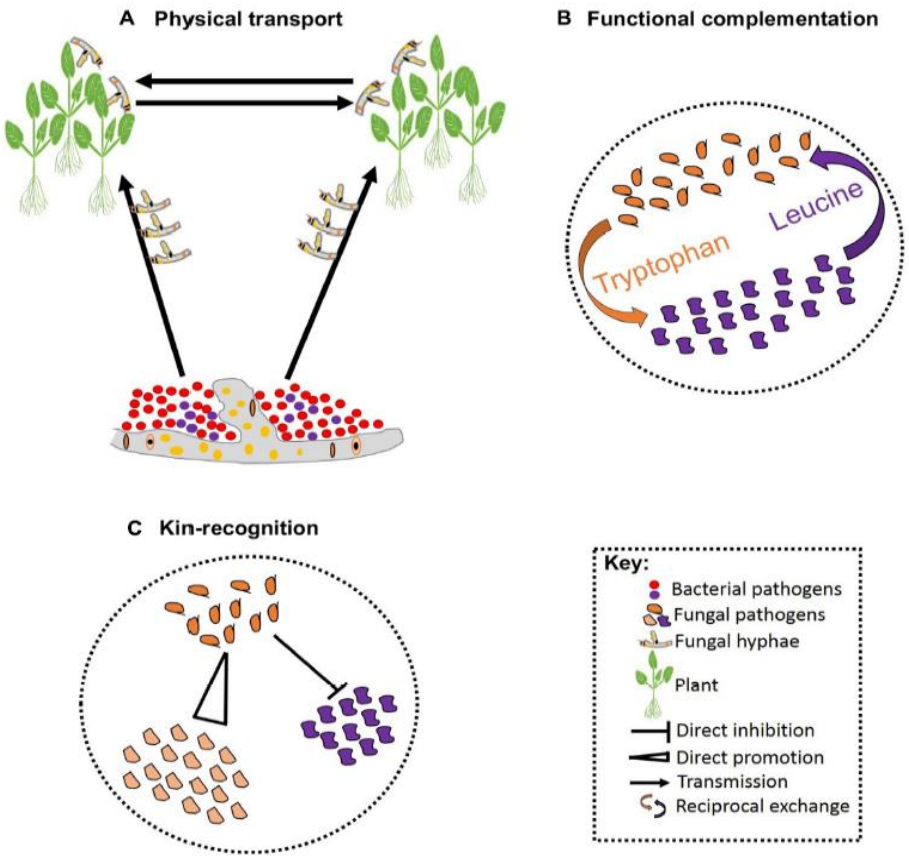

Figure 1.2. Schematic representation of pathogen-pathogen cooperation. Some bacteria can establish symbiotic associations with fungi that allow them to exploit new niches and move across infected hosts (A). Cooperation can be vital for the survival of both parties involved leading to a reciprocal exchange of vital growth substrates (B). Cooperation can also involve kinship and some pathogens can facilitate fitness of their kin while restricting the fitness of non-kin (C).

Mutualistic cooperation between pathogens can have major epidemiological implications, and certain plant pathogens are only host-destructive when they cooperate with other independent pathogens. For example, obligate mutualism between maize dwarf mosaic virus and wheat streak mosaic virus causes lethal maize necrosis – neither of these viruses is known to cause lethal necrosis alone (Uyemoto, 1983). Similarly, co-infection of tobacco mosaic virus and potato virus cause defoliation streak and a high rate of mortality in young tomato leaves (Hull, 2014). Cooperation can also enhance pathogen persistence by supporting greater reproduction rates, increasing the chance of the host being a source of inoculum in the next season (Fondong et al., 2000). Co-infection of *Nicotiana benthamiana*

plants with two strains of the cassava mosaic virus showed symptoms covering all leaves, while single-strain infection exhibited partial coverage and some leaves remained asymptomatic (Fondong et al., 2000).

Reciprocal exchange of growth substrates is a common strategy through which pathogens establish stable cooperation. Such cooperative associations are prominent when resources are deficient, and one species produces the growth substrates required by the other (Figure 1.2B). Hence, cooperation in such cases is vital for the success of all species involved (Hoek et al., 2016). In addition, there are a few well-characterised studies of altruistic cooperation between closely related species. Altruistic cooperation occurs when co-infection leads to the reduced availability of resources per species, such that the less competitive species experience reduced reproduction rates preserving resources for the reproduction of the other species (Kummerli et al., 2009; West et al., 2002). Hence, the reproductive advantage of the competitive species is dependent on the other species (Figure 1.2C). Hamilton's kin-selection theory provides a plausible explanation for the altruistic association between relatives: by helping a close relative, a pathogen is indirectly passing its genes to the next generation (Hamilton, 1963). This can occur when the degree of relatedness between the benefactor and the beneficiary is high, and the benefit outweighs the cost of the cooperation (Chao et al., 2000; Eberhard, 1975). Coexisting pathogens that exhibit altruism may display rapid evolution to overcome pesticides as a result of the reproductive advantage of the more competitive species. Furthermore, initiating defence responses against various pathogens acting together may prove costly to host resources and defence systems, although evidence for such interactions in plant pathogens is currently lacking.

1.6 Evolution of pathogens in co-infections

Recent research into pathogen interactions has considered the genetic adaptation that close proximity facilitates. It has been suggested that genomes of some species display reduced mutation rates as an adaptation strategy to the presence of other coexisting species (Cordero and Polz, 2014). Fungi isolated from tree-hole rainwater pools exhibited similar resource acquisition strategies that should lead to severe competition. However, culturing these isolates on media that resembled their natural habitat resulted in a reciprocal exchange of growth substrates (Madsen et al., 2016). When multiple species are in close proximity,

genetic recombination may occur through fusion of haploid cells. For instance, reshuffling of alleles between genetically-distant fungi resulted in novel genetic diversity in *Zymoseptoria pseudotritici* (Stukenbrock et al., 2012). Novel hybrids often display new characteristics that enable colonisation of previously unexploited niches. For example, the horizontal transfer of the gene *ToxA* from *P. nodorum* to *P. tritici repentis* allows *P. tritici repentis* to invade ToxA sensitive wheat cultivars on a large scale (Friesen et al., 2006).

Co-infection can also provide a selective advantage for the adaptation of low-frequency pathogen populations. For example, the persistence of avirulent strains of *P. syringae* was partially linked to their growth advantage through coexistence with virulent strains (Barrett et al., 2011). Similarly, laboratory-based co-infection studies demonstrated a fitness advantage to less competent pathogens conditional on their coexistence with fully-adapted pathogens (Bashey, 2015). Perhaps the simplest explanation for such fitness advantage would be a mass-action mechanism– i.e., more disease load within the plant implies greater disease transmission rates and greater infection opportunities for both species (Perefarres et al., 2014). A less direct explanation, especially applicable for viruses, may involve heteroencapsidation. This may occur when two co-infecting species display sufficient genetic variability in which case the more competent species may complement the less competent species providing benefits in accumulation and transmission within and among plants (Perefarres et al., 2014). Direct testing of mechanisms by which co-infection contributes to the maintenance of pathogen diversity is an exciting research area.

1.7 Evolution of virulence in co-infecting pathogens

Current knowledge suggests that virulence is an inevitable requirement for host exploitation. Evolution of virulence can be constrained by the reproduction rate of a pathogen (Alizon et al., 2013). Hence, increased virulence may initially be advantageous, but subsequent consequences resulting from increased host mortality are not (Chao et al., 2000; Ebert and Bull, 2003). This is particularly true in pathosystems where both the host and pathogen have comparable generation times, in which case the costs of increased virulence are spread among all species sharing the host – the so-called tragedy of the commons (Hardin, 1968). Under co-infection conditions, pathogens are thought to utilise host-limited resources more efficiently with natural selection favouring the coexistence of

pathogens that are less harmful to their hosts (Brown et al., 2002; Van Baalen and Sabelis, 1995). Early insights into the evolution of virulence were provided by the classical three-way model of Levin and Pimentel (1981) which included a host and two pathogens differing in virulence. Based on this model, when two pathogens invade the same host, virulence of one species is always considered relative to the virulence of the other species (Brown et al., 2002; Levin and Pimentel, 1981).

Early during co-infection, the more virulent pathogen may quickly take over. Nevertheless, both more and less virulent pathogens can coexist (Van Baalen and Sabelis, 1995). *In vitro* experiments suggest that coexistence between two pathogen species varying in virulence can occur. In one system, the population of the more virulent pathogen *U. maydis* was able to reach higher frequencies over the less virulent species *F. verticillioides*, though both species coexisted (Jonkers et al., 2012). However, when the same system was conducted *in planta* using maize, the less virulent species experienced lower resistance from the host and hence gained a competitive advantage over the more virulent pathogen (Estrada et al., 2012). As the less virulent species dominate, local competition of some degree takes place, and the balance may shift to favour the more virulent species (Macho et al., 2007). Once again, as the more virulent pathogen becomes abundant, plant defence systems prioritise responses against the more virulent pathogen, thereby indirectly allowing the less virulent pathogen to regain lost ground (Cobey and Lipsitch, 2013; de Roode et al., 2005; Thieme, 2007). This cycle is key for pathogen coexistence in space and time and implies, from an evolutionary perspective, that neither too high nor too low levels of virulence are advantageous.

1.8 Concluding remarks

If we are to make significant progress in plant disease management, research efforts should embrace field representative systems including multiple-pathogen infections. The role of pathogen-pathogen interactions and their impact on plant defence systems should increasingly be recognised as a priority of equal importance to studying single plant-pathogen interactions. Although rare, interaction between pathogens potentially allows the exchange of genes encoding virulence factors broadening pathogen infection strategies and allowing them to exploit new niches (Friesen et al., 2006). However, some interactions can

alert the defence system of the plant making subsequent infections less likely. Progress in utilising pathogen-pathogen interactions for developing holistic disease management strategies has been underwhelming, indicating an area that requires attention (Martinez-Medina et al., 2016).

In co-infection, pathogens can produce antimicrobial compounds toxic to other pathogens sharing the same host. However, whether production of such compounds truly represents an adaptation strategy to competition is unclear. It would be debilitating for a pathogen to produce compounds towards future threats if these threats are not realised. Such pathogens would be selected against under a reasonable assumption that the pathogen must target direct enemies or risk wasting resources. Nevertheless, pathogens can coexist and share a host, mainly due to conditions favouring the occurrence of multiple pathogens. An outstanding question is how changes in natural (e.g., climatic) and man-made (e.g., new varieties) conditions alter coexistence in the long-term. Changes to conditions may favour one pathogen over another, leading to a potential invasion by large-scale aggressive pathogens. Other challenges that require future attention are cases of below- and above-ground co-infections. Pathogens colonising various plant parts can interact via systemic host defences, making the study of these interactions particularly intriguing (Filgueiras et al., 2016). Other challenging questions that may have significant epidemiological implications are cases where pathogens invade novel niches/species. The metabolic changes that are required for a pathogen to optimise nutrient acquisition from novel niches remain unclear. High-throughput multi-species transcriptomics and metabolomics should help to unravel some of the mechanisms. Such methods will provide a better understanding of pathogen interactions allowing the development of disease control measures against multiple pathogens.

References

Adee, S., Pfender, W., and Hartnett, D. (1990). Competition between *Pyrenophora tritici-repentis* and *Septoria nodorum* in the wheat leaf as measured with de Wit replacement series. *Phytopathology* **80**, 1177-1182.

Aghnoum, R., and Niks, R. E. (2012). Compatible *Puccinia hordei* infection in barley induces basal defense to subsequent infection by *Blumeria graminis*. *Physiological and Molecular Plant Pathology* **77**, 17-22.

Aime, S., Alabouvette, C., Steinberg, C., and Olivain, C. (2013). The endophytic strain *Fusarium oxysporum* Fo47: a good candidate for priming the defense responses in tomato roots. *Molecular Plant-Microbe Interactions* **26**, 918-926.

Alizon, S., de Roode, J. C., and Michalakis, Y. (2013). Multiple infections and the evolution of virulence. *Ecology Letters* **16**, 556-567.

Alizon, S., and Lion, S. (2011). Within-host parasite cooperation and the evolution of virulence. *Proceedings of the Royal Society of London B: Biological Sciences* **278**, 738–747.

Al-Naimi, F., Garrett, K., and Bockus, W. W. (2005). Competition, facilitation, and niche differentiation in two foliar pathogens. *Oecologia* **143**, 449-457.

Barrett, L. G., Bell, T., Dwyer, G., and Bergelson, J. (2011). Cheating, trade-offs and the evolution of aggressiveness in a natural pathogen population. *Ecology Letters* **14**, 1149-1157.

Bashey, F. (2015). Within-host competitive interactions as a mechanism for the maintenance of parasite diversity. *Philsophical Transactions Royal Society B* **370**, 1-8.

Brown, J. K. (2015). Durable resistance of crops to disease: a Darwinian perspective. *Annual Review of Phytopathology* **53**, 513-539.

Brown, S. P., Hochberg, M. E., and Grenfell, B. T. (2002). Does multiple infection select for raised virulence? *Trends in Microbiology* **10**, 401-405.

Castrillo, G., Teixeira, P. J. P. L., Paredes, S. H., Law, T. F., De Lorenzo, L., Feltcher, M. E., Finkel, O. M., Breakfield, N. W., Mieczkowski, P., and Jones, C. D. (2017). Root microbiota drive direct integration of phosphate stress and immunity. *Nature* **543**, 513-518.

Chao, L., Hanley, K. A., Burch, C. L., Dahlberg, C., and Turner, P. E. (2000). Kin selection and parasite evolution: higher and lower virulence with hard and soft selection. *Quarterly Review of Biology* **75**, 261-275.

Chesson, P. (2000). Mechanisms of maintenance of species diversity. *Annual Review of Ecology and Systematics* **31**, 343-366.

Cobey, S., and Lipsitch, M. (2013). Pathogen diversity and hidden regimes of apparent competition. *The American Naturalist* **181**, 12-24.

Conrath, U., Beckers, G. J., Langenbach, C. J., and Jaskiewicz, M. R. (2015). Priming for enhanced defense. *Annual Review of Phytopathology* **53**, 97-119.

Cooper, A., Latunde-Dada, A., Woods-Tör, A., Lynn, J., Lucas, J., Crute, I., and Holub, E. (2008). Basic compatibility of *Albugo candida* in *Arabidopsis thaliana* and *Brassica juncea* causes broad-spectrum suppression of innate immunity. *Molecular Plant-Microbe Interactions* **21**, 745-756.

Cordero, O. X., and Polz, M. F. (2014). Explaining microbial genomic diversity in light of evolutionary ecology. *Nature Reviews Microbiology* **12**, 263.

Cornelis, P., and Dingemans, J. (2013). *Pseudomonas aeruginosa* adapts its iron uptake strategies in function of the type of infections. *Frontiers in Cellular and Infection Microbiology* **3**, 1-7.

Cui, J., Bahrami, A. K., Pringle, E. G., Hernandez-Guzman, G., Bender, C. L., Pierce, N. E., and Ausubel, F. M. (2005). *Pseudomonas syringae* manipulates systemic plant defenses against pathogens and herbivores. *Proceedings of the National Academy of Sciences of the United States of America* **102**, 1791-1796.

Dangl, J. L., and Jones, J. D. (2001). Plant pathogens and integrated defence responses to infection. *Nature* **411**, 826-833.

de Roode, J. C., Pansini, R., Cheesman, S. J., Helinski, M. E., Huijben, S., Wargo, A. R., Bell, A. S., Chan, B. H., Walliker, D., and Read, A. F. (2005). Virulence and competitive ability in genetically diverse malaria infections. *Proceedings of the National Academy of Sciences of the United States of America* **102**, 7624-7628.

de Torres-Zabala, M., Truman, W., Bennett, M. H., Lafforgue, G., Mansfield, J. W., Egea, P. R., Bögre, L., and Grant, M. (2007). *Pseudomonas syringae* pv. tomato hijacks the Arabidopsis abscisic acid signalling pathway to cause disease. *The EMBO journal* **26**, 1434-1443.

De Vos, M., Van Oosten, V. R., Van Poecke, R. M., Van Pelt, J. A., Pozo, M. J., Mueller, M. J., Buchala, A. J., Métraux, J.-P., Van Loon, L., and Dicke, M. (2005). Signal signature and transcriptome changes of Arabidopsis during pathogen and insect attack. *Molecular Plant-Microbe Interactions* **18**, 923-937.

De Weert, S., Kuiper, I., Lagendijk, E. L., Lamers, G. E., and Lugtenberg, B. J. (2004). Role of chemotaxis toward fusaric acid in colonization of hyphae of *Fusarium oxysporum* f. sp. *radicis-lycopersici* by *Pseudomonas fluorescens* WCS365. *Molecular Plant-Microbe Interactions* **17**, 1185-1191.

Eberhard, M. J. W. (1975). The evolution of social behavior by kin selection. *Quarterly Review of Biology* **50**, 1-33.

Ebert, D., and Bull, J. J. (2003). Challenging the trade-off model for the evolution of virulence: is virulence management feasible? *Trends in Microbiology* **11**, 15-20.

Estrada, A. E. R., Jonkers, W., Kistler, H. C., and May, G. (2012). Interactions between *Fusarium verticillioides*, *Ustilago maydis*, and *Zea mays*: an endophyte, a pathogen, and their shared plant host. *Fungal Genetics and Biology* **49**, 578-587.

Filgueiras, C. C., Willett, D. S., Junior, A. M., Pareja, M., El Borai, F., Dickson, D. W., Stelinski, L. L., and Duncan, L. W. (2016). Stimulation of the salicylic acid pathway aboveground recruits entomopathogenic nematodes belowground. *Plos One* **11**, e0154712.

Fitt, B. D., Huang, Y.-J., van den Bosch, F., and West, J. S. (2006). Coexistence of related pathogen species on arable crops in space and time. *Annual Review of Phytopathology* **44**, 163-182.

Fondong, V., Pita, J., Rey, M., De Kochko, A., Beachy, R., and Fauquet, C. (2000). Evidence of synergism between African cassava mosaic virus and a new double-recombinant geminivirus infecting cassava in Cameroon. *Journal of General Virology* **81**, 287-297.

Friesen, T. L., Stukenbrock, E. H., Liu, Z., Meinhardt, S., Ling, H., Faris, J. D., Rasmussen, J. B., Solomon, P. S., McDonald, B. A., and Oliver, R. P. (2006). Emergence of a new disease as a result of interspecific virulence gene transfer. *Nature Genetics* **38**, 953-959.

Gazzarrini, S., and Mccourt, P. (2003). Cross-talk in plant hormone signalling: what arabidopsis mutants are telling us. *Annals of Botany* **91**, 605-612.

Ghoul, M., West, S., Diggle, S., and Griffin, A. (2014). An experimental test of whether cheating is context dependent. *Journal of Evolutionary Biology* **27**, 551-556.

Glazebrook, J. (2005). Contrasting mechanisms of defense against biotrophic and necrotrophic pathogens. *Annual Review of Phytopathology* **43**, 205-227.

Glenn, A. E., Zitomer, N. C., Zimeri, A. M., Williams, L. D., Riley, R. T., and Proctor, R. H. (2008). Transformation-mediated complementation of a FUM gene cluster deletion in *Fusarium verticillioides* restores both fumonisin production and pathogenicity on maize seedlings. *Molecular Plant-Microbe Interactions* **21**, 87-97.

Grant, M. R., and Jones, J. D. (2009). Hormone (dis) harmony moulds plant health and disease. *Science* **324**, 750-752.

Greenberg, J. T., and Yao, N. (2004). The role and regulation of programmed cell death in plant–pathogen interactions. *Cellular Microbiology* **6**, 201-211.

Grube, M., Fürnkranz, M., Zitzenbacher, S., Huss, H., and Berg, G. (2011). Emerging multi-pathogen disease caused by *Didymella bryoniae* and pathogenic bacteria on Styrian oil pumpkin. *European Journal of Plant Pathology* **131**, 539-548.

Hacquard, S., Kracher, B., Hiruma, K., Munch, P. C., Garrido-Oter, R., Thon, M. R., Weimann, A., Damm, U., Dallery, J.-F., and Hainaut, M. (2016). Survival trade-offs in plant roots during colonization by closely related beneficial and pathogenic fungi. *Nature Communications* **7**, 1-12.

Hamilton, W. D. (1963). The evolution of altruistic behavior. *The American Naturalist* **97**, 354-356.

Hardin, G. (1968). The tragedy of the commons. Science **162**, 1243-1248.

Harrison, F., Browning, L. E., Vos, M., and Buckling, A. (2006). Cooperation and virulence in acute *Pseudomonas aeruginosa* infections. *BMC Biology* **4**, 21-29.

Hauck, P., Thilmony, R., and He, S. Y. (2003). A *Pseudomonas syringae* type III effector suppresses cell wall-based extracellular defense in susceptible Arabidopsis plants. *Proceedings of the National Academy of Sciences of the United States of America* **100**, 8577-8582.

Hentzer, M., Wu, H., Andersen, J. B., Riedel, K., Rasmussen, T. B., Bagge, N., Kumar, N., Schembri, M. A., Song, Z., and Kristoffersen, P. (2003). Attenuation of *Pseudomonas aeruginosa* virulence by quorum sensing inhibitors. *The EMBO Journal* **22**, 3803-3815.

Hibbing, M. E., Fuqua, C., Parsek, M. R., and Peterson, S. B. (2010). Bacterial competition: surviving and thriving in the microbial jungle. *Nature Reviews Microbiology* **8**, 15-25.

Hoek, T. A., Axelrod, K., Biancalani, T., Yurtsev, E. A., Liu, J., and Gore, J. (2016). Resource availability modulates the cooperative and competitive nature of a microbial cross-feeding mutualism. *Plos Biology* **14**, 1-17.

Hull, R. (2014). Plant virology, Academic press, San Diego, CA.

Jonkers, W., Estrada, A. E. R., Lee, K., Breakspear, A., May, G., and Kistler, H. C. (2012). Metabolome and transcriptome of the interaction between *Ustilago maydis* and *Fusarium verticillioides in vitro*. *Applied and Environmental Microbiology* **78**, 3656-3667.

Kamilova, F., Lamers, G., and Lugtenberg, B. (2008). Biocontrol strain *Pseudomonas fluorescens* WCS365 inhibits germination of *Fusarium oxysporum* spores in tomato root exudate as well as subsequent formation of new spores. *Environmental Microbiology* **10**, 2455-2461.

Katsir, L., Schilmiller, A. L., Staswick, P. E., He, S. Y., and Howe, G. A. (2008). COI1 is a critical component of a receptor for jasmonate and the bacterial virulence factor coronatine. *Proceedings of the National Academy of Sciences of the United States of America* **105**, 7100-7105.

Khan, A., Geetha, R., Akolkar, A., Pandya, A., Archana, G., and Desai, A. J. (2006). Differential cross-utilization of heterologous siderophores by nodule bacteria of *Cajanus cajan* and its possible role in growth under iron-limited conditions. *Applied Soil Ecology* **34**, 19-26.

Kozanitas, M., Osmundson, T. W., Linzer, R., and Garbelotto, M. (2017). Interspecific interactions between the Sudden Oak Death pathogen *Phytophthora ramorum* and two sympatric *Phytophthora* species in varying ecological conditions. *Fungal Ecology* **28**, 86-96.

Kummerli, R., Griffin, A. S., West, S. A., Buckling, A., and Harrison, F. (2009). Viscous medium promotes cooperation in the pathogenic bacterium *Pseudomonas aeruginosa*. *Proceedings of the Royal Society B* **276**, 3531-3538.

Levin, S., and Pimentel, D. (1981). Selection of intermediate rates of increase in parasite-host systems. *American Naturalist* **117**, 308-315.

Macho, A. P., Zumaquero, A., Ortiz-Martin, I., and Beuzon, C. R. (2007). Competitive index in mixed infections: a sensitive and accurate assay for the genetic analysis of *Pseudomonas syringae*–plant interactions. *Molecular Plant Pathology* **8**, 437-450.

Madsen, J. S., Roder, H. L., Russel, J., Sorensen, H., Burmolle, M., and Sorensen, S. J. (2016). Co-existence facilitates interspecific biofilm formation in complex microbial communities. *Environmental Microbiology* **18**, 2565–2574.

Martinez-Medina, A., Flors, V., Heil, M., Mauch-Mani, B., Pieterse, C. M., Pozo, M. J., Ton, J., van Dam, N. M., and Conrath, U. (2016). Recognizing plant defense priming. *Trends in Plant Science* **21**, 818-822.

Maurhofer, M., Keel, C., Schnider, U., Voisard, C., Haas, D., and Défago, G. (1992). Influence of enhanced antibiotic production in *Pseudomonas fluorescens* strain CHA0 on its disease suppressive capacity. *Phytopathology* **82**, 190-195.

Millet, Y. A., Danna, C. H., Clay, N. K., Songnuan, W., Simon, M. D., Werck-Reichhart, D., and Ausubel, F. M. (2010). Innate immune responses activated in Arabidopsis roots by microbe-associated molecular patterns. *The Plant Cell* **22**, 973-990.

Moffat, C. S., Ingle, R. A., Wathugala, D. L., Saunders, N. J., Knight, H., and Knight, M. R. (2012). ERF5 and ERF6 play redundant roles as positive regulators of JA/Et-mediated defense against *Botrytis cinerea* in Arabidopsis. *Plos One* **7**, e35995.

Monod, J. (1949). The growth of bacterial cultures. *Annual Reviews in Microbiology* **3**, 371-394.

Mordecai, E. A., Gross, K., and Mitchell, C. E. (2016). Within-host niche differences and fitness trade-offs promote coexistence of plant viruses. *The American Naturalist* **187**, E13-E26.

Mousa, W. K., Schwan, A., Davidson, J., Strange, P., Liu, H., Zhou, T., Auzanneau, F.-I., and Raizada, M. N. (2015). An endophytic fungus isolated from finger millet (*Eleusine coracana*) produces anti-fungal natural products. *Frontiers in Microbiology* **6**, 1-16.

Mousa, W. K., Schwan, A. L., and Raizada, M. N. (2016a). Characterization of antifungal natural products isolated from endophytic fungi of finger millet (*Eleusine coracana*). *Molecules* **21**, 1171.

Mousa, W. K., Shearer, C., Limay-Rios, V., Ettinger, C. L., Eisen, J. A., and Raizada, M. N. (2016b). Root-hair endophyte stacking in finger millet creates a physicochemical barrier to trap the fungal pathogen *Fusarium graminearum*. *Nature Microbiology* **1**, 16167.

Notz, R., Maurhofer, M., Dubach, H., Haas, D., and Défago, G. (2002). Fusaric acid-producing strains of *Fusarium oxysporum* alter 2, 4-diacetylphloroglucinol biosynthetic gene expression in *Pseudomonas fluorescens* CHA0 in vitro and in the rhizosphere of wheat. *Applied and Environmental Microbiology* **68**, 2229-2235.

Ongena, M., Jourdan, E., Schafer, M., Kech, C., Budzikiewicz, H., Luxen, A., and Thonart, P. (2005). Isolation of an N-alkylated benzylamine derivative from *Pseudomonas putida* BTP1 as elicitor of induced systemic resistance in bean. *Molecular Plant-Microbe Interactions* **18**, 562-569.

Orton, E. S., and Brown, J. K. (2016). Reduction of growth and reproduction of the biotrophic fungus *Blumeria graminis* in the presence of a necrotrophic pathogen. *Frontiers in Plant Science* **7**, 1-12.

Partida-Martinez, L. P., and Hertweck, C. (2005). Pathogenic fungus harbours endosymbiotic bacteria for toxin production. *Nature* **437**, 884-888.

Perefarres, F., Thebaud, G., Lefeuvre, P., Chiroleu, F., Rimbaud, L., Hoareau, M., Reynaud, B., and Lett, J.-M. (2014). Frequency-dependent assistance as a way out of competitive exclusion between two strains of an emerging virus. *Proceedings of the Royal Society of London B: Biological Sciences* **281**, 1-9.

Petrosino, J. F., Highlander, S., Luna, R. A., Gibbs, R. A., and Versalovic, J. (2009). Metagenomic pyrosequencing and microbial identification. *Clinical Chemistry* **55**, 856-866.

Pfennig, K. S., and Pfennig, D. W. (2009). Character displacement: ecological and reproductive responses to a common evolutionary problem. *The Quarterly Review of Biology* **84**, 253–276.

Pieterse, C. M., Leon-Reyes, A., Van der Ent, S., and Van Wees, S. C. (2009). Networking by small-molecule hormones in plant immunity. *Nature Chemical Biology* **5**, 308-316.

Rankin, D. J., Bargum, K., and Kokko, H. (2007). The tragedy of the commons in evolutionary biology. *Trends in Ecology and Evolution* **22**, 643-651.

Ravensdale, M., Rocheleau, H., Wang, L., Nasmith, C., Ouellet, T., and Subramaniam, R. (2014). Components of priming-induced resistance to Fusarium head blight in wheat revealed by two distinct mutants of *Fusarium graminearum*. *Molecular Plant Pathology* **15**, 948-956.

Ren, N., and Gijzen, M. (2016). Escaping host immunity: new tricks for plant pathogens. *Plos Pathogens* **12**, e1005631.

Robert-Seilaniantz, A., Grant, M., and Jones, J. D. (2011). Hormone crosstalk in plant disease and defense: more than just jasmonate-salicylate antagonism. *Annual Review of Phytopathology* **49**, 317-343.

Rohmer, L., Hocquet, D., and Miller, S. I. (2011). Are pathogenic bacteria just looking for food? Metabolism and microbial pathogenesis. *Trends in Microbiology* **19**, 341-348.

Saunders, M., and Kohn, L. M. (2008). Host-synthesized secondary compounds influence the in vitro interactions between fungal endophytes of maize. *Applied and Environmental Microbiology* **74**, 136-142.

Schenk, P. M., Carvalhais, L. C., and Kazan, K. (2012). Unraveling plant-microbe interactions: can multi-species transcriptomics help? *Trends in Biotechnology* **30**, 177-184.

Smith, K. P., Handelsman, J., and Goodman, R. M. (1999). Genetic basis in plants for interactions with disease-suppressive bacteria. *Proceedings of the National Academy of Sciences of the United States of America* **96**, 4786-4790.

Song, Y. Y., Zeng, R. S., Xu, J. F., Li, J., Shen, X., and Yihdego, W. G. (2010). Interplant communication of tomato plants through underground common mycorrhizal networks. *Plos One* **5**, e13324.

Spoel, S. H., Johnson, J. S., and Dong, X. (2007). Regulation of tradeoffs between plant defenses against pathogens with different lifestyles. *Proceedings of the National Academy of Sciences of the United States of America* **104**, 18842-18847.

Spoel, S. H., Koornneef, A., Claessens, S. M., Korzelius, J. P., Van Pelt, J. A., Mueller, M. J., Buchala, A. J., Métraux, J.-P., Brown, R., and Kazan, K. (2003). NPR1 modulates cross-talk between salicylate-and jasmonate-dependent defense pathways through a novel function in the cytosol. *The Plant Cell* **15**, 760-770.

Stukenbrock, E. H., Christiansen, F. B., Hansen, T. T., Dutheil, J. Y., and Schierup, M. H. (2012). Fusion of two divergent fungal individuals led to the recent emergence of a unique widespread pathogen species. *Proceedings of the National Academy of Sciences of the United States of America* **109**, 10954-10959.

Susi, H., Barres, B., Vale, P. F., and Laine, A.-L. (2015). Co-infection alters population dynamics of infectious disease. *Nature Communications* **6**, 1-8.

Thieme, H. R. (2007). Pathogen competition and coexistence and the evolution of virulence. *In* "Mathematics for Life Science and Medicine", pp. 123-153. Springer, Berlin.

Tollenaere, C., Lacombe, S., Wonni, I., Barro, M., Ndougonna, C., Gnacko, F., Sérémé, D., Jacobs, J. M., Hebrard, E., and Cunnac, S. (2017). Virus-bacteria rice co-Infection in Africa: field estimation, reciprocal effects, molecular mechanisms, and evolutionary implications. *Frontiers in Plant Science* **8**, 1-13.

Tollenaere, C., Susi, H., and Laine, A.-L. (2016). Evolutionary and epidemiological implications of multiple infection in plants. *Trends in Plant Science* **21**, 80-90.

Tollenaere, C., Susi, H., Nokso-Koivisto, J., Koskinen, P., Tack, A., Auvinen, P., Paulin, L., Frilander, M. J., Lehtonen, R., and Laine, A.-L. (2012). SNP design from 454 sequencing of *Podosphaera plantaginis* transcriptome reveals a genetically diverse pathogen metapopulation with high levels of mixed-genotype infection. *Plos One* **7**, e52492.

Toscano-Underwood, C., Huang, Y., Fitt, B. D., and Hall, A. (2003). Effects of temperature on maturation of pseudothecia of *Leptosphaeria maculans* and *L. biglobosa* on oilseed rape stem debris. *Plant Pathology* **52**, 726-736.

Uyemoto, J. (1983). Biology and control of maize chlorotic mottle virus. *Plant Disease* **67**, 7-10.

Van Baalen, M., and Sabelis, M. W. (1995). The scope for virulence management: a comment on Ewald's view on the evolution of virulence. *Trends in Microbiology* **3**, 414-416.

Van der Ent, S., Van Wees, S. C., and Pieterse, C. M. (2009). Jasmonate signaling in plant interactions with resistance-inducing beneficial microbes. *Phytochemistry* **70**, 1581-1588.

Walsh, U. F., Morrissey, J. P., and O'Gara, F. (2001). *Pseudomonas* for biocontrol of phytopathogens: from functional genomics to commercial exploitation. *Current Opinion in Biotechnology* **12**, 289-295.

West, S. A., Griffin, A. S., Gardner, A., and Diggle, S. P. (2006). Social evolution theory for microorganisms. *Nature Reviews Microbiology* **4**, 597-607.

West, S. A., Pen, I., and Griffin, A. S. (2002). Cooperation and competition between relatives. *Science* **296**, 72-75.

2 Development of a qPCR methodology for diagnosis of co-infecting Ptr and Pan[II]

Abstract

This chapter addresses the need for an assay to simultaneously quantify the abundance of two pathogens from a single leaf sample. The chapter reports on a duplex quantitative PCR assay that simultaneously distinguishes and quantifies co-infections by two important fungal pathogens of wheat: *Pyrenophora tritici-repentis* and *Parastagonospora nodorum*. These fungi share common characteristics and host species, creating a challenge for conventional disease diagnosis and subsequent management strategies. The assay uses uniquely assigned fluorogenic probes to quantify fungal biomass as nucleic acid equivalents. The probes provide highly specific target quantification with accurate discrimination against non-target closely related fungal species and host genes. Quantification of the fungal targets is linear over a wide dynamic range (5000 to 0.5 pg DNA μl^{-1}) with high reproducibility (RSD $\leq$10%). In the presence of host DNA in the assay matrix, fungal biomass can be quantified up to a fungal to wheat DNA ratio of 1 to 200. The utility of the method was demonstrated using field samples of a cultivar susceptible to both pathogens. While visual and culturing diagnosis suggested the presence of only one of the pathogen species, the assay revealed not only presence of both co-infecting pathogens (hence enabling asymptomatic detection) but also allowed quantification of relative abundances of the pathogens as a function of disease severity. Thus, the assay provides for accurate diagnosis; and is suitable for high-throughput screening of co-infections for epidemiological studies, and for exploring pathogen-pathogen interactions and dynamics, none of which would be possible with the conventional approaches.

[II]This chapter was published in August 2018: Abdullah, A. S., Turo, C., Moffat, C. S., Lopez-Ruiz, F. J., Gibberd, M. R., Hamblin, J. and Zerihun, A. Real-time PCR for detection and quantification of co-infection by two globally distributed fungi of wheat. Frontiers Plant Science, | doi.org/10.3389/fpls.2018.01086.

Authors' contribution: Araz Abdullah contributed to the conception of the idea, defined/selected the primers, conducted the experiments, analysed the data and drafted the manuscript. Chala Turo assisted in setting up the conventional PCR and testing of the primers. Caroline Moffat, Fran Lopez, Ayalsew Zerihun, Mark Gibberd, and John Hamblin supervised the work and provided critical suggestions on the article. All authors read and approved the final version of the article.

2.1 Introduction

Co-infections, whereby a host-plant is invaded by multiple pathogens or multiple strains of the same pathogen, are common in the field and can have major consequences for disease ecology and pathogen evolution (Alizon et al., 2013). Despite the recognition of the significance of co-infection (Savary and Zadoks, 1992; Tack et al., 2012; Zadoks, 1999), empirical studies are still few, due mainly to the complexity of distinguishing/quantifying multiple pathogens, which often requires suitable molecular tools (Tollenaere et al., 2016; Tollenaere et al., 2012). As a result, the theoretical understanding of co-infection has largely outpaced experimental studies in natural and agricultural systems (Abdullah et al., 2017; Hood, 2003). Our capacity to understand and manage the processes and consequences of co-infection is limited until current and future theoretical models can be validated by reliable data.

Methods that have previously been used for distinguishing multiple pathogens from co-infected tissues involve detection of nucleic acid targets using metagenome sequencing and/or analysis of melt-curves from PCR primers with various annealing properties (Brandfass and Karlovsky, 2006; Gelaye et al., 2017; Tollenaere et al., 2012). Such methods enable multiple pathogen detections but provide limited quantitative information on the relative abundance of each pathogen and their effects on overall disease (Bernreiter, 2017). The quantification of pathogen abundance is critical, as many pathogens are naturally present within plants, but their infection levels, pathogenicity and hence relative impacts can differ vastly (Bakker et al., 2014). At present, real-time quantitative PCR (qPCR) is the most reliable technique for measuring disease load in a sample while providing species specificity (Bates et al., 2001; Holland et al., 1991; Schena et al., 2006). Successful qPCR-based multiplexed assays have been developed for detection of *Phytophthora* diseases of soybean (Rojas et al., 2017), but the accuracy of quantification is often compromised in samples with unbalanced target ratios (Atallah et al., 2007; Klerks et al., 2004). Thus, to ensure reliable quantification, co-infection studies often analyse the abundance of multiple pathogens in separate reactions. However, this approach, due to the cost of labour and resources required, is limited to small-scale investigations restrcting our capacity to investigate co-infections over large-scale host populations.

In order to address the limitations of current approaches, dual-labelled species-specific probes were employed in detection and quantification of two major fungi of wheat: *Pyrenophora tritici-repentis* (Ptr) and *Parastagonospora nodorum* (Pan). These two foliar fungi cause tan (yellow) spot and septoria nodorum blotch in wheat, respectively, damaging photosynthetically active leaf area and causing substantial yield losses (Bhathal et al., 2003). Symptoms caused by these two diseases are difficult to distinguish visually and may be misdiagnosed as other unrelated wheat diseases (Blixt et al., 2010), creating a challenge for conventional disease diagnosis and subsequent management strategies. Interestingly, Ptr carries a pathogenicity-related gene, *ToxA*, thought to have been acquired laterally from Pan (Friesen et al., 2006). This suggests that co-infection by these two fungi is likely to occur in nature and may have consequences for disease management strategies. Despite the high likelihood of co-infection by these two fungi and difficulties of identification, no tools have been developed for the diagnosis of their abundance in co-infected host materials.

This chapter reports on a duplex qPCR assay that distinguishes specific DNA sequences unique to Ptr and Pan and quantifies their presence by direct comparison to standards amplified in parallel reactions. The basis of this method is the uniquely assigned fluorogenic reporters for each species sequence. The fluorogenic reporters, when bound to the target, quantify fungal biomass as nucleic acid equivalents. In this chapter, a series of experiments are conducted to demonstrate the specificity and sensitivity of the method. These use both a simulated genomic DNA matrix of both fungi at varying ratios as well as naturally infected wheat leaves collected from the field. The chapter also examines the capacity of the method to show that a species that is present at very low abundance can be detected and quantified, with very limited interference, in the presence of an abundant species.

2.2 Materials and methods

2.2.1 PCR primers and conditions

Ptr primers were designed to target a species-specific multicopy genomic region described previously (Moffat et al., 2015; See et al., 2016). Briefly, a 4.65 kb region of the Ptr isolate Pt-1CBFP carrying the *ToxA* gene (supercontig_1.4) was aligned to an orthologous genomic region of the Pan isolate SN15 (scaffold_55). Three known isolates of the targeted

fungi were included in this step to ensure that the primers amplify all isolates of the pathogens of interest. A pair of primers that target a 99-bp fragment located 701-bp upstream of the *ToxA* coding region was designed to detect Ptr (Table 2.1). These primers amplify a short fragment (99-bp) within the promoter region of a low molecular weight host-selective toxin. This region has been detected in a number of races of Ptr isolates collected from around the world (Moolhuijzen et al., 2018). The size of the primer pair was restricted to 99-bp to ensure comparable amplicon sizes between Ptr and Pan.

Table 2.1. List of the oligonucleotides used in this study. Primers and probes were designed to amplify short fragments of the targeted pathogen DNA.

Sequence ID*	5′→3′ sequence	Product length (bp)	GC (%)
Ptr–Forward	GTCTCCTCTGGTGGTATG		
Ptr–Reverse	GCTCTTAGTGAAGTTCAATC	99	55.6
Ptr–Probe	TACCTCTACTCGGTCGCCTATGG		
Pan–Forward	**ACCGCATTACCAAAGTTC**		
Pan–Reverse	**ACTGGAACTGGAACAATAAG**	112	45.8
Pan–Probe	CCTGAATGCTCTTGACACTTGGTT		

* Ptr and Pan refer to *P. tritici-repentis* and *P. nodorum*, respectively. Sequences in bold are pre-published primers modified from Oliver et al. (2008). Other sequences are designed in this study.

Pan DNA was amplified using primers modified from those previously described by Oliver et al. (2008). Additional 3-bp was included at the beginning of each primer sequence to allow the probe to overcome the issue of primer-dimer association (Barbisin et al., 2009). Pan primers amplify a 112-bp fragment of a highly conserved anonymous gene (SNOG_01116·1). This gene has no significant similarity to any other sequences in the publically available genome databases (Oliver et al., 2008). All primers were designed using OligoArchitect™ primer analyser (Sigma, Life Science) and scanned against the National Centre for Biotechnology Information GenBank database using basic local alignment search tools to ensure their specificity.

The designed primers were subjected to conventional PCR to confirm their specificity. Each PCR reaction contained 1xMyTaq buffer, 250 nM forward primer, 250 nM reverse primer, 1 unit MyTaq DNA polymerase (Bioline), and 5 ng DNA template. Reactions were performed as follows: 3 min initial denaturation at 95˚C, 35 cycles of 30 s denaturation at

95˚C, 30 s of annealing at 58˚C and 1 min extension at 72˚C. Electrophoresis of PCR products was performed on 2% agarose gels stained with SyberSafe (Life Technologies) and visualised under UV light. Reproducibility of the results was confirmed by running the PCR with negative controls in duplicates. The PCR step also included DNA samples from five common fungal pathogens of cereals as negative controls. Colonies of *Pyrenophora teres* f.sp. *maculata*, *Pyrenophora teres* f.sp. *teres*, *Blumeria graminis* f.sp. *tritici*, *Alternaria alternata*, and *Fusarium graminearum* were kindly provided by Steven Chang, Curtin University/Centre for Crop and Disease Management. Species identity was confirmed by sequencing the internal transcribed spacer of the ribosomal DNA (Schoch et al., 2012). All sequence analyses and multiple sequence alignments were carried out using Geneious version R6.1.6.

2.2.2 Real-time PCR probes and conditions

Two dual-labelled hydrolysis probes were custom-designed and assigned to hybridise with a complementary region between the forward and the reverse primers. The Ptr and Pan probes were 23-bp and 20-bp in length, respectively. The length of each probe was chosen to ensure probe-primer hybrids are formed in a complementary manner with the length of the primers. Each probe was labelled with a unique fluorogenic reporter to ensure that target sequences of both pathogens were amplified simultaneously but detected independently. The Ptr probe was labelled with 6-carboxyfluorescein (FAM™; Sigma-Aldrich). The Pan probe was labelled with CAL Fluor Gold® (CFG; Sigma-Aldrich). FAM has emission maxima between 494 nm and 518 nm and CFG emission peaks between 538 nm and 559 nm. The fluorogenic reporters were selected based on the capacity of the CFX96 detection system, the instrument used in this study, to resolve overlapping spectra. This was determined prior to carrying out the experiments using a spectra overlay tool available at http://www.Qpcrdesign.com/spectral-overlay. Both probes were paired with the non-fluorescent black hole quencher-1 (BHQ-1®; Sigma-Aldrich).

Probes and their matching primers were run on a 96-well spectrofluorometric thermal cycler (Bio-Rad CFX96) with the following conditions: 15 min at 95˚C, 15 s denaturation at 95˚C, 20 s at 72˚C followed by 40 cycles of 15 s at 95˚C and 30 s at 58˚C. Each 20 µl reaction volume contained 5 µl of the sample and 12 µl iQ™ Multiplex Powermix (Bio-Rad). For a fixed amount of target template, Ptr DNA was amplified faster than Pan DNA.

Hence, probe and primers of Ptr were restricted to obtain comparable quantification cycles (Cq) to that of Pan. In a preliminary experiment, the concentrations of primers and probes were gradually increased from 50 nM up to 450 nM at 50 nM intervals. Ptr DNA was amplified using 200 nM forward primer, 200 nM reverse primer and 100 nM probe. Pan DNA was amplified using 250 nM forward primer, 250 nM reverse primer and 150 nM probe. Unless specified, reactions were carried out in duplex where primers and probes for both species were applied together. A preliminary experiment showed a comparable amplification efficiency between duplex and singleplex reactions and no evidence of cross-amplification among primers and probes of the two species was observed (Table 2.2). Presence of any nonspecific amplicon was examined using post-PCR melt curve analysis.

Table 2.2. Parameter estimates and reaction efficiencies of the triplicated standard curves constructed in singleplex and duplex settings.

Target species	Singleplex reactions				Duplex reactions				
	R^2	Slope	Intercept	E* (%)	R^2	Slope	Intercept	E* (%)	*P*-value†
Ptr	0.997	-3.504	21.018	92.92	0.993	-3.550	21.095	91.28	>0.05
Pan	0.996	-3.210	21.305	104.89	0.995	-3.344	21.238	99.25	>0.05

*E refers to the calculated efficiency of the reaction (E=10(-1/slope) – 1).

†Comparison of parameter estimates between the regressions in singleplex and duplex settings.

2.2.3 DNA extraction and quantification

Pure genomic DNA from fungal colonies was extracted using the Bio-sprint 15 plant DNA kit (Qiagen) as per the manufacturer's protocol. Fungal cultures were maintained on V8 potato dextrose agar (V8-DPA) plates as described elsewhere (Moffat et al., 2015). Mycelia were harvested from these cultures and ground into a fine powder in liquid nitrogen. Subsamples (40 mg ground tissue) were placed into 1.5-ml microtubes, which were then used for DNA extraction. The concentration of DNA in each subsample was determined using a NanoDrop 2000 UV-Vis spectrophotometer (Thermo Scientific) and diluted to 50 ng μl^{-1} in ultrapure PCR grade water. DNA was stored at -20˚C until used. Aerosol protected pipette tips were used throughout the extraction and quantification steps to prevent DNA contamination. DNA from infected wheat leaves was extracted using the same DNA extraction kit and quantified as described above.

2.2.4 DNA spiking and field validation

In two independent experiments, a fixed concentration of fungal DNA of one pathogen (5 ng μl^{-1}) was spiked into a progressively decreasing DNA concentration of the other pathogen (5, 0.5, 0.05 and 0.005 ng DNA μl^{-1}). This generated a ratio of DNA concentration from one pathogen to the other in the sample ranging from 1:1 down to 1:10000. The spiking aimed to simulate the analysis of samples derived from infection conditions whereby the two species occur at different relative abundance, which is typical of many foliar fungal infections. Recovery of fungal DNA for the respective pathogens was expressed as the ratio of the total concentration of fungal DNA quantified using the qPCR method to the amount of DNA added x 100.

In a third experiment, the recovery of fungal DNA was measured in fungal DNA samples spiked with abundant wheat DNA. The concentration of fungal DNA in the samples was progressively decreased from 5 down to 0.05 ng μl^{-1} while background wheat DNA was increased from 5 to 100 ng μl^{-1}. The experiment simulated analytical conditions where fungal DNA is present in small concentrations against a background of ample wheat DNA, such as would occur where infection severity and/or incidence are low.

To evaluate how well the assay works for field samples, diseased leaves from the wheat variety Scout were collected from a site in the southwest of Western Australia (31°.74S,116°.70E). Scout is rated as susceptible to very susceptible to both Ptr and Pan (DAFWA, 2016). Sampled leaves were visually inspected for diseased leaf area and given scores on 0 to100 scale. Leaves were then split into two groups; one group (n=9) was surface-sterilized in 2% chlorine and incubated on V8-PDA agar Petri-dishes in an attempt to characterise the causal agent of the disease. Leaves from the second group (n=9) were ground in liquid nitrogen and used for DNA extraction. 50 ng μl^{-1} gDNA from the infected leaves, along with 50 ng μl^{-1} gDNA from uninfected leaves from glasshouse-grown plants (negative controls), were first analysed by conventional PCR. A further 50 ng μl^{-1} gDNA from the same infected leaves and controls were then analysed using qPCR.

2.2.5 Detection and quantification of fungal abundance

Fluorescence data from the qPCR machine were retrieved during the annealing step of every Cq. Threshold fluorescence was set automatically by the instrument manager system (CFX Manager Version 2.0.8) before carrying out the assay. A log-linear standard curve of

a 10-fold dilution series corresponding to 5000 to 0.5 pg μl^{-1} was generated by plotting the logarithms of known concentrations of fungal DNA against the Cq values. The resulting regression equations were used to calculate fungal DNA in unknown samples. No-template controls, where sterile water was added instead of DNA, were included in each reaction. Limit of detection of the duplex assay, the lowest concentration at which reliable detection can be achieved, was determined following Armbruster and Pry (2008). All reactions were run with three replicates and samples that gave positive fluorescence before no-template controls were considered positive.

2.3 Results

2.3.1 Specificity of the assay

To test how well Ptr and Pan could be distinguished from each other, as well as from other common wheat pathogens and the host, two conventional PCR assays each using 5 ng gDNA were carried out. Five non-target controls of DNA from closely related cereal fungal pathogens and DNA from the wheat cultivar Scout were included in this step. Reactions were run in separate wells (i.e., singleplex). Conventional PCR provided amplicons of the expected sizes, and Ptr and Pan were distinguished based on the size of the amplicons (Figure 2.1A). Ptr and Pan primers only amplified the respective pathogen DNA. None of the five non-target controls or DNA from wheat gave specific amplicons that could be detected by conventional PCR (Figure 2.1B, C).

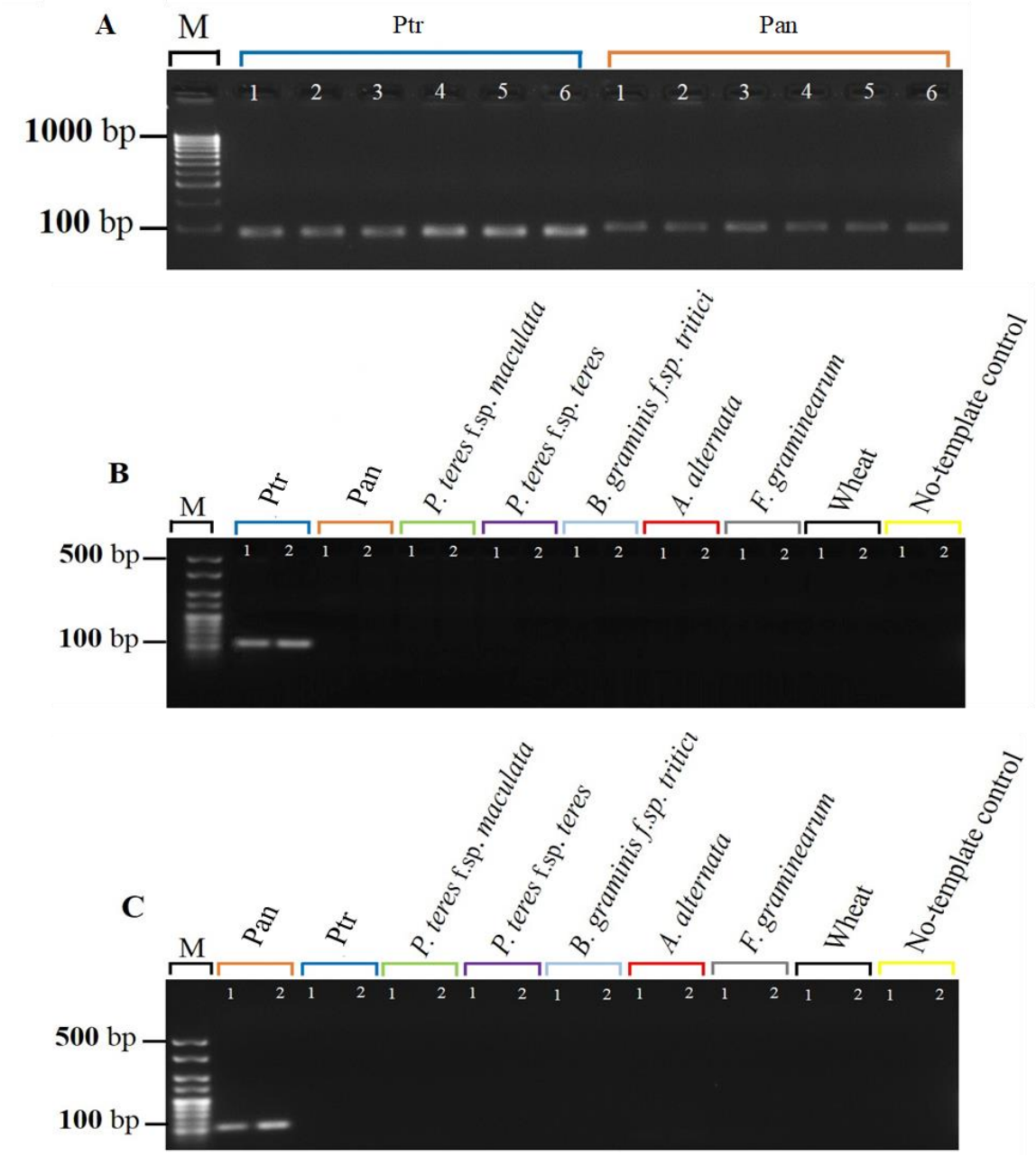

Figure 2.1. Specificity testing of primers by agarose gel electrophoresis. (A) Testing of Ptr amplicons (99-bp) as compared in size to Pan amplicons (112-bp). Reactions were run in six replicates. (B) Primers of Ptr, Ptr-Forward and Ptr-Reverse, were tested against Pan DNA, and (C) primers of Pan, Pan-Forward and Pan-Reverse, were tested against Pan DNA in two separate PCR reactions. Reactions included negative controls of DNA samples from

five cereal fungal pathogens. Reactions including positive and negative controls were electrophoresed on 2% agarose with two technical replicates.

The specificity of the probes and their matching primers was then tested in two-singleplex real-time qPCR assays each containing 5 ng gDNA. Detection only occurred for probes that were complementary to the expected sequences, and none of the five non-target controls or the wheat DNA had specific amplification during 40 real-time qPCR cycles (Figure 2.2A, B). Samples that included no-template DNA or those that contained wheat DNA were negative during the course of the reaction (Figure 2.2A, B). Ptr and Pan were distinguished based on the emission spectra of the fluorogenic reporters that were used to label each pathogen probe.

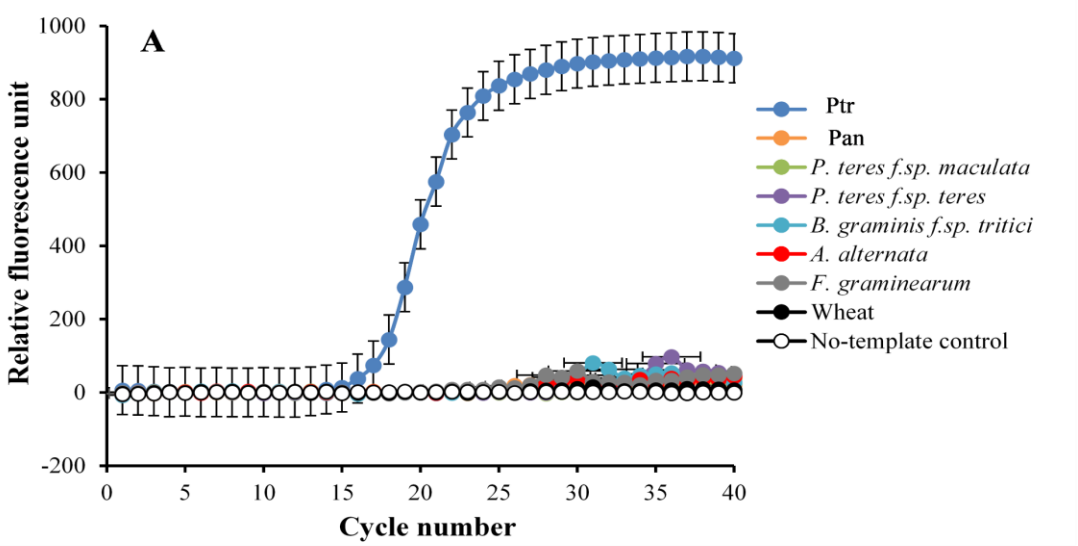

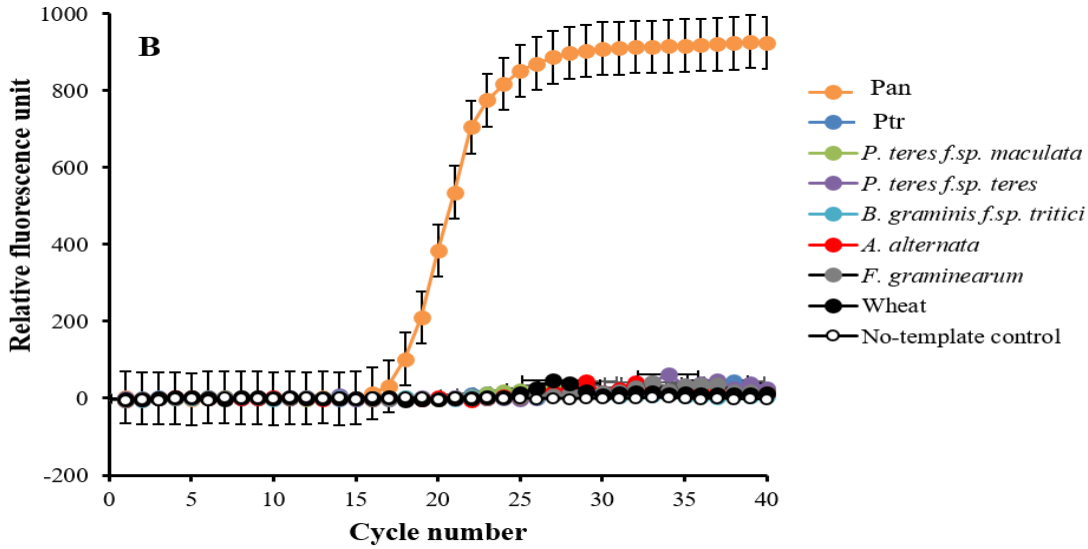

Figure 2.2. Specificity testing of primers and their matching probes in singleplex real-time qPCR settings. Amplification curve of Ptr is plotted in blue (A) and the amplification curve of Pan is plotted in orange (B). Primers and probes (Table 2.1) were tested against DNA from five fungal species, negative wheat control, and a no template control and reactions were run separately. Data represent means ± standard deviation (n=3).

2.3.2 Dynamic range, efficiency, and reproducibility of the assay

Two duplexed standard curve experiments were carried out on DNA of Ptr and Pan mixed at equal ratios. A 10-fold dilution series in the range of 5000 to 0.5 pg μl^{-1} was generated, analysed and plotted against the number of Cq required to detect fluorescence signals. Each dilution was prepared with three replicates except the no-template control, which was analysed using 10 replicates. Fitting log-linear standard curves between Cq and fungal DNA resulted in correlation coefficients (r) -0.997 and -0.996 for Ptr and Pan, respectively. The standard curves for both species were linear over 10000-fold dilution, and the calculated amplification efficiency was 91.28% for Ptr and 99.25% for Pan (Figure 2.3A, B). The slopes and intercepts of the log-linear curves were comparable between Ptr and Pan (p> 0.05). Mean Cq value (± standard deviation bars, where visible) of three replicated reactions was highly reproducible with relative standard deviation ≤10% (Figure 2.3A, B). The variation around the mean was independent of template concentration, and the Cq value for 10 no-template controls averaged 36.62 with a relative standard deviation of 0.35%.

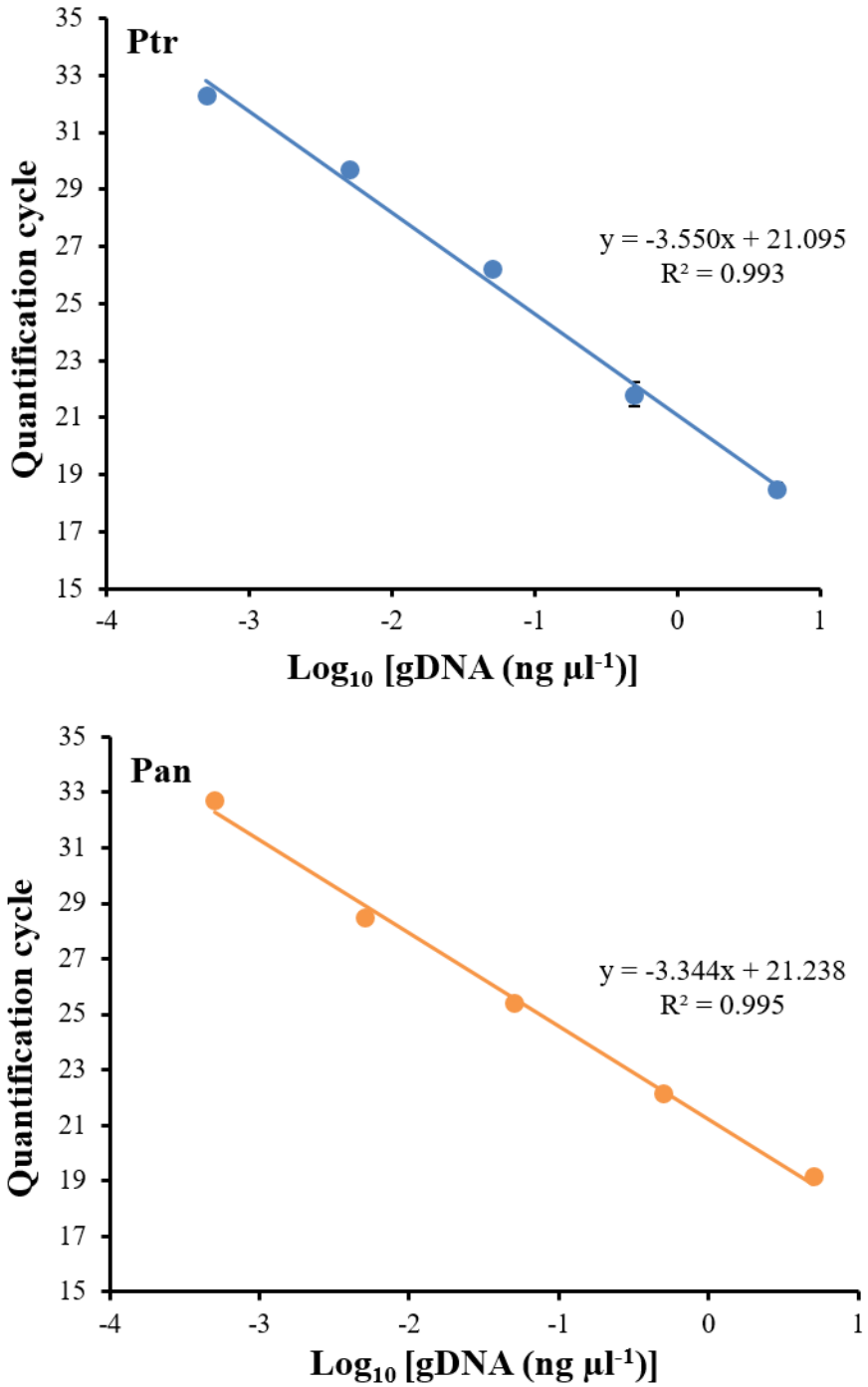

Figure 2.3. The relationship between the quantification cycle and the logarithm of the concentration of fungal DNA in duplexed qPCR settings. Triplicate dilution series corresponding to gDNA concentrations of 5000, 500, 50, 5 and 0.5 pg μl^{-1} were prepared. No-template samples were included in every reaction as negative controls (*n*=10). The quantification cycle at which fluorescent signals were observed is plotted against the

logarithm of DNA concentrations of Ptr (A) and Pan (B). The corresponding regression equations and coefficient of determinations (R^2) are shown on the plot. Data are means ± standard deviation where visible (*n*=3).

2.3.3 Sensitivity and limit of detection of the assay

Two spiking experiments were carried out using a simulated matrix of Ptr and Pan DNA mixed at various ratios. Results of the spiking experiments demonstrated that reducing DNA ratio of one species while keeping DNA of the other species constant did not affect the detection limit of the assay. The assay was able to accurately quantify fungal DNA of Ptr and Pan down to a relative ratio of 1:100 (Figure 2.4A, B). However, further reduction of the DNA ratio to 1:1000 underestimated the amount of Ptr by 11.75% and Pan by 18.55%. This underestimation became more pronounced with further dilution, and at 100 ppm (i.e., DNA ratios of 1:10000), neither pathogen was quantifiable in the presence of the other (Figure 2.4A, B). The minimal DNA concentration for detection was 0.59 pg μl^{-1} for Ptr and 0.36 pg μl^{-1} for Pan.

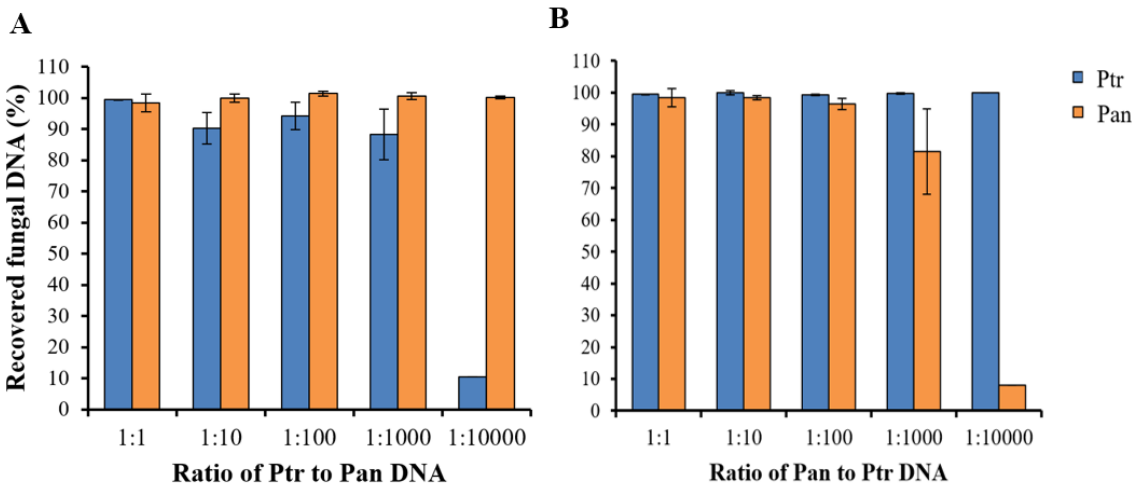

Figure 2.4. Detection and quantification of Ptr and Pan in a simulated DNA matrix of various ratios. Starting concentration was 5 ng μl^{-1} of each pathogen DNA. (A) Ptr DNA was spiked with Pan DNA at ratios of 1:1, 1:10, 1:100, 1:1000 and 1:10000. (B) Pan DNA was spiked with Ptr DNA at the same ratios. Data represent means ± standard deviation (*n*=6).

The ability of the assay to detect and quantify fungal DNA in a sample that included abundant wheat DNA was also tested. The assay was able to quantify both fungal species

with high accuracy up to a Ptr: Pan: wheat DNA ratio of 1:1:200 (Figure 2.5). Recovery of fungal DNA, the total amount of DNA quantified using the qPCR method, was high at 95.69% for Ptr and 94.20% for Ptr when the fungal to wheat DNA ratios dropped to 1:1:2000. At these ratios, however, relative standard deviations were 10.23% and 13.90% for Ptr and Pan, respectively, affecting the reliability of DNA quantification.

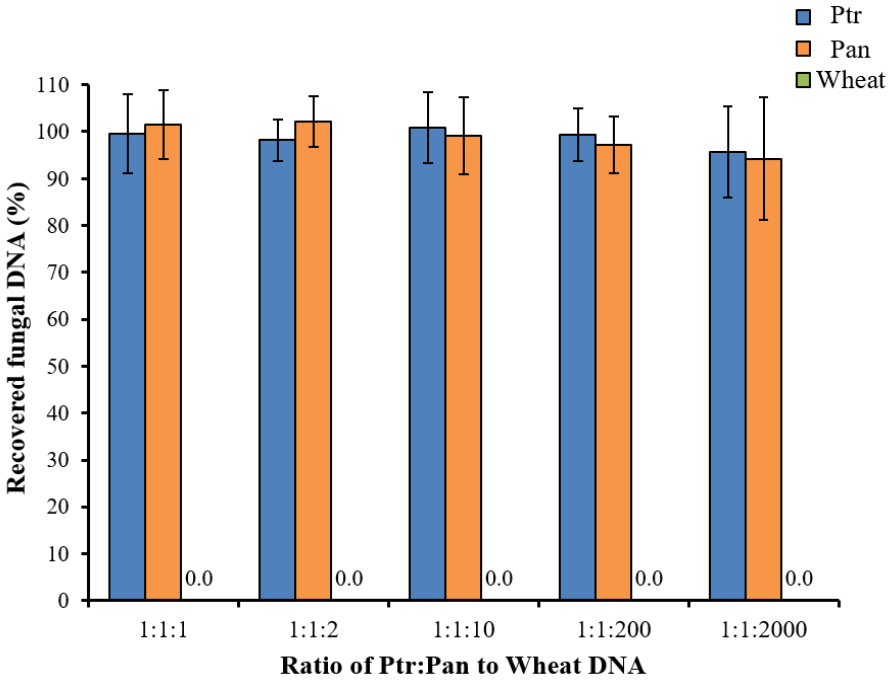

Figure 2.5. Simulated DNA matrix of various ratios of fungi to wheat DNA. Increasing quantities (5 to 100 ng µl-1) of wheat DNA was spiked with decreasing quantities of fungal DNA (5 to 0.05 ng µl-1). Quantification was done using quantitative PCR and reactions were duplexed each containing four fungal-specific primers and two complementary probes (Table 2.1). Data represent means ± standard deviation (*n*=6). Wheat DNA was not quantified/detected hence zero.

2.3.4 Field evaluation of naturally infected plants

Eighteen naturally infected wheat leaves were collected from a site in the southwest of Western Australia (31.74998° N, 116.68289° E). These leaves showed typical symptoms of tan spot with distinct yellow halos and tan chlorotic lesions (Figure 2.6A). No apparent symptoms of septoria nodorum blotch were visible on these leaves. Leaves were split into two groups; one group (*n*=9) was incubated on V8-PDA agar Petri-dishes in an attempt to

characterise the causal agent of the disease. Incubation on agar only yielded colonies typical of Ptr (data not shown).

DNA was extracted from the second leaf group (n=9) and analysed using conventional PCR. Only one out of nine duplicated PCR reactions tested positive to Pan. All reactions were positive to Ptr. DNA from the same leaves, that were used in the conventional PCR, was then analysed using qPCR. The duplex qPCR assay was able to detect signals corresponding to sequences of Ptr and Pan despite the absence of any visible symptoms of Pan on these leaves (Figure 2.6B). There was a good agreement (r=-0.82) between total fungal DNA quantified by qPCR and conventional disease scores that were collected in the field (Figure 2.6B; black circles/line). Conventional disease scores were significantly correlated with the increase in Ptr DNA, and Ptr DNA was a greater contributor to the disease scores than Pan DNA (Figure 2.6B; blue and orange circles/lines).

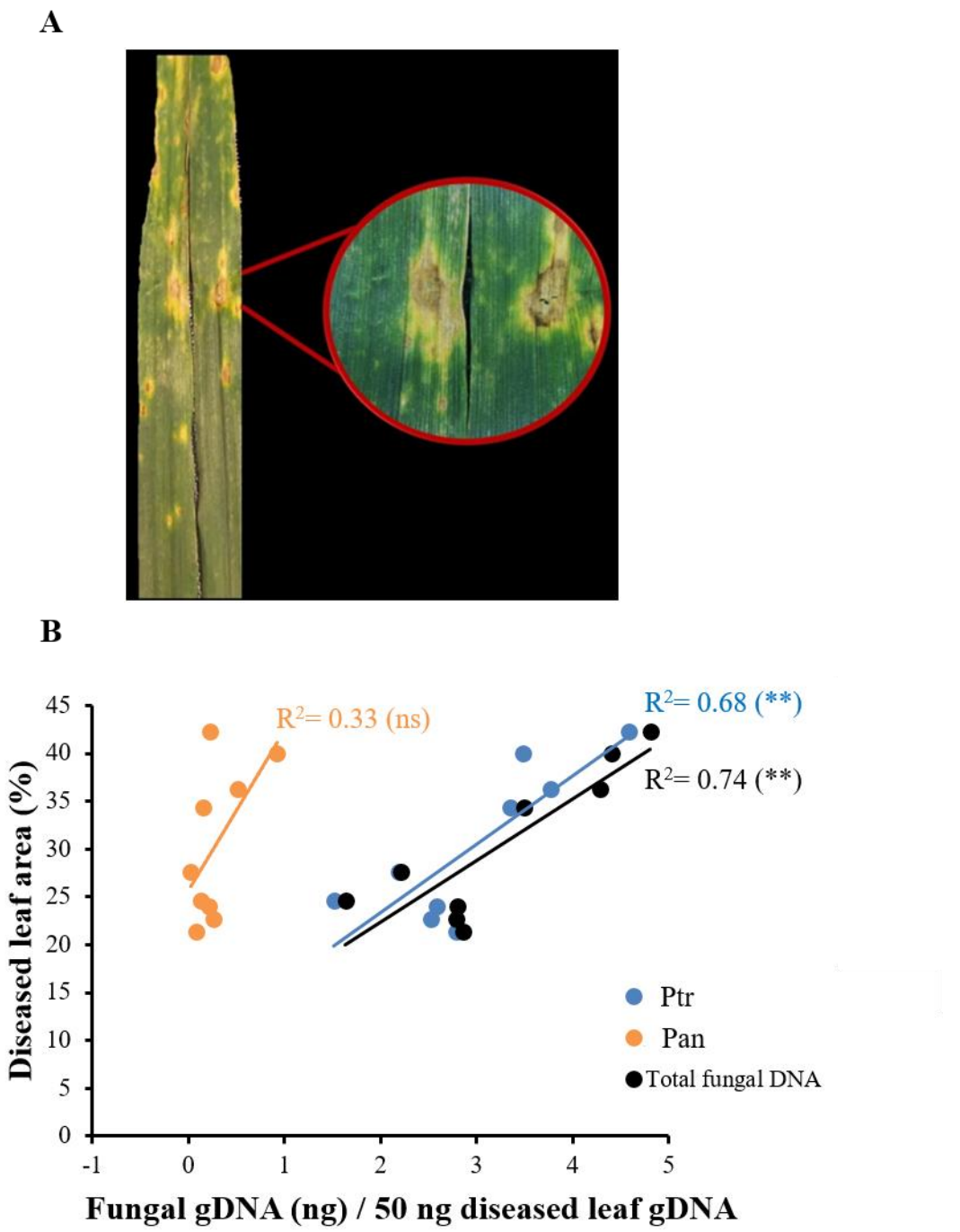

Figure 2.6. Quantification of fungal DNA in naturally infected wheat leaves. (A) Leaves displaying tan spot symptoms with tan necrotic centres and yellow halos. (B) A linear model fitted into the relationship between fungal DNA measured using quantitative PCR and conventional disease score. The corresponding regression equation and coefficient of determination (R2) are shown on the plot. ns and ** refer to not significant and significant ($P < 0.01$), respectively.

2.4 Discussion

Quantification of the relative abundance of co-infecting pathogens requires selection of primers and probes that are compatible with each other whilst distinguishing between the co-infecting species. Recent work has identified a 235-bp multicopy region present in the Ptr genome, and primers designed in this region were able to detect Ptr from wheat leaves, even prior to the visible appearance of tan spot lesions (See et al., 2016). However, these primers cross-hybridised with *Pyrenophora teres* f.sp. *teres*, which the authors suggested may be overcome by the addition of fluorescence-labelled probes in the middle of the amplicon.

In this chapter, primers were chosen to produce relatively smaller amplicons (99-112 bp) that are more efficient for amplifying specific products than longer primers (Bustin et al., 2009). The primers successfully distinguished targeted pathogens from non-target closely related fungal species and host genes. However, for increased specificity, fluorogenic probes were designed to hybridise to sequences within the primers enabling the assay to simultaneously distinguish and quantify DNA associated with Ptr from that associated with Pan. The length of the probes was designed to ensure that stable primer-probe hybrids were formed at the same annealing temperature for both species, irrespective of the length of the primers. Furthermore, probes were labelled with a unique fluorogenic-reporter allowing DNA sequences from Ptr and Pan to be amplified simultaneously but independent of each other. The choice of the fluorogenic reporter was decided based on instrument capability in resolving overlapping spectra. FAM-labelled probes are excited at lower emission spectra than CFG-labelled probes and hence are expected to produce stronger signals. Nevertheless, restricting the concentration of the FAM-labelled probe in the reaction optimised the fraction of the amplicon that is bound to the probe and produced comparable signals for Ptr and Pan. In addition to the fluorogenic reporters, probes were labelled with dark-hole quenchers to inhibit probe signals when probes are free in the solution (Holland et al., 1991). The dark-hole quencher was sufficient to inhibit signals from probes that are not in perfect contact with the target, resulting in accurate species-specific quantifications.

A series of experiments were conducted demonstrating the specificity, efficiency, and reproducibility of this assay for simultaneous detection and quantification of Ptr and Pan. The method reported here resolved two signals each unique to the assayed species. No

cross-amplification with either host plant DNA or DNA from other closely related fungal pathogens of cereals was observed. The assay amplified the targeted sequences with high specificity and was able to detect the presence of Ptr at 0.59 pg μl^{-1} and Pan at 0.36 pg μl^{-1} in mixed fungal DNA matrices. Furthermore, in mixed gDNA matrices of both targeted species, the assay was able to detect fungal signals at a relative abundance as low as 1 in 10000 with ≤10% RSD. Similarly, the assay was able to quantify the presence of Pan DNA down to 23-pg in leaf samples naturally co-infected by abundant Ptr up to 2192-pg. Nonetheless, there was a slight interference to the quantification of the less abundant target when DNA of the other target and/or wheat DNA was highly abundant. This may occur because reaction components including DNA polymerase, dNTPs, and $MgCl_2$ become limiting in later qPCR cycles. The more abundant target may compete for reaction components with the less abundant target, delaying its amplification (Bustin et al., 2009). As a result, the quantification of the less abundant target, although remaining specific and within the detection limit, may be compromised. One way to minimise this interference is to optimise concentrations of reaction components sequentially (Bustin et al., 2009). Regardless, the assay is highly stable and reproducible. The reproducibility was confirmed by the small standard deviations of triplicate samples in the standard curves (≤10%). The amplification curves of replicate runs showed strong overlap indicating stability and reproducibility.

A limitation of most nucleic acid-based assays is an inability to distinguish between DNA from living and dead cells (Pinheiro et al., 2016). Although fungal cell viability was not assessed in this work, the high correlation coefficient, 0.826, especially between Ptr DNA and the conventional disease score, suggests that viability may not have a significant impact on measuring disease as DNA equivalent. Quantification of fungal DNA has been shown to provide accurate measurement of disease severity for Ptr (See et al., 2016) and Pan (Oliver et al., 2008). Another limitation, more specific to qPCR, is that only a few targets can readily be accommodated in a single homogeneous assay. The number of targets that can be fitted in one assay depends on the design of the assay and the ability of the instrument to resolve overlapping spectra. The instrument used in this study has a blue monochromatic laser source for the excitation of fluorophores, and can simultaneously detect five targets on five different channels. This limits the fluorophores that could be efficiently excited by the blue laser to those that are distant from the far-red wavelengths. Instruments with high

resolution-detectors and variable-wavelength light sources may allow more targets to be included in an assay. Instruments with such specifications are available and can be employed for detection and quantification of large-scale screening of co-infection by multiple pathogens.

Detection of multiple pathogens has also been achieved by the use of post-PCR dissociation curve analysis. Such methods use a set of primers with different melting temperatures and G + C contents. Using this technique, up to ten microbial pathogens of humans have been distinguished in a single assay (Gelaye et al., 2017; Jiang et al., 2017). Post-PCR methods, although specific and accommodating several targets in a single assay, do not provide quantitative information on the level of disease. Plant tissues can be inhabited by a large number of pathogenic and non-pathogenic microbes. Nevertheless, infection levels of these microbes and the damage they cause to the plant can vary greatly (Bakker et al., 2014). The assay reported on in this chapter offers several advantages over the dissociation curve analysis and many other methods for diagnosis of co-infection. First, no post-reaction processing is required. Reactions are driven to completion allowing higher levels of sensitivity even when target sequences are present at low concentrations. Second, the assay provides quantitative data on the level of disease load in a sample, which other methods including metagenome sequencing do not offer. Finally, the cost-effectiveness, although not directly estimated, of testing multiple agents in a single test allows more testing using the same amount of reagents and staff time. When coupled with a 96-well capacity, this assay offers a sensitive and quantitative high throughput methodology for detection of co-infection by Ptr and Pan in wheat plants. The method can also be used to study the epidemiological consequences of co-infection by Ptr and Pan in the field.

References

Abdullah, A. S. A., Moffat, C., Lopez Ruiz, F. J. L., Gibberd, M. G., Hamblin, J., and Zerihun, A. Z. (2017). Host-multi-pathogen warfare: pathogen interactions in co-infected plants. *Frontiers in Plant Science* **8:1806**, 1-12.

Alizon, S., de Roode, J. C., and Michalakis, Y. (2013). Multiple infections and the evolution of virulence. *Ecology Letters* **16**, 556-567.

Armbruster, D. A., and Pry, T. (2008). Limit of blank, limit of detection and limit of quantitation. *The Clinical Biochemist Reviews* **29 (Suppl 1)**, S49-S52.

Atallah, Z., Bae, J., Jansky, S., Rouse, D., and Stevenson, W. (2007). Multiplex real-time quantitative PCR to detect and quantify *Verticillium dahliae* colonization in potato lines that differ in response to Verticillium wilt. *Phytopathology* **97**, 865-872.

Bakker, M. G., Schlatter, D. C., Otto-Hanson, L., and Kinkel, L. L. (2014). Diffuse symbioses: roles of plant-plant, plant-microbe and microbe-microbe interactions in structuring the soil microbiome. *Molecular Ecology* **23**, 1571-1583.

Barbisin, M., Fang, R., O'Shea, C. E., Calandro, L. M., Furtado, M. R., and Shewale, J. G. (2009). Developmental validation of the Quantifiler® Duo DNA quantification kit for simultaneous quantification of total human and human male DNA and detection of PCR inhibitors in biological samples. *Journal of Forensic Sciences* **54**, 305-319.

Bates, J., Taylor, E., Kenyon, D., and Thomas, J. (2001). The application of real-time PCR to the identification, detection and quantification of *Pyrenophora* species in barley seed. *Molecular Plant Pathology* **2**, 49-57.

Bernreiter, A. (2017). Molecular diagnostics to identify fungal plant pathogens–a review of current methods. *Ecuador Se Calidad-Revista Científica Ecuatoriana* **4**, 26-35.

Bhathal, J., Loughman, R., and Speijers, J. (2003). Yield reduction in wheat in relation to leaf disease from yellow (tan) spot and septoria nodorum blotch. *European Journal of Plant Pathology* **109**, 435-443.

Blixt, E., Olson, A., Lindahl, B., Djurle, A., and Yuen, J. (2010). Spatiotemporal variation in the fungal community associated with wheat leaves showing symptoms similar to stagonospora nodorum blotch. *European Journal of Plant Pathology* **126**, 373-386.

Brandfass, C., and Karlovsky, P. (2006). Simultaneous detection of *Fusarium culmorum* and *F. graminearum* in plant material by duplex PCR with melting curve analysis. *BMC Microbiology* **6:4**, 1-10.

Bustin, S. A., Benes, V., Garson, J. A., Hellemans, J., Huggett, J., Kubista, M., Mueller, R., Nolan, T., Pfaffl, M. W., and Shipley, G. L. (2009). The MIQE guidelines: minimum information for publication of quantitative real-time PCR experiments. *Clinical Chemistry* **55**, 611-622.

DAFWA (2016). Wheat variety guide for Western Australia. *Department of Agriculture and Food Western Australia.* **Online publication. www.agric.wa.gov.au/cropdisease.**

Friesen, T. L., Stukenbrock, E. H., Liu, Z., Meinhardt, S., Ling, H., Faris, J. D., Rasmussen, J. B., Solomon, P. S., McDonald, B. A., and Oliver, R. P. (2006). Emergence of a new disease as a result of interspecific virulence gene transfer. *Nature Genetics* **38**, 953-959.

Gelaye, E., Mach, L., Kolodziejek, J., Grabherr, R., Loitsch, A., Achenbach, J. E., Nowotny, N., Diallo, A., and Lamien, C. E. (2017). A novel HRM assay for the simultaneous detection and differentiation of eight poxviruses of medical and veterinary importance. *Scientific Reports* **7**, 1-12.

Holland, P. M., Abramson, R. D., Watson, R., and Gelfand, D. H. (1991). Detection of specific polymerase chain reaction product by utilizing the 5'----3'exonuclease activity of *Thermus aquaticus* DNA polymerase. *Proceedings of the National Academy of Sciences of the United States of America* **88**, 7276-7280.

Hood, M. (2003). Dynamics of multiple infection and within-host competition by the anther-smut pathogen. *The American Naturalist* **162**, 122-133.

Jiang, Y., He, L., Wu, P., Shi, X., Jiang, M., Li, Y., Lin, Y., Qiu, Y., Bai, F., and Liao, Y. (2017). Simultaneous identification of ten bacterial pathogens using the multiplex ligation reaction based on the probe melting curve analysis. *Scientific Reports* **7:5902**, 1-9.

Klerks, M., Zijlstra, C., and Van Bruggen, A. (2004). Comparison of real-time PCR methods for detection of *Salmonella enterica* and *Escherichia coli* O157: H7, and introduction of a general internal amplification control. *Journal of Microbiological Methods* **59**, 337-349.

Moffat, C., See, P. T., and Oliver, R. (2015). Leaf yellowing of the wheat cultivar Mace in the absence of yellow spot disease. *Australasian Plant Pathology* **44**, 161-166.

Moolhuijzen, P., See, P. T., Hane, J. K., Shi, G., Liu, Z., Oliver, R. P., and Moffat, C. S. (2018). Comparative genomics of the wheat fungal pathogen *Pyrenophora tritici-repentis* reveals chromosomal variations and genome plasticity. *BMC genomics* **19**, 279.

Oliver, R. P., Rybak, K., Shankar, M., Loughman, R., Harry, N., and Solomon, P. (2008). Quantitative disease resistance assessment by real-time PCR using the *Stagonospora nodorum*-wheat pathosystem as a model. *Plant Pathology* **57**, 527-532.

Pinheiro, E. T., Neves, V. D., Reis, C. C., Longo, P. L., and Mayer, M. P. (2016). Evaluation of the propidium monoazide–quantitative polymerase chain reaction method for the detection of viable *Enterococcus faecalis*. *Journal of Endodontics* **42**, 1089-1092.

Rojas, J. A., Miles, T. D., Coffey, M. D., Martin, F. N., and Chilvers, M. I. (2017). Development and application of qPCR and RPA genus-and species-specific detection of *Phytophthora sojae* and *P. sansomeana* root rot pathogens of soybean. *Plant Disease* **101**, 1171-1181.

Savary, S., and Zadoks, J. (1992). Analysis of crop loss in the multiple pathosystem groundnut-rust-late leaf spot. *Crop Protection* **11**, 229-239.

Schena, L., Hughes, K. J., and Cooke, D. E. (2006). Detection and quantification of *Phytophthora ramorum*, *P. kernoviae*, *P. citricola* and *P. quercina* in symptomatic leaves by multiplex real-time PCR. *Molecular Plant Pathology* **7**, 365-379.

Schoch, C. L., Seifert, K. A., Huhndorf, S., Robert, V., Spouge, J. L., Levesque, C. A., Chen, W., Bolchacova, E., Voigt, K., and Crous, P. W. (2012). Nuclear ribosomal internal transcribed spacer (ITS) region as a universal DNA barcode marker for Fungi. *Proceedings of the National Academy of Sciences of the United States of America* **109**, 6241-6246.

See, P. T., Moffat, C. S., Morina, J., and Oliver, R. P. (2016). Evaluation of a multilocus Indel DNA region for the detection of the wheat tan spot pathogen *Pyrenophora tritici-repentis*. *Plant Disease* **100**, 2215-2225.

Tack, A. J., Thrall, P. H., Barrett, L. G., Burdon, J. J., and Laine, A. L. (2012). Variation in infectivity and aggressiveness in space and time in wild host-pathogen systems: causes and consequences. *Journal of Evolutionary Biology* **25**, 1918-1936.

Tollenaere, C., Susi, H., and Laine, A.-L. (2016). Evolutionary and epidemiological implications of multiple infection in plants. *Trends in Plant Science* **21**, 80-90.

Tollenaere, C., Susi, H., Nokso-Koivisto, J., Koskinen, P., Tack, A., Auvinen, P., Paulin, L., Frilander, M. J., Lehtonen, R., and Laine, A.-L. (2012). SNP design from 454 sequencing of *Podosphaera plantaginis* transcriptome reveals a genetically diverse pathogen metapopulation with high levels of mixed-genotype infection. *Plos One* **7**, e52492.

Zadoks, J. (1999). Reflections on space, time, and diversity. *Annual Review of Phytopathology* **37**, 1-17.

3 Prevalence of Ptr and Pan Co-infection in Wheat Fields of Western Australia[III]

Abstract

The pathogenic fungal species *Pyrenophora tritici-repentis* (Ptr) and *Parastagonospora nodorum* (Pan) are common in many wheat-producing regions of the world. These two fungi cause tan spot and septoria nodorum blotch, respectively, frequently co-infecting wheat leaves. Empirical studies of this, and other co-infections, are rare because of the visual similarity in symptoms and the lack of robust methods for quantifying the relative abundance of pathogens associated with the co-infection. This chapter uses the qPCR method developed in chapter 2 to investigate the prevalence of co-infection by Ptr and Pan at three field sites and on three wheat cultivars varying in disease resistance. Co-infection by Ptr and Pan was almost ubiquitous (overall prevalence 94%) and Pan DNA was only detected in association with Ptr. While Ptr and Pan commonly co-infected, Ptr was more abundant early and mid-season, 80 and 67% of total fungal abundance, respectively, when crops were tillering and booting. Pan became equally abundant to Ptr when crops reached flowering. Variability in total fungal abundance and disease severity was primarily determined by cultivar; although Ptr was the most abundant pathogen despite differences in cultivar resistance to this pathogen.

[III]This chapter was published in February 2020: Abdullah, Gibberd, M. R., and Hamblin, J. Co-infection of wheat by *Pyrenophora tritici-repentis* and *Parastagonospora nodorum* in the wheatbelt of Western Australia. Crop and Pasture Science 71(2) | doi.org/10.1071/CP19412

Authors' contribution: Araz Abdullah conceived the idea of the research, collected and analysed the samples, performed the data analysis and drafted the manuscript. Mark Gibberd and John Hamblin supervised the work and provided critical suggestions on the article. All authors read and approved the final version of the article.

3.1 Introduction

There is emerging recognition that wheat plants are naturally co-infected by multiple pathogen species or genotypes. For example, genetically diverse populations of the obligate biotroph *Puccinia striiformis* f. sp. *tritici* were found co-infecting leaves of wheat crops grown across the UK (Hubbard et al., 2015). Similarly, widespread co-infection of wheat by foot and crown rots, caused by multiple *Fusarium* spp. has been reported in Poland (Kuzdralinski et al., 2014) and co-infection of wheat by *Septoria tritici* and *Septoria nodorum* was found to be common in several areas within the USA (Shaner and Buechley, 1995). Despite the common occurrence and significance of co-infection, studies targeting these interacting infections are rare (Abdullah et al., 2017; Savary and Zadoks, 1992; Tack et al., 2012; Zadoks, 1999).

Pyrenophora tritici-repentis (Ptr) and *Parastagonospora nodorum* (Pan) are amongst the most common necrotrophic fungal pathogens of wheat causing the diseases tan spot (TS) and septoria nodorum blotch (SNB), respectively. These fungi commonly infect leaves and cause yield losses by reducing leaf area available for photosynthesis (Bhathal et al., 2003; Johnson, 1987; Salam et al., 2013). Symptoms caused by these fungi are foliar necrosis, chlorosis or both and symptoms are often difficult to distinguish visually (Abdullah et al., 2018). Symptoms can also be confused as other wheat diseases (Blixt et al., 2010), further complicating accurate disease diagnosis. The infection process of Ptr and Pan is primarily determined by the secretion of necrotrophic effectors or host-selective toxins. These facilitate *in planta* growth of these pathogens by triggering cell death in wheat cultivars carrying matching sensitivity genes (Ciuffetti et al., 2010; Pandelova et al., 2009; Solomon et al., 2006). Interestingly, Ptr possesses a potent toxin, *ToxA*, the gene encoding this toxin is thought to have been inter-specifically transferred from Pan (Friesen et al., 2006). Sharing such a pathogenicity gene suggests that co-infection of wheat leaves by these two species is probable. Nonetheless, the occurrence scale of such co-infection and its effect on disease severity in the field have not been previously quantified and reported.

The main objective of this chapter was to investigate the prevalence of co-infection by two common and destructive fungal pathogens, Ptr and Pan, in naturally infected wheat fields. The chapter explores temporal patterns of fungal abundance and corresponding disease severity across three sites in the main wheat-growing area of Western Australia. Three

wheat cultivars, of varying resistance ratings, were examined in this study, and the chapter used the qPCR method developed in the previous chapter (Abdullah et al., 2018). Results suggest that Ptr and Pan coexist widely in infected wheat leaves. Molecular evidence suggests temporal differences in the relative abundance of these two species and fungal DNA abundance appeared to be a reliable predictor of overall disease severity.

3.2 Materials and methods

3.2.1 Field sites and sampling

Field studies were conducted between May and October 2016 at three sites in the main wheat-growing area of Western Australia. Sites were located on commercial properties at Mingenew (29°11′38″S, 115°26′28″E), Muresk (31°44′57″S, 116°41′02″E) and Wagin (33°19′00″S, 117°21′00″E). Sites were grown to wheat for the previous two years. At each site, three wheat (*Triticum aestivum*) cultivars, Emu Rock, Yitpi and Magenta, were evaluated. These were selected to provide varying level of genetic resistance backgrounds to the targeted diseases (Table 3.1). Wheat seeds, 190 to 200 seeds m^{-2}, were planted in plots containing the preceding season's wheat stubble, cultivar Scout, to promote natural infection. Scout is susceptible to very susceptible to the diseases caused by Ptr and Pan and is known to support Ptr-Pan co-infection (Abdullah et al., 2018). At each site, plots were 1.44 m x 12 m and identical Scout buffer plots were planted between each trial plot. Trials were set up in a randomised complete block design with three blocks and the full set of cultivars assigned in each block at random. Site management including fertilisation, herbicide and insecticide applications were consistent across sites.

Table 3.1. Disease resistance rating (DAFWA 2016) for the wheat cultivars used in this study.

Cultivar	Disease resistance rating*	
	Tan spot (Ptr)	Septoria nodorum blotch (Pan)
Emu Rock	MR/MS	S/VS
Yitpi	S/VS	MS
Magenta	MR	MR/MS

*MR/MS = moderately resistance to moderately susceptible. S/VS = susceptible to very susceptible. MR = moderately resistance. MS = moderately susceptible.

Plants were sampled at Zadoks growth stages (Zadoks et al., 1974) 24-26, 36-39 and 55-62 in Muresk and Wagin and at 36-39 and 55-62 in Mingenew. At each sampling event, fully unfolded and non-senescent leaves were collected from nine randomly selected plants of each wheat cultivar. Two leaves were sampled from each of the selected plants from the upper and the lower-canopy position. Samples from the two canopy positions were kept separate to assess the effect of canopy position on infection prevalence. Sampled leaves were visually scored for percentage of diseased leaf area (necrotic and chlorotic); no distinction was made between TS and SNB lesions. After scoring, leaves were excised using sterile scissors and forceps and individually stored in microtubes (2 ml volume). Immediately after collection, samples were placed on dry ice for transport to the laboratory and then stored at -80˚C until DNA was extracted. When sampling across cultivars and replicates, scissors and forceps were sterilised in 10% sodium hypochlorite (4% chlorine) to prevent cross-contamination.

3.2.2 DNA extraction and quantification

DNA was extracted using a Bio-sprint 15 plant DNA kit (Qiagen) following the manufacturer's protocol. Leaf samples were ground into a fine powder in liquid nitrogen. Sub-samples (40 mg) of ground leaf tissue were placed into 1.5 ml microtubes for DNA extraction as described previously (Abdullah et al., 2018). DNA concentration was determined using a NanoDrop 2000 UV-Vis spectrophotometer (Thermo Scientific) and confirmed with fluorescent dye thiazole orange (Nygren et al., 1998). Extracted DNA was diluted to a 50 ng μl^{-1} working solution with ultrapure, PCR-grade water. DNA samples were stored at -20˚C until required. Throughout the extraction and quantification of DNA, aerosol barrier filter tips were used to prevent cross-contamination. Pure genomic DNA, for constructing standard curves, was extracted from fungal colonies using the DNA kit described above. Fungal cultures were maintained on V8-PDA agar plates as described elsewhere (Moffat et al., 2015; Pijls et al., 1994). Mycelia from these cultures were harvested, finely ground in liquid nitrogen and used for DNA extraction.

3.2.3 Detection and quantification of fungal DNA

This study used a qPCR assay that simultaneously distinguishes and quantifies the presence of Ptr and Pan (Abdullah et al., 2018). Briefly, the assay utilises a set of four molecular primers and two matching probes. Primers and probes target unique genomic sequences

within each targeted species. Conservation of the sequences across various isolates of the targeted species was evaluated by aligning the sequence of interest against available genome sequences of the pathogens. Probes were incorporated in the middle of each sequence of interest to increase detection specificity and allow duplexing (Abdullah et al., 2018; Timken et al., 2005). Probes were also differentially tagged with fluorophores so that both species can be quantified simultaneously but detected independently on different channels of the qPCR machine. Reactions were carried out in a 20-µl volume of 96-well reaction plates (capped MicroAmp Optical, Applied Biosystems) on a CFX96 real-time PCR detection system (Bio-Rad). Regression equations for each target were constructed from a 10-fold dilution series (100, 10, 1, 0.1 and 0.01 ng μl^{-1}) containing an equal abundance of DNA from both fungal species. The resulting equations were then used to convert quantification cycles to equivalent DNA concentrations in unknown samples (Abdullah et al., 2018). Sterile water controls were below threshold detection limits and hence were negative while samples spiked with various concentrations of fungal DNA were positive. All reactions were run with three technical repeats and samples that gave positive fluorescence before no-template controls were considered positive.

3.2.4 Data analysis

The limit of detection (LoD, Ptr=0.64 pg μl^{-1}; Pan=0.42 pg μl^{-1}), the lowest concentration at which reliable detection could be achieved with the qPCR method, was used to convert fungal DNA concentrations into a binary variable (co-infected or non-co-infected). Samples that gave positive DNA detection for both pathogens were defined as co-infected. All other samples (i.e. below the LoD or infected by one of the pathogen species only) were pooled together and categorised as not co-infected. Using Pearson chi-square statistic, these data were used to test whether the prevalence of co-infection was similar across sites, cultivars, crop developmental stages and leaves (upper or lower) from which the samples were collected.

Pathogen relative abundance in the co-infected samples was analysed as the proportion of Ptr or Pan to the total fungal DNA in the co-infected samples. Changes in the proportions across sites and cultivars were examined using analysis of variance (ANOVA). Normality of the residual was assessed, visually and statistically, using the Shapiro-Wilk test (Shapiro and Wilk, 1965). Fungal DNA abundance and disease severity data were right-skewed;

these were Log_{10}-transformed to comply with the ANOVA assumptions. Where a factor (i.e. site, cultivar or crop developmental stage) or an interaction showed an effect on relative abundance, the least significant difference value at P=0.05 was used for mean separation. Partial correlation analysis was used to assess the magnitude of the association between visual disease severity and abundance of Ptr and Pan while controlling for the association of the other pathogen. The analysis was done using GenStat 17th edition.

3.3 Results

3.3.1 Co-infection by Ptr and Pan was almost ubiquitous, but Pan DNA was only detected in co-infected leaves

Disease incidence, as determined by the positive detection of one or both pathogens by the qPCR, was >99% across sites and cultivars. Co-infection by Ptr and Pan was highly prevalent and found on 94% of the samples collected (Table 3.2). Of these, all lower leaves were co-infected whilst 87.5% of the upper leaves were co-infected. Prevalence of co-infection was independent of cultivar disease resistance ratings, and the frequency of co-infection by Ptr and Pan was similar across all varieties (χ^2=5.0, P=0.1, df=2).

The concentration of Ptr DNA in the co-infected samples averaged around 7 ng per 40 mg leaf tissue, which was 1.9-fold the DNA found in samples infected by Ptr alone (n=9). Ptr DNA (i.e. single pathogen) was detected in 14% of the samples in Mingenew and 5.6% of the samples in Wagin (Table 3.2). Samples from Muresk were all co-infected, and disease incidence on these samples was 100%. Across all sites, when detected, Pan DNA was only detected in association with Ptr. None of the samples tested positive for Pan DNA on its own as a single pathogen (Table 3.2).

Table 3.2. Disease incidence and prevalence of co-infection in leaves as determined by qPCR on three wheat varieties grown at three locations in Western Australia in 2016. Figures in parentheses represent the number of samples averaged across crop growth stages and canopy positions. The uninfected category denotes samples for which Ptr and Pan DNA were below the limits of detection of the qPCR method.

Site	Cultivar	Disease incidence (%)	Percentage of samples			
			Uninfected	Ptr only	Pan only	Co-infected
Mingenew	Emu Rock	100	0 (0)	33.3 (4)	0 (0)	66.6 (8)
	Magenta	100	0 (0)	0 (0)	0 (0)	100 (12)
	Yitpi	100	0 (0)	8.3 (1)	0 (0)	91.6 (11)
Muresk	Emu Rock	100	0 (0)	0 (0)	0 (0)	100 (18)
	Magenta	100	0 (0)	0 (0)	0 (0)	100 (18)
	Yitpi	100	0 (0)	0 (0)	0 (0)	100 (18)
Wagin	Emu Rock	100	0 (0)	5.6 (1)	0 (0)	94.4 (17)
	Magenta	94.4	5.6 (1)	11.1 (2)	0 (0)	83.3 (15)
	Yitpi	100	0 (0)	0 (0)	0 (0)	100 (18)

3.3.2 Relative abundance of Ptr and Pan was dynamic throughout the season and influenced by site, host genotype and growth stage of the crop

Disease severity and fungal DNA abundance increased as the season progressed and the crop developed (Figure 3.1A, B). Disease severity on lower leaves was generally greater than upper leaves (fungal DNA mean ± s.e. were 4.5±0.61 and 1.0±0.30 ng per 40 mg leaf tissue, respectively). Variation in disease severity and fungal DNA abundance were mostly influenced by site, host cultivar and growth stage of the crop. The most diseased sites were Mingenew and Muresk; the least diseased site was Wagin (Figure 3.1A, B). Leaves collected from the host varieties Emu Rock and Yitpi were consistently more diseased (fungal DNA was 3.29±0.69 and 4.63±0.84 ng per 40 mg leaf tissue, respectively) than Magenta leaves (fungal DNA was 0.23±0.12 ng per 40 mg leaf tissue).

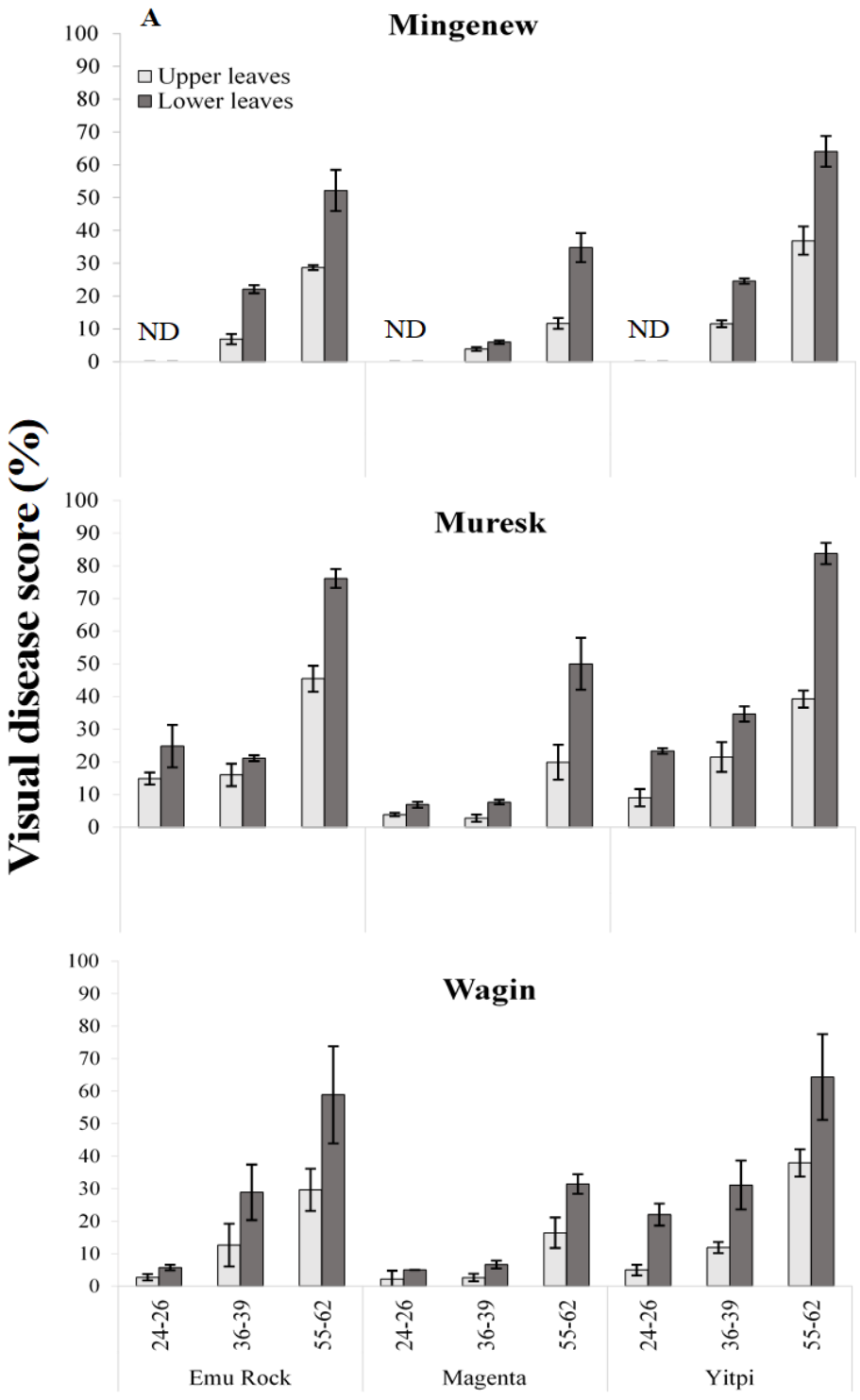
A
Mingenew
Upper leaves
Lower leaves
ND
ND
ND
Muresk
Wagin
Visual disease score (%)
24-26
36-39
55-62
Emu Rock
Magenta
Yitpi

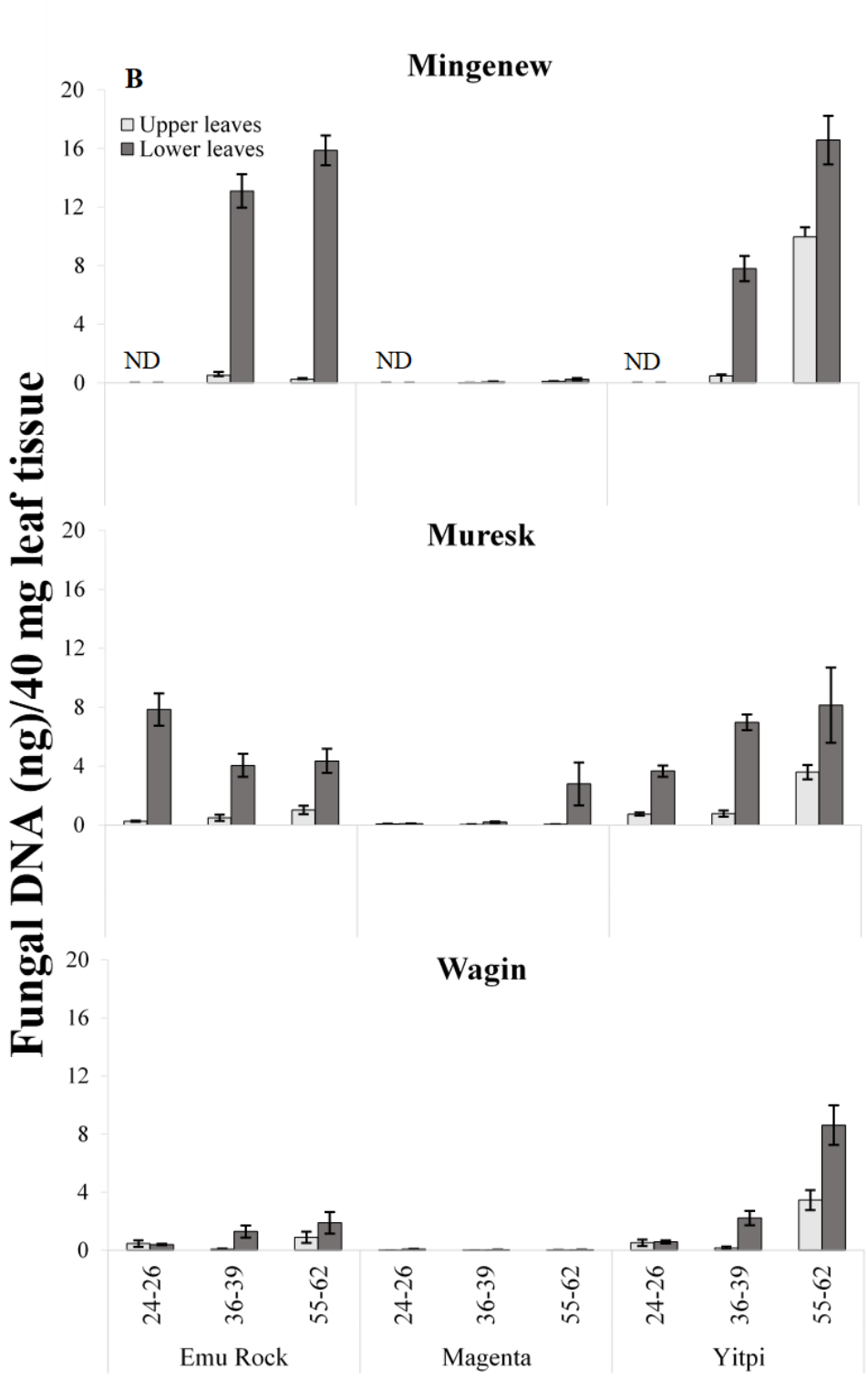

Figure 3.1. Disease dynamics of naturally infected wheat fields across three sites and three cultivars. (A) Percentage of visual disease severity measured on a 0-100 scale. (B) Total fungal DNA measured by the qPCR method. Growth stages are based on Zadocks decimal

code for cereals (Zadoks et al. 1974). Data are means ± standard errors. ND refers to no data.

At the Mingenew site, Ptr DNA was more abundant, than Pan DNA, in samples collected from both upper and lower leaves (Figure 3.2). At Wagin, Ptr DNA was generally more abundant early in the season, but Pan became equally or more abundant towards mid to late season. At the Muresk site, both pathogens had similar relative abundances (Figure 3.2). Ptr DNA on leaves collected from Emu Rock and Yitpi constituted 75% and 67% of the total fungal DNA, respectively. Pan DNA was equally abundant (58%; $P>0.05$) as Ptr DNA on leaves collected from Magenta (Figure 3.2). The abundance of DNA associated with Ptr was 2 to 4-fold higher than Pan DNA early and mid-season (growth stages 24 and 39) on both upper and lower leaves (Figure 3.2). Pan DNA only made up 20% and 33% of total fungal DNA between growth stages 24 and 39, respectively. The proportion of Pan DNA increased throughout the season and by growth stage 55-62, Ptr and Pan DNA were at parity ($P>0.05$) on both upper and lower leaves in Muresk and Wagin (Figure 3.2).

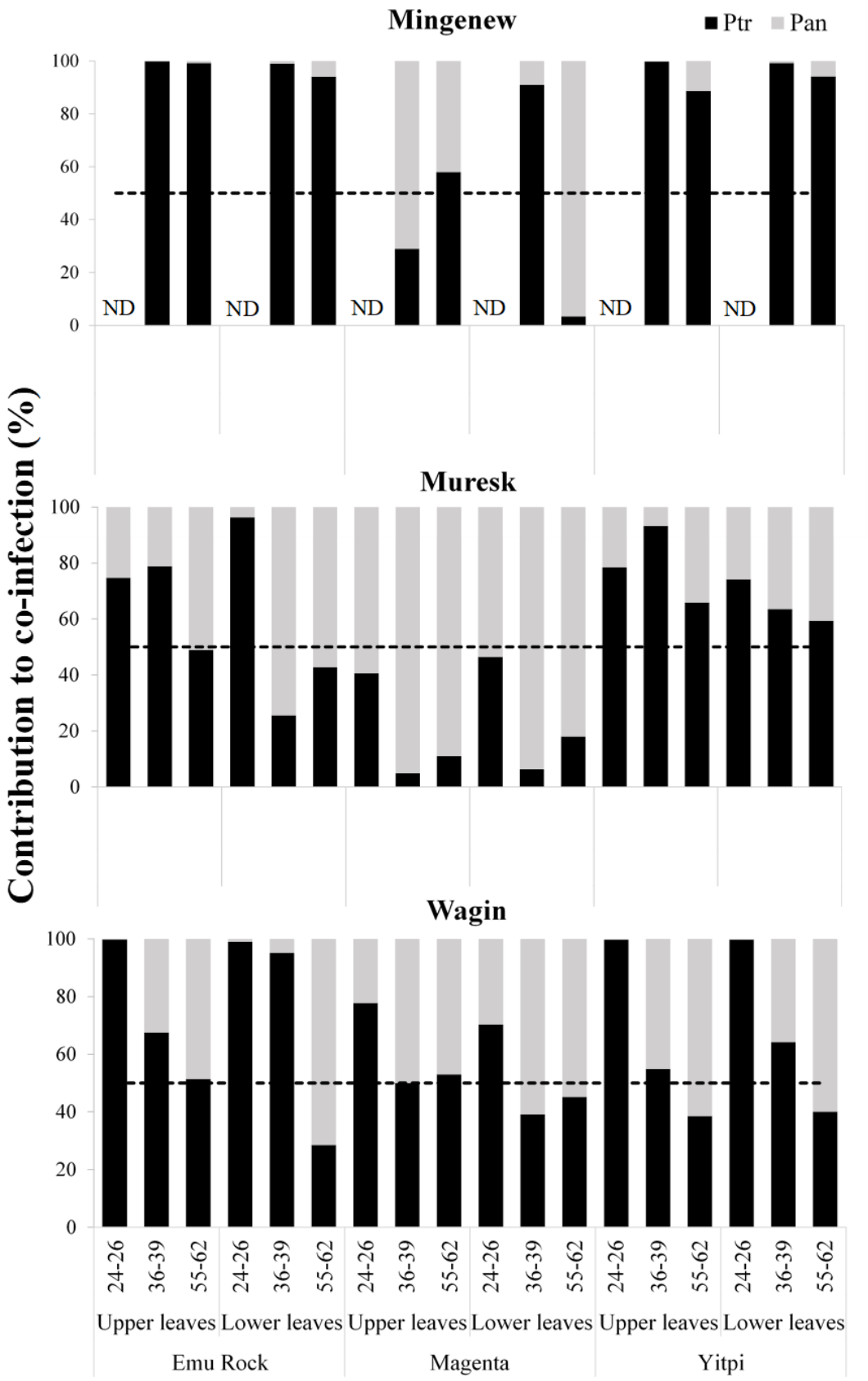
Mingenew
Ptr
Pan
Muresk
Wagin
Contribution to co-infection (%)
100
80
60
40
20
0
ND
24-26
36-39
55-62
Upper leaves
Lower leaves
Emu Rock
Magenta
Yitpi

Figure 3.2. Dynamics of Ptr and Pan DNA contribution to the total fungal DNA in co-infected samples collected from upper leaves and lower leaves. Data are the percentage contribution of Ptr and Pan to total fungal DNA in the co-infected leaves. ND refers to no data. The dotted black line is the line of parity.

3.3.3 Fungal DNA abundance is a reliable predictor of disease severity

Variation in total fungal abundance, DNA of both Ptr and Pan measured by qPCR, in samples explained 54% of the observed visual disease damage over the three growth stages (log-log $P<0.05$). Total fungal DNA abundance significantly increased as the crops developed (Figure 3.3). Across sites, the linear model based on total fungal DNA accounted for a more significant proportion of the variance (69%) in visual disease score at crop growth stage 36-39 (Figure 3.3B) than at the other stages (Figure 3.3A, C).

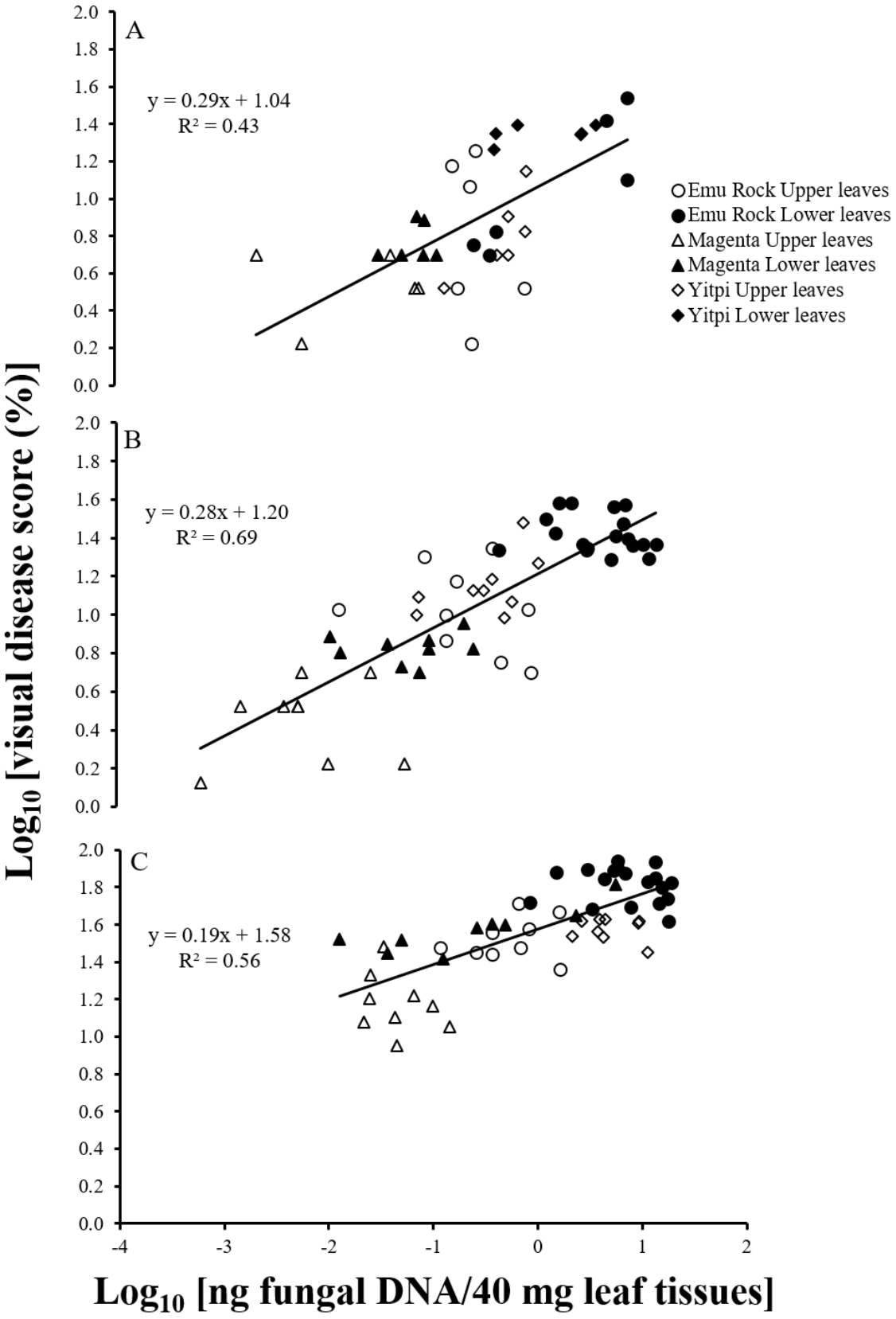
A
y = 0.29x + 1.04
R² = 0.43
B
y = 0.28x + 1.20
R² = 0.69
C
y = 0.19x + 1.58
R² = 0.56
Emu Rock Upper leaves
Emu Rock Lower leaves
Magenta Upper leaves
Magenta Lower leaves
Yitpi Upper leaves
Yitpi Lower leaves
Log10 [visual disease score (%)]
Log10 [ng fungal DNA/40 mg leaf tissues]

Figure 3.3. Linear relationship between visual disease scores measured in the field and total fungal DNA abundance measured on leaf samples from the same plants with qPCR. Data combine all locations for (A) growth stage 24-26, (B) growth stage 36-39 and (C) growth stage 55-62.

The strength of the relationship between the abundance of Ptr and Pan DNA with visual disease score was assessed for each growth stage and each canopy position (Figure 3.4). For this analysis, data from the three sites were combined. The strength of the association of the DNA abundance of the two pathogens and visual disease scores varied with the growth stage of the crops and canopy position from where leaves were collected. Early in the season (growth stage 24-26), DNA abundance of Pan showed significant partial correlations with visual disease scores for samples from upper leaves (Figure 3.4). However, for samples from lower leaves at the same growth stages, the DNA abundance of Ptr had a higher partial correlation with the visual disease scores than that of Pan (Figure 3.4). As the crop developed (growth stage 36-39), visual disease scores were more strongly associated with the DNA abundance of Ptr than Pan on lower leaves (Figure 3.4). As crops reached flowering (growth stage 55-62), Ptr continued its dominance except on the lower leaves where the DNA abundance of Ptr and Pan had a similar magnitude on the observed visual disease scores (Figure 3.4).

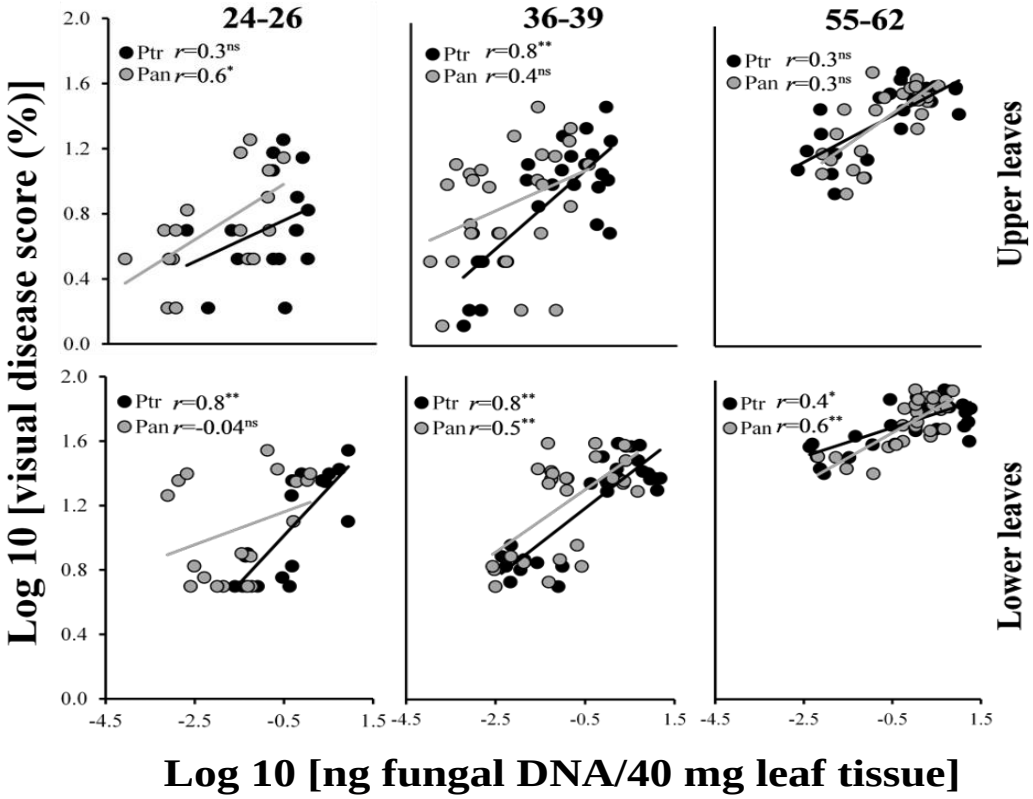

Figure 3.4. Relationship between fungal DNA abundance for Ptr and Pan determined by qPCR and visual disease scores of leaves assessed in-field for three growth stages for upper leaves and lower leaves. Plots combine data for host genotypes and site location. Partial correlation coefficients (*r*) are shown on the plots. *, ** and ns refer to significant at ≤0.05, significant at <0.05, and not significant, respectively (ANOVA).

3.4 Discussion

This chapter investigated the occurrence of co-infection by Ptr and Pan across three naturally infected wheat fields and three wheat cultivars varying in their resistance ratings to both diseases. Ptr and Pan cause similar disease symptoms and are often difficult to distinguish visually (Abdullah et al., 2018). However, analysis of fungal abundance using the qPCR method suggests that co-infection of wheat by Ptr and Pan is widespread and likely to be a common phenomenon. Other fungal pathogens, such as the ascomycete *Zymoseptoria tritici* (Desm.) causing septoria tritici blotch (STB), are also known to occur with Ptr and Pan. Comprehensive analysis of the fungal community that can occur with Ptr

and Pan is reported elsewhere (Blixt et al., 2010). While STB epidemics pose a significant threat to many wheat-growing regions (Stukenbrock et al., 2006; Suffert et al., 2011), its impact on wheat in Australia is limited and is not thought to be a disease of significance in Western Australia (Murray and Brennan, 2009). The focus on Ptr and Pan reflects their relative impact on wheat industry and widespread occurrence in Western Australian (Murray and Brennan, 2009).

Ptr DNA abundance within samples collected early in the season was greater than Pan DNA abundance. This may have resulted from differences between Ptr and Pan in ascospore maturation and timing of primary infection or growth response to the prevailing weather conditions or rates of re-infection or combinations of these. In the wheatbelt of Western Australia, the timing of Ptr ascopore release vary geographically and seasonally (Galloway et al., 2017). Nonetheless, at a given site, it is likely that some overlap occurs with Pan ascospore release periods since ascospore releases of both pathogens occur over several weeks coinciding with the early crop growth stages (Bathgate and Loughman, 2001; Galloway et al., 2017). However, at the earliest sampling time, in this study, plants were between mid- and late-tillering (growth stage 24-26). Therefore, it was not possible to determine whether ascospore maturation and subsequent onset of Ptr and Pan primary infection differed and contributed to the observed difference in the relative abundances. Nonetheless, due to the stubble-born nature of Ptr and Pan, management of stubble is likely to have an impact on the inoculum of both pathogens. On the other hand, the increased abundance of Pan later in the season can have a potential impact on yield by reducing photosynthesis of leaves that contribute directly to grain filling. Disease management tactics must then protect heads and flag leaves during the grain-filling period. This indicates the use of targeted mid/late-season fungicide application, especially when yield potential is high and conditions are conducive for SNB epidemics, will be beneficial.

In Mediterranean climates, ascospores of Ptr and Pan over-summer on stubble and previous season crop debris. Ascospores initiate the infection and can transmit the disease to asymptomatic leaves and neighbouring crops (Bathgate and Loughman, 2001). The position of ascospores on the stubble may contribute to separation in time of ascospore release. The lower parts of the standing stubble are close to the soil and thus more likely to have higher moisture content than the upper portions that are further away from the soil.

Since sufficient moisture is a requirement for Ptr ascospore release (Bathgate and Loughman, 2001; Bhathal et al., 2003), this suggests that the disease expression of TS would occur on lower leaves early in the season. However, data presented in this chapter showed no evidence of apparent vertical stratification and both upper and lower leaves had similar disease scores and Ptr abundance. Differences in weather conditions experienced at each site may have contributed to the early onset of TS as Ptr grows actively at low temperatures while Pan grows faster as temperatures increase late in the season (Bathgate and Loughman, 2001). Climate conditions experienced at each site in 2016 can be obtained from the Bureau of Meteorology (http://www.bom.gov.au/climate/data/). GPS locations, page 54, can be used to locate the nearest weather station. While, climate conditions are known to affect disease development, studying the extent of this effect would require extensive sampling regime and larger spatiotemporal coverage. Such coverage was outside the scope of this study but would warrant an entire PhD project on its own.

This chapter also sought to evaluate whether cultivar disease resistance rating influences the prevalence of Ptr-Pan co-infection. Cultivars were chosen to provide varying levels of resistance to one or both diseases. Regardless of the resistance level of the cultivars used, co-infection by Ptr and Pan was highly prevalent across all sites (overall prevalence was 94%). Under the conditions studied, Ptr DNA was either as or more abundant than Pan DNA on both Emu Rock and Yitpi despite reported differences in disease resistance ratings between these cultivars (Table 3.1). Therefore, for diseases that occur as a complex, rating for individual disease resistance may not reflect rating under co-infection conditions. It is suggested that, for the diseases reported on in this chapter, assessment of cultivars for disease resistance should be carried out in the context of the complex.

The other cultivar included in this study, Magenta, displayed good resistance against both Ptr and Pan consistent with its resistance rating (Table 3.1). The low disease levels observed in Magenta may indicate it is either insensitive to or lacks the recognition products of the genes that match with Ptr and Pan main effector toxins (See et al., 2018; Tan et al., 2015). It is also plausible that host resistance to these two pathogens is under similar genetic control. It may be possible to develop improved resistance to these two pathogens simultaneously utilising similar/same genetic background. Such a case has been substantiated for other wheat diseases including leaf rust and powdery mildew (Li et al.,

2014; Milus et al., 2015). However, for the diseases studied here, such a phenomenon has not been reported, and there may be a benefit from undertaking a review of the sensitivity of existing wheat cultivars under co-infection conditions.

Both Ptr and Pan can penetrate wheat leaf tissues either through the cuticle or, less commonly, through stomata (Dushnicky et al., 1996; Solomon et al., 2006). However, following penetration, Ptr grows more rapidly than Pan colonising larger portion within the mesophyll in susceptible wheat cultivars (chapter 4). Pan, on the other hand, rarely invades the mesophyll, and often remains visible in the deeper leaf tissues around the vascular bundle (chapter 4). These differences in the post-penetration strategies may contribute to the ability of these two pathogens to co-exist through niche separation. Since symptoms caused by these two pathogens are difficult to distinguish, observation of the impact of post-penetration processes on the interactions between these two fungi is difficult. Furthermore, the two fungi can form undistinguishable joint lesions (Abdullah et al., 2018) suggesting that both species may also be able to occupy overlapping niches. Recent developments in fluorescent dye labelling and reporter genes may allow the situation to be unravelled, and this is an active area of research.

References

Abdullah, A. S., Turo, C., Moffat, C. S., Lopez-Ruiz, F. J., Gibberd, M. R., Hamblin, J., and Zerihun, A. (2018). Real-time PCR for diagnosing and quantifying co-infection by two globally distributed fungal pathogens of wheat. *Frontiers in Plant Science* **9**, 1086.

Abdullah, A. S. A., Moffat, C., Lopez Ruiz, F. J. L., Gibberd, M. G., Hamblin, J. H., and Zerihun, A. Z. (2017). Host-multi-pathogen warfare: pathogen interactions in co-infected plants. *Frontiers in Plant Science* **8**, 1806.

Bathgate, J., and Loughman, R. (2001). Ascospores are a source of inoculum of *Phaeosphaeria nodorum*, *P. avenaria* f. sp. *avenaria* and *Mycosphaerella graminicola* in Western Australia. *Australasian Plant Pathology* **30**, 317-322.

Bhathal, J., Loughman, R., and Speijers, J. (2003). Yield reduction in wheat in relation to leaf disease from yellow (tan) spot and septoria nodorum blotch. *European Journal of Plant Pathology* **109**, 435-443.

Blixt, E., Olson, A., Lindahl, B., Djurle, A., and Yuen, J. (2010). Spatiotemporal variation in the fungal community associated with wheat leaves showing symptoms similar to stagonospora nodorum blotch. *European Journal of Plant Pathology* **126**, 373-386.

Ciuffetti, L. M., Manning, V. A., Pandelova, I., Betts, M. F., and Martinez, J. P. (2010). Host-selective toxins, Ptr ToxA and Ptr ToxB, as necrotrophic effectors in the *Pyrenophora tritici-repentis*–wheat interaction. *New Phytologist* **187**, 911-919.

DAFWA (2016). Wheat variety guide for Western Australia. Department of Agriculture and Food Western Australia. Online publication. www.agric.wa.gov.au/cropdisease.

Dushnicky, L., Ballance, G., Sumner, M., and MacGregor, A. (1996). Penetration and infection of susceptible and resistant wheat cultivars by a necrosis toxin-producing isolate of *Pyrenophora tritici-repentis*. *Canadian Journal of Plant Pathology* **18**, 392-402.

Friesen, T. L., Stukenbrock, E. H., Liu, Z., Meinhardt, S., Ling, H., Faris, J. D., Rasmussen, J. B., Solomon, P. S., McDonald, B. A., and Oliver, R. P. (2006). Emergence of a new disease as a result of interspecific virulence gene transfer. *Nature Genetics* **38**, 953-959.

Galloway, J., Salam, M., and Pip, P. (2017). Less yellow spot in wheat: progress towards a decision support tool that will predict when yellow spot spores are released from the previous season stubble. In "Crop Updates", pp. 1-3. Grains Research and Development Corporation, Perth, Western Australia.

Hubbard, A., Lewis, C. M., Yoshida, K., Ramirez-Gonzalez, R. H., de Vallavieille-Pope, C., Thomas, J., Kamoun, S., Bayles, R., Uauy, C., and Saunders, D. G. (2015). Field pathogenomics reveals the emergence of a diverse wheat yellow rust population. *Genome Biology* **16**, 1-15.

Johnson, K. (1987). Defoliation, disease, and growth: a reply. *Phytopathology* **77**, 393-398.

Kuzdralinski, A., Szczerba, H., Tofil, K., Filipiak, A., Garbarczyk, E., Dziadko, P., Muszynska, M., and Solarska, E. (2014). Early PCR-based detection of *Fusarium culmorum, F. graminearum, F. sporotrichioides* and *F. poae* on stem bases of winter wheat throughout Poland. *European Journal of Plant Pathology* **140**, 491-502.

Li, Z., Lan, C., He, Z., Singh, R. P., Rosewarne, G. M., Chen, X., and Xia, X. (2014). Overview and application of QTL for adult plant resistance to leaf rust and powdery mildew in wheat. *Crop Science* **54**, 1907-1925.

Milus, E. A., Moon, D. E., Lee, K. D., and Mason, R. E. (2015). Race-specific adult-plant resistance in winter wheat to stripe rust and characterization of pathogen virulence patterns. *Phytopathology* **105**, 1114-1122.

Moffat, C., See, P. T., and Oliver, R. (2015). Leaf yellowing of the wheat cultivar Mace in the absence of yellow spot disease. *Australasian Plant Pathology* **44**, 161-166.

Murray, G. M., and Brennan, J. P. (2009). Estimating disease losses to the Australian wheat industry. *Australasian Plant Pathology* **38**, 558-570.

Nygren, J., Svanvik, N., and Kubista, M. (1998). The interactions between the fluorescent dye thiazole orange and DNA. *Biopolymers* **46**, 39-51.

Pandelova, I., Betts, M. F., Manning, V. A., Wilhelm, L. J., Mockler, T. C., and Ciuffetti, L. M. (2009). Analysis of transcriptome changes induced by Ptr ToxA in wheat provides insights into the mechanisms of plant susceptibility. *Molecular Plant* **2**, 1067-1083.

Pijls, C., Shaw, M., and Parker, A. (1994). A rapid test to evaluate *in vitro* sensitivity of *Septoria tritici* to flutriafol, using a microtitre plate reader. *Plant Pathology* **43**, 726-732.

Salam, K. P., Thomas, G. J., Beard, C., Loughman, R., MacLeod, W. J., and Salam, M. U. (2013). Application of meta-analysis in plant pathology: a case study examining the impact of fungicides on wheat yield loss from the yellow spot-septoria nodorum blotch disease complex in Western Australia. *Food Security* **5**, 319-325.

Savary, S., and Zadoks, J. (1992). Analysis of crop loss in the multiple pathosystem groundnut-rust-late leaf spot. I. Six experiments. *Crop Protection* **11**, 99-109.

See, P. T., Marathamuthu, K., Iagallo, E., Oliver, R., and Moffat, C. (2018). Evaluating the importance of the tan spot ToxA–Tsn1 interaction in Australian wheat varieties. *Plant Pathology* **67**, 1066-1075.

Shaner, G., and Buechley, G. (1995). Epidemiology of leaf blotch of soft red winter wheat caused by *Septoria tritici* and *Stagonospora nodorum*. *Plant Disease* **79**, 928-938.

Shapiro, S. S., and Wilk, M. B. (1965). An analysis of variance test for normality (complete samples). *Biometrika* **52**, 591-611.

Solomon, P. S., Wilson, T. G., Rybak, K., Parker, K., Lowe, R. G., and Oliver, R. P. (2006). Structural characterisation of the interaction between *Triticum aestivum* and the dothideomycete pathogen *Stagonospora nodorum*. *European Journal of Plant Pathology* **114**, 275-282.

Stukenbrock, E. H., Banke, S., Javan-Nikkhah, M., and McDonald, B. A. (2006). Origin and domestication of the fungal wheat pathogen *Mycosphaerella graminicola* via sympatric speciation. *Molecular Biology and Evolution* **24**, 398-411.

Suffert, F., Sache, I., and Lannou, C. (2011). Early stages of septoria tritici blotch epidemics of winter wheat: build-up, overseasoning, and release of primary inoculum. *Plant Pathology* **60**, 166-177.

Tack, A. J., Thrall, P. H., Barrett, L. G., Burdon, J. J., and Laine, A. L. (2012). Variation in infectivity and aggressiveness in space and time in wild host–pathogen systems: causes and consequences. *Journal of Evolutionary Biology* **25**, 1918-1936.

Tan, K.-C., Phan, H. T. T., Rybak, K., John, E., Chooi, Y. H., Solomon, P. S., and Oliver, R. P. (2015). Functional redundancy of necrotrophic effectors – consequences for exploitation for breeding. *Frontiers in Plant Science* **6**, 1-13.

Timken, M. D., Swango, K. L., Orrego, C., and Buoncristiani, M. R. (2005). A duplex real-time qPCR assay for the quantification of human nuclear and mitochondrial DNA in forensic samples: implications for quantifying DNA in degraded samples. *Journal of Forensic Science* **50**, 1044–1060.

Zadoks, J. (1999). Reflections on space, time, and diversity. *Annual Review of Phytopathology* **37**, 1-17.

Zadoks, J. C., Chang, T. T., and Konzak, C. F. (1974). A decimal code for the growth stages of cereals. *Weed Research* **14**, 415-421.

4 Co-inoculation under Controlled-Environment Conditions[IV]

Abstract

Plants host a mycobiome including pathogens that can form complexes. In these complexes, pathogens of otherwise distinctly different genotypes can interact within their shared host causing similar or indistinct disease symptoms. The consequences of their interactions on disease severity and pathogen development represent a novel area of research. This chapter investigates pathogen interactions and their consequences for disease development and severity. The chapter uses a tripartite pathosystem consisting of the host wheat and two major foliar fungal pathogens: *Pyrenophora tritici-repentis* (Ptr) and *Parastagonospora nodorum* (Pan). Results show that the infection process of Ptr and Pan appear to be complemented in co-inoculated leaves, reducing the lag-phase of visible disease symptoms by 50% and significantly increasing disease severity thereafter. The mechanisms underlying this complementation are unclear but cytological observations suggest an anatomical separation between leaf tissues during the pre-necrotic phase that is likely to enable Ptr-Pan co-infection. Pathogen success at causing significant disease was influenced by time and sequence of co-inoculation, with prior inoculation by Pan (up to 48 hours) exacerbated Ptr aggressiveness toward the host. These results suggest that Ptr and Pan can endure and/or benefit from their mutual presence indicating a close ecological trajectory and overlapping niche distribution.

[IV]Manuscript prepared for publication entitled "Co-inoculation of two foliar pathogens of wheat leads to accelerated disease symptoms and disease progression"

4.1 Introduction

Studies of plant-pathogen interactions have historically focused on experimental systems utilising a single-pathotype. However, in natural and agroecosystems, plants often interact with several pathogenic genotypes, exhibiting complexities not captured by the widely used single-pathotype system (Abdullah et al., 2017; Tollenaere et al., 2016). Co-infection has long been recognised for its significance on pathogen fitness and disease severity but rarely empirically studied (Alizon et al., 2013; Savary and Zadoks, 1992; Tack et al., 2012). Co-infecting pathogens are thought to compete for limited host resources. Competition leads to a higher exploitation rate by more competitive species, or all co-infecting species may succumb (Hamilton, 1972; Hardin, 1968). Hence, with co-infection, disease dynamics are expected to vary from a simplified single pathotype system, and this is at the heart of several mechanistic models predicting an increase/decrease in overall disease damage where more than one pathogen infects a host (Alizon et al., 2013; Fournier et al., 2006; May and Nowak, 1995).

Disease damage in co-infected plants is a consequence of three concurrent interactions: (i) host-pathogen; (ii) pathogen-pathogen, and (iii) host-multi-pathogen complexes (Abdullah et al., 2017). These interactions can lead to either additive effects when total disease damage equals the sum of individual effects or non-additive synergistic or antagonistic effects. Synergistic interactions favour the success of at least one pathogen, and overall disease damage is likely to be greater than additive damage (Fournier et al., 2006; Syller, 2012). Antagonistic interactions can lead to exclusion, where only one pathogen benefits (Seabloom et al., 2015). In this case, the overall disease damage is likely to be less than the potential additive effect due to the costs associated with pathogen to pathogen competition ultimately benefiting the host (Alizon et al., 2013; Alizon and Baalen, 2008). Hence, it may be possible to view co-infecting pathogens as a network. The success of each pathogen in the network is not only influenced by its abilities to overcome host defences, but also by interactions with other co-infection species (Christensen et al., 1987; Pedersen and Fenton, 2007). However, if the plant exhibits resistance or susceptibility to one of the co-infecting pathogens, the overall disease damage may not simply be a direct reflection of pathogen interactions (Arfi et al., 2013; Conrath et al., 2006; Cui et al., 2005). In fact, the plant may show little or no resistance to one pathogen (Adhikari and McIntosh, 1998), but eventually,

plant responses may deteriorate when disease intensity overwhelms plant resistance mechanisms (Estrada et al., 2012). Despite the considerable biological interest, little is known about the interactions that determine disease severity in co-infected plants.

Previous studies have focused on how co-infection influences the evolution of virulence (Alizon et al., 2013; May and Nowak, 1995; van Baalen and Sabelis, 1995), pathogen transmission (Elena et al., 2014; Susi et al., 2015) and sex ratio in pathogens (Giraud et al., 2008; López-Villavicencio et al., 2007). Collectively, these studies demonstrate that co-infection can have major consequences for host fitness and the spread of diseases in a host population. A few attempts have also been made to understand host defence responses to multiple pathogens including bacteria, fungi and insects (Cui et al., 2005; De Vos et al., 2005; Glazebrook, 2005; McGrann et al., 2014). However, none of these studies assess co-infection directly. Instead, host immunity to several single-infections is integrated to draw potential conclusions on co-infections. Such systems may not directly reflect the heterogeneous nature of diseases in the field. Moreover, large variations in environmental conditions and plant ages among these studies make it difficult to integrate results and draw conclusions. Therefore, information on how co-infection influences pathogen dynamics and disease severity is needed to make reliable conclusions of pathogen interactions.

The main objectives of this chapter were to investigate (i) expression of disease symptoms, (ii) disease development and (iii) pathogen-pathogen interactions in a co-inoculated wheat host. The chapter combines molecular, histological and cytological approaches to improve our understanding of the influence of co-inoculation on disease development. A tripartite pathosystem involving the wheat host and two fungal species: *Pyrenophora tritici-repentis* (Ptr) and *Parastagonospora nodorum* (Pan) was used in this chapter. These two fungi are common to many wheat-producing regions of the world. They cause yield loss by inducing chlorosis and necrosis subsequently reducing green leaf area (Bhathal et al., 2003; Johnson, 1987; Oliver et al., 2008). Separately, Ptr causes tan spot while Pan causes septoria nodorum blotch (Bhathal and Loughman, 2001). Jointly, these fungi cause a leaf spot complex in wheat (Abdullah et al., 2018). The field survey presented in chapter 3 provided evidence suggesting that co-infection by Ptr and Pan is common in Western Australia and Pan is likely to only occur in association with Ptr (Abdullah et al., 2020). This suggests that the presence of Ptr may predispose the host to subsequent infection by Pan. This issue has

practical implications, especially for diseases that occur in complexes. In such situations, studying one component of the complex will provide incomplete information about host-pathogen interactions. Although this chapter focuses on Ptr-Pan co-inoculation in wheat, knowledge gained from this pathosystem may also apply to other species. The current focus on these species reflects their widespread occurrence and relevance to global food security (Bhathal and Loughman, 2001; Liu et al., 2015; Murray and Brennan, 2009; Oliver et al., 2008).

4.2 Materials and methods

4.2.1 Fungal isolates, culturing conditions

All fungal isolates used in this chapter were maintained on V8-PDA Petri-dishes as described elsewhere (Moffat et al., 2015; Pijls et al., 1994). Only pathogenic wild type (wt) Ptr, collected from a site in Muresk (31°44′57″S 116°41′02″E), and pathogenic (wt) Pan, collected from a site close to Geraldton (28°46′28″S 114°36′32″E), were evaluated. Conidia of Ptr were produced as described previously (Lamari and Bernier, 1989). Conidia of Pan were produced by spreading a concentrated inoculum stock evenly across freshly plated PDA Petri-dishes. The Petri-dishes were then placed 10 cm beneath continuous cool white florescent lights for 7 to 9 days during which time they produced conidia. Conidia of Ptr and Pan were suspended in sterile water, and counted using a hemocytometer. Regular re-isolation of all fungal isolate occurred after every experimental use to maintain virulence.

4.2.2 Fungal transformation with green fluorescent protein

Green fluorescent protein (GFP) in Pan was achieved with protoplast transformation of the wt SN15 isolate using the vector pGpdGFP (Sexton and Howlett, 2001). To produce the protoplast, a spore suspension containing 5×10^7 Pan conidia was incubated in a 1 L flasks filled with 400 ml liquid medium plus 4 mM sterilised L-tryptophan. Flasks were placed on a shaker (140 rpm) at 23°C for 24 h. Flasks were then centrifuged at 10000 × g for 10 min at 4°C. The supernatant was discarded and the remaining cells were washed with 600 mM $MgSO_4$ and resuspended in 20 ml filter-sterilised $MgSO_4$ (1.2M; pH 5.8) with 10 mM phosphate buffer containing 15 mg glucanex per ml (Novo Nordisk). The resuspended solution was then transferred into glass Petri-dishes and incubated for 2 h at 27°C. The solution was transferred to a sterile centrifuge tube and 5 ml of 600 mM sorbitol in 10 mM

Tris (pH 7.5) was added. Tubes were centrifuged at 1500 × g for 30 min at 4°C and washed with 3 ml STC buffer (1.2 M sorbitol, 10 mM calcium chloride, 10 mM Tris, pH 7.5) and carefully resuspended in 0.5 ml of the same buffer until the protoplast was produced.

Protoplast suspension (100 µl; adjusted to a cell density of 5 x 10^7) was mixed with 7 µg transforming DNA dissolved in 25 µl STC buffer in a disposable plastic centrifuge tube and incubated at 23°C for 25 min (Yelton et al., 1984). Negative control was also prepared, in which the protoplast received an equivalent volume of STC buffer. After that, 200 µl of 60% (wt/vol) polyethene glycol 4000/10 mM Tris (pH 7.5)/ 10 mM $CaCl_2$ was added and the tubes were hand-agitated gently. This was followed by a further two additions of the same solution (200 and 800 µl) with gentle mixing after each addition. The protoplasts were then incubated for 20 min at 23°C and the mixture was centrifuged at 12,000 × g for 5 min. The protoplasts were then carefully resuspended in 1 ml STC buffer. The resultant protoplasts were transformed with *Not*I-digested plasmid DNA and plated on hygromycin (50 µg ml^{-1}) as described previously (Sexton and Howlett, 2001). Screening for positive transformation followed a standard PCR protocol (Hobert, 2002). The transformed isolate was obtained after three rounds of PDA culturing with hygromycin and two rounds of single sporing.

4.2.3 Synchronous co-inoculation – Experiment 1

A synchronous co-inoculation experiment was conducted in a glasshouse with controlled temperature set to 22/15°C day/night. Four wheat (*Triticum aestivum*) cultivars were included in this experiment: Emu Rock, Yitpi, Halberd and Magenta. These were selected to provide varying resistance levels to the diseases caused by Ptr and Pan (Table 4.1). Plants were grown in round polyvinyl chloride pots (15 cm diameter and 20 cm deep) filled with a commercial potting mix (Richgro®). Four-week-old seedlings were inoculated using a hand-held airbrush sprayer containing conidia of either Ptr, Pan or they were co-inoculated (Table 4.2). Plants from the same inoculation treatment were grouped together and sprayed with 100 ml conidial suspension in 0.3% (w/v) gelatine. The concentration of spores in the suspension was adjusted to 3 x 10^3 and 1 x 10^5 conidia ml^{-1} for Ptr and Pan, respectively. These concentrations were determined in a preliminary experiment based on a 0 to 10 disease damage scale from a single inoculation of the wheat cultivar Halberd. A 0 score indicates no visible symptoms while 10 indicates a fully necrotised/chlorotic leaf.

Inoculation at the above concentrations provided similar disease scores (7.2 ± 0.9 for Ptr and 6.6 ± 0.8 for Pan) measured 15 days post-inoculation (dpi).

Table 4.1. Disease resistance rating (DPIRD, 2018) for the wheat cultivars used in this chapter.

Cultivar	Disease resistance rating*	
	Tan spot (Ptr)	Septoria nodorum blotch (SNB)
Emu Rock	MR/MS	S/VS
Yitpi	S/VS	MS
Halberd	S	S
Magenta	MR	MR/MS

*MR/MS = moderately resistant to moderately susceptible. S/VS = susceptible to very susceptible. MR = moderately resistant. MS = moderately susceptible.

Co-inoculated plants received a mixture of inoculum from both fungi in equal volume. The mixture was prepared from the same initial stock solutions as used for single inoculation. Total inoculum volume was kept consistent as in the single inoculation treatment. Control plants were inoculated with water in 0.3% gelatine. Plants were inoculated in enclosed chambers and were kept protected from air movement for 30 min to dry. After inoculation, plants were placed in enclosed incubation chambers and kept at ~90% humidity for 48 h to promote infection. Plastic dividers (90 cm height) were placed between the different treatment groups to prevent diseases from spreading between treatments. There were six biological replicates per treatment group; these were arranged in a randomised complete block design. Plants in each treatment were monitored daily for visible disease symptoms. Days to 50% of the inoculated plants showing visible disease symptoms were calculated. Plants were also scored for disease severity on the penultimate leaves at 3-day intervals starting from 6 dpi up to 15 dpi. Plants from all treatments were given a disease score on a 0 to 10 scale as described above. After scoring, leaves were excised and stored in 2-ml volume microtubes and kept in liquid nitrogen during sampling and transport. Leaves were stored at -80°C until used.

4.2.4 Asynchronous co-inoculation – Experiment 2

Growth and inoculation conditions were the same as in Experiment 1, except that three wheat cultivars were included in this experiment: Emu Rock, Yitpi and Halberd (Table 4.1). In this experiment, the inoculation order of Ptr and Pan was manipulated so that one species

was inoculated 24, 48, and 72 h before or after inoculation by the other species (Table 4.2). Synchronously co-inoculated and mock-inoculated plants served as controls for this experiment. Paired gelatine inoculations were also included as controls for each asynchronous co-inoculation. Inoculation treatments were carried out using six biological replicates and the treatments were arranged in a randomised complete block design. All co-inoculated plants received conidial suspension of Ptr and Pan as in Experiment 1. Clean, sterilised spray equipment was used on each inoculation day. Inoculations on different days used fresh conidial suspensions that were prepared from the same batch of V8-PDA agar cultures and adjusted to the same concentration as in Experiment 1. Inoculation on different days was in enclosed chambers to avoid cross-contamination. Disease assessment and leaf sampling were carried out as in Experiment 1.

Table 4.2. Treatment structure of the two co-inoculation experiments described in this study.

Synchronous co-infection (Experiment 1)	Asynchronous co-infection* (Experiment 2)
Ptr in single inoculation	Ptr + Pan in co-inoculation
Pan in single inoculation	Ptr + Pan 24h later
Ptr + Pan in co-inoculation	Ptr + Pan 48h later
Mock, no inoculation	Ptr + Pan 72h later
	Pan + Ptr 24h later
	Pan + Ptr 48h later
	Pan + Ptr 72h later
	Mock, no inoculation

*Paired control with 0.3% gelatine were included when different arrival sequences were used.

4.2.5 DNA extraction, quantification and qPCR

Analysis of fungal abundance was done on penultimate leaves collected from Experiments 1 and 2. Leaves were cut and placed into a 2 ml volume safe cap microtube. These were ground into a fine powder in liquid nitrogen with the aid of tungston-carbide beads. Sub-samples (40 mg) of ground leaf tissues were used for DNA extraction. DNA was extracted using a Bio-sprint 15 plant DNA kit (Qiagen) as per the manufacturer's protocol. DNA concentration was determined using a NanoDrop 2000 UV-Vis spectrophotometer (Thermo Scientific) and diluted to 50 ng μl^{-1} working solutions. DNA samples were stored at -20˚C until required. Pure genomic DNA, for constructing standard curves, was extracted from fungal colonies using the same DNA kit described above. Fungal cultures were maintained

on V8-PDA agar plates (Pijls et al., 1994, Moffat et al., 2015). Mycelia from these cultures were harvested and finely ground in liquid nitrogen and used for DNA extraction.

Extracted DNA was assayed for fungal DNA abundance using a previously described qPCR protocol (Abdullah et al., 2018). Briefly, the method uses a set of four specialised primers and two matching probes to target unique genomic regions within Ptr and Pan. Probes are differentially tagged with fluorophores so that both fungi are quantified simultaneously but on different channels of the qPCR machine. All qPCR reactions were carried out on a CFX96 real-time PCR system (Bio-Rad), and quantification was achieved using the standard curve method (Abdullah et al., 2018). All reactions were run with three technical and two biological replicates.

4.2.6 Detached leaf assay – Experiment 3

A modified detached leaf assay from Benedikz et al. (1981) was used to evaluate the pathogenicity of the GFP-Pan as well as to test the co-inoculation by Ptr and Pan. Seeds of wheat (Halberd and Emu Rock) were planted in individual trays containing the same commercial potting mix used in Experiment 1. Leaves of two-week-old seedlings were excised and attached adaxial side up onto clear polystyrene boxes containing 50 ml benzimidazole agar (75 mg/L). Leaves in boxes were prepared in three biological replicates and the full set of inoculation treatment (Ptr, Pan and their co-inoculation) was randomised within each box. A small cylindrical mycelial plug of hyphae and V8-PDA agar (diameter ~5 mm) were placed onto the excised leaves. When mycelial plugs were not used, 20 μl^{-1} conidial suspension in 0.3% gelatine of Ptr and Pan mixed in equal volume was used instead. The concentration of conidia in the suspension was as in Experiment 1. After inoculation, the ends of the leaf cuts were covered with an additional layer of benzimidazole agar and boxes were placed in plastic containers lined with damp cotton fibre to raise humidity. Leaves were maintained in high relative humidity (~85%) at 23°C and kept under continuous cool white fluorescent light until the damage on the leaf was visible.

4.2.7 Spot inoculation assay – Experiment 4

This assay used the same detached leaves assay described above except that leaves (9 cm in length) of 4 week-old Emu Rock seedlings were used. These were spot-inoculated with a conidial suspension of Ptr and Pan alongside the leaf midveins. Leaves were arranged in three randomly allocated biological replicates each inoculated with conidial suspension as

in Experiment 1. The distance between spots was kept consistent at ~1 cm apart. Five inoculation spots were made on each leaf using a sterile surgical pipet. Each spot received 20 μl^{-1} spore suspension in 0.3% gelatine. After inoculation, boxes were placed in covered plastic trays lined with misted cotton fibre sheets and leaves were inspected daily and observed microscopically

4.2.8 *In vitro* hyphal interaction assay – Experiment 5

Two independent *in vitro* experiments were conducted to study hyphal interaction between Ptr and Pan. In the first experiment, 10 µl of inoculum containing 3 x 10^3 and 1 x 10^5 conidia ml^{-1} of Ptr and Pan, respectively, were placed onto water agar cushions on glass microscope slides coated with a thin layer of PDA agar. Slides were placed in double-sealed plastic containers and incubated at 25°C under continuous cool white light. Three fungal isolates were included: wt-Ptr, wt-Pan and GFP-Pan. Separate spore suspensions of wt-Ptr and wt-Pan or wt-Ptr and GFP-Pan were placed on either end of the microscope slides. Fungal colonies were placed ~4 cm apart and they were allowed to grow until hyphal growth overlapped. On each end of the microscope slides, two growth zones were identified. The inner zone of the slides, where the growth of Ptr and Pan overlapped, were called confrontation zones (CZ). The outer sides of the slides were called by their respective species either Ptr zone or Pan zone.

In total, 36 microscope slides were inoculated. These were split into three groups each containing four replicates. The first group (n=12) was inoculated with wt-Ptr and wt-Pan. Fungal colonies were allowed to grow until growth at the CZ reached its maximum. These slides were stained with Evans blue and assessed for fungal vitality. The second group (n=12) was left unstained and inoculated with wt-Ptr and wt-Pan. These slides were imaged (X40) over a period of 7 days using a light microscope. The third group (n=12) included the GFP-Pan and wt-Ptr. These were overlaid with a fluorescent stain and imaged using a confocal microscope.

In the subsequent experiment, 20 µl of inoculum, adjusted to 3 x 10^3 and 1 x 10^5 conidia ml^{-1} for Ptr and Pan respectively, were placed onto PDA in Petri-dishes (n=36). All possible combinations, including plating only Ptr or Pan (control), co-plating on distal/polar ends of Petri-dishes and co-plating on the same spot (no-distance). After inoculation, dishes were

sealed with laboratory parafilm tape to prevent the spore suspension drying out. Plates were then incubated at 25/15°C light/dark and monitored daily. Where co-plating was made at a distance, Ptr and Pan inoculums were placed ~4 cm apart. Plates were imaged using a 20 megapixel high resolution camera (Canon EOS 5DS) and fungal colonies were examined for any signs of interaction including those described by Skidmore and Dickinson (1976). Colony diameter was measured over time until colonies achieved maximum growth covering the dish. Where dual/co-plating was made, colony diameter was measured when the growth of one or both fungi reached maximum.

4.2.9 Cytological techniques

Interactions between Ptr and Pan, *in planta* and *in vitro*, were examined using a spinning disc confocal microscope with a VisiScope Confocal Cell Explorer (Visitron System, Munich, Germany). A microscope (Olympus, Hamburg, Germany), fitted with an inverted IX81 motorised imaging unit, a PlanApo UPlanSApo objective (Olympus, Hamburg, Germany) and a Photometrics CoolSNAP HQ2 camera (Roper Scientific, Germany), was used for imaging. Ptr was stained with the Calcofluor-White® (CW; Sigma-Aldrich) as per the manufacturer's protocol and visualised under UV (420 nm/100mW). GFP-Pan was visualised under the pre-optimised GFP channel (560 nm/100mW). The reporters of both pathogens were excited using a VS-KMS6 laser merge system with two solid-state diode lasers with a 50/50 split intensity. The co-observation of the GFP and CW was achieved using an OptoSplit II LS image splitter controlled by VisiView (Visitron System). Dual-channel imaging was carried out using a dual-view micro imager equipped with a dual-line beam splitter. All parts of the microscope were under the control of MetaMorph (MDS Analytical Technologies, Winnersh, UK).

Scanning electron microscopy was performed on detached leaves of wheat (Halberd). Leaves were prepared as described above and spray inoculated with conidial suspension of wt-Ptr and wt-Pan using small handheld cosmetic spray bottles. Conidial concentration in the suspension was as in Experiment 1. Inoculated leaves were covered with plastic coverlids. Moistened sterilised fibreglass cotton was placed in the corners of each coverlid to maintain high humidity. Inoculated leaves were cut around the infected spots into small discs (~10-mm). Leaf discs were coated with a gold sputter coating in an Alto 2100 chamber and observed with a Jeol JSM-6390LV scanning electron microscope (JEOL, Ltd, Welwyn

Garden City, UK). All microscopic analyses were done on at least three biological replicates, and representative images are shown. Optical leaf sections were handmade as described in Solomon et al. (2006). Evans blue staining was performed as per the manufacturer protocol and visualised using an optical view microscope (Olympus, Hamburg, Germany).

4.3 Results

4.3.1 Co-inoculation leads to accelerated appearance of symptoms associated with the early development of Ptr (Experiment 1 and 2)

Depending on host genotype, inoculation with either Ptr or Pan resulted in visible disease symptoms 6 to 9 dpi (Figure 4.1A). Symptoms on these plants were large necrotic lesions scattered throughout the leaves (Figure 4.1B). In contrast, synchronous co-inoculation with both pathogens halved the length of time required for the disease to appear on susceptible genotypes, with symptoms visible at 3 dpi (Figure 4.1A, C). Symptoms on these plants were depicted as numerous closely located necrotic lesions mostly along the midrib of leaves (Figure 4.1B). On all cultivars, except Magenta, Ptr abundance on the co-inoculated plants reached detectable DNA levels 3 dpi. At this time, Pan DNA was below the limit of detection (Figure 4.1C; Table insert). The host genotype Magenta showed delayed visible disease appearance (7 to 9 dpi) and Ptr DNA detection compared to the other genotypes (Figure 4.1A, C).

Plants inoculated with Pan 24 h prior to Ptr inoculation also showed earlier symptom development by 3 dpi (Figure 4.2). However, the reverse order (i.e. Ptr and then Pan 24 h later) did not lead to accelerated development of disease symptoms. The more rapid onset of disease symptoms following Ptr-Pan synchronous and asynchronous co-inoculation is consistent with observations from a preliminary experiment undertaken under glasshouse conditions (Appendix 1). As in synchronous co-inoculation, Ptr also benefited from asynchronous co-inoculation reaching detectable abundances 3 dpi (Figure 4.2; data labels). Pan DNA was not detectable at this same time point, however. These results suggest that co-inoculation of wheat with Ptr and Pan can cause accelerated disease development that is primarily associated with the increased growth of Ptr.

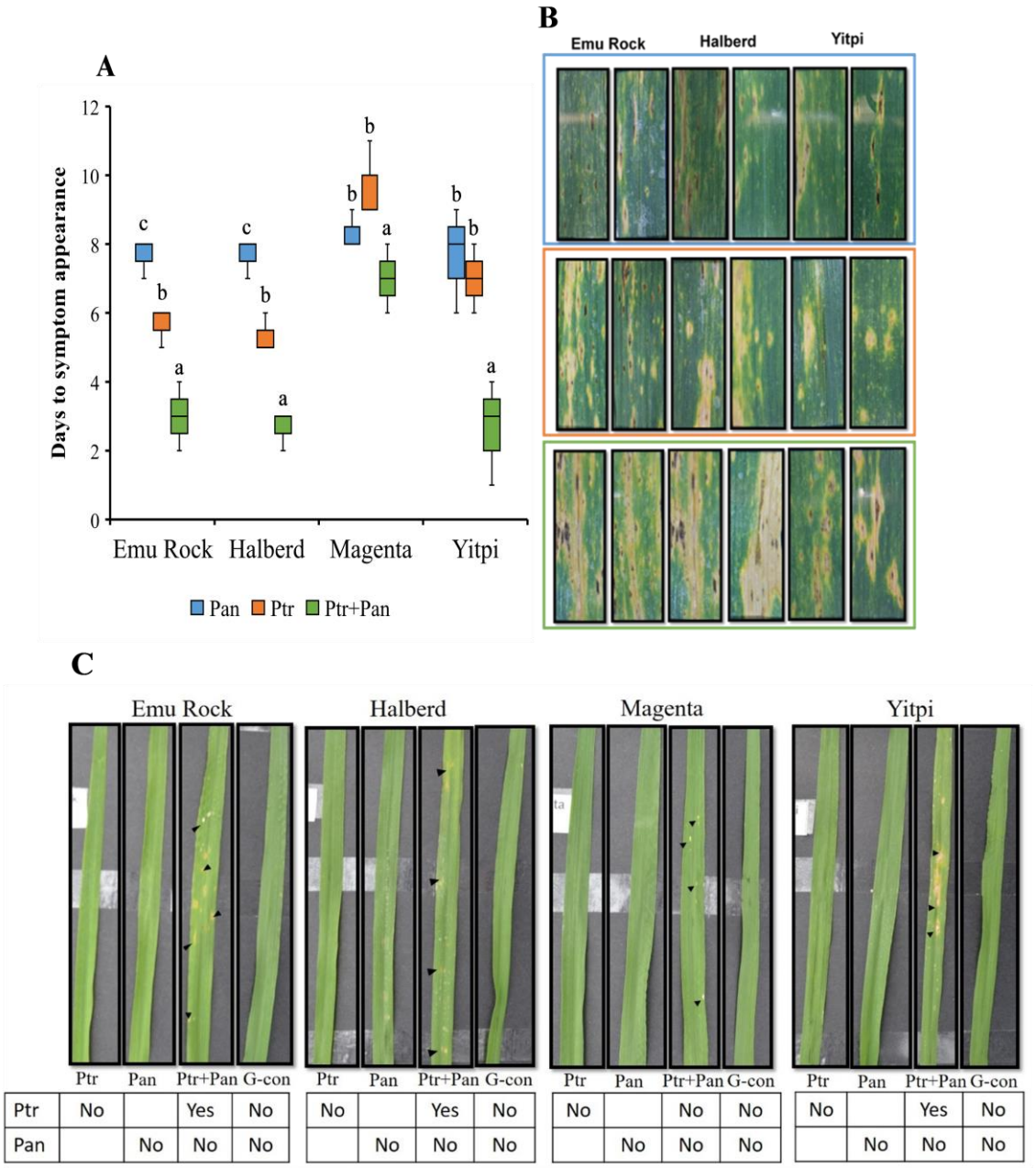

Ptr	Pan	Ptr+Pan	G-con
Ptr	No	Yes	No
Pan	No	No	No

Ptr	Pan	Ptr+Pan	G-con
No		Yes	No
	No	No	No

Ptr	Pan	Ptr+Pan	G-con
No		No	No
	No	No	No

Ptr	Pan	Ptr+Pan	G-con
No		Yes	No
	No	No	No

Figure 4.1. Development of visible disease symptoms on wheat cultivars inoculated with various pathogen treatments (Experiment 1). (A) Boxplot showing days until 50% of the plants showed disease symptoms following inoculation with Ptr, Pan or their synchronous co-inoculation. The horizontal black line crossing the box is the median, the bottom and top of the box are the lower and upper quartiles and whiskers are the minimum and maximum values where visible. Boxes with the same letter code are not significantly different (Tukey multiple comparison of means at $P \leq 0.05$). (B) Example of leaves from

three wheat cultivars showing symptoms of Pan infection (blue box), Ptr infection (orange box), and their co-infection (green box). Pictures were captured 9 dpi and shown in two biological repeats. Disease symptoms on Magenta were low and hence not shown. (C) Examples of leaves showing disease symptoms 3 dpi. Insert table shows the result of the qPCR assay on leaves showing disease symptoms collected 3 dpi. Yes and No refer to assay results above and below the limit of detection (LoD), respectively. The LoD for Ptr=0.52 pg μl^{-1} and Pan=0.39 pg μl^{-1}.

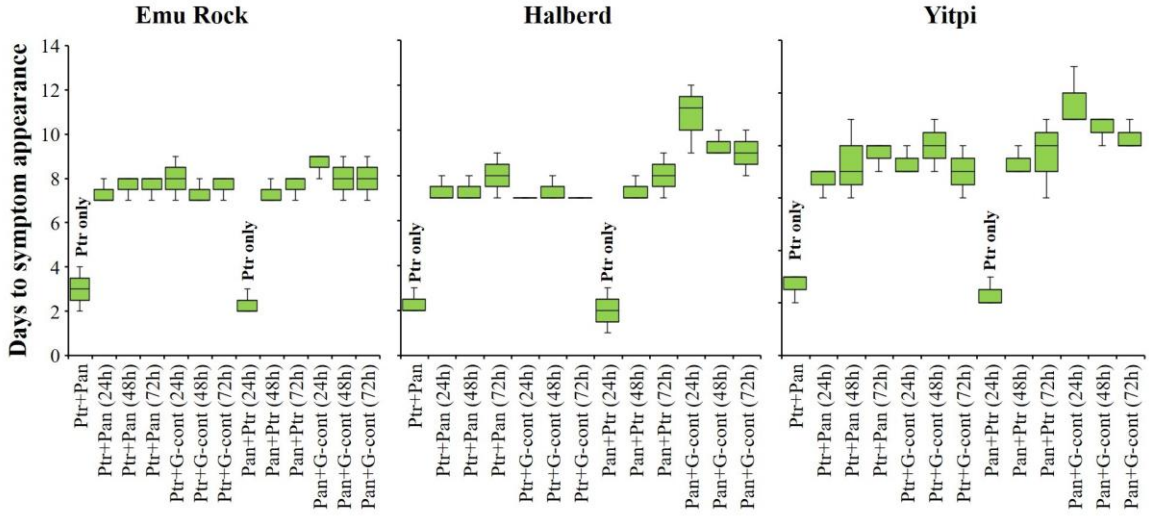

Figure 4.2. Boxplot showing days until 50% of the plants showed disease symptoms following Ptr-Pan asynchronous co-inoculation (Experiment 2). The horizontal black line crossing the box is the median, the bottom and top of the box are the lower and upper quartiles and whiskers are the minimum and maximum values where visible. Data labels represent results of the qPCR assay on leaves showing disease symptoms. Ptr was within the LoD of the qPCR assay and hence labelled; Pan was below the LoD and not labelled. G-cont refers to gelatine-only, paired control.

4.3.2 Co-inoculation leads to greater disease damage mostly driven by a rapid abundance of Ptr (Experiment 1 and 2)

Variation in disease damage score was mostly related to host genotype with the host cultivar Magenta having the lowest level of disease development. Magenta did not develop significant disease throughout the experiment and there was no significant difference between single and co-inoculation treatments (Figure 4.3). In all other host cultivars, synchronous co-inoculation of Ptr and Pan exacerbated disease damage, and by 9 dpi, disease damage scores on co-inoculated plants were significantly greater than disease

damage caused by either Ptr or Pan alone (Figure 4.3). At this time, the damage from the co-inoculation treatment was equivalent to the sum damage of Ptr and Pan combined (i.e. additive damage). The trend of higher disease damage scores induced by co-inoculation continued throughout the experiment, but the level of damage caused by the co-inoculation treatment became less than additive towards 12 and 15 dpi (Figure 4.3).

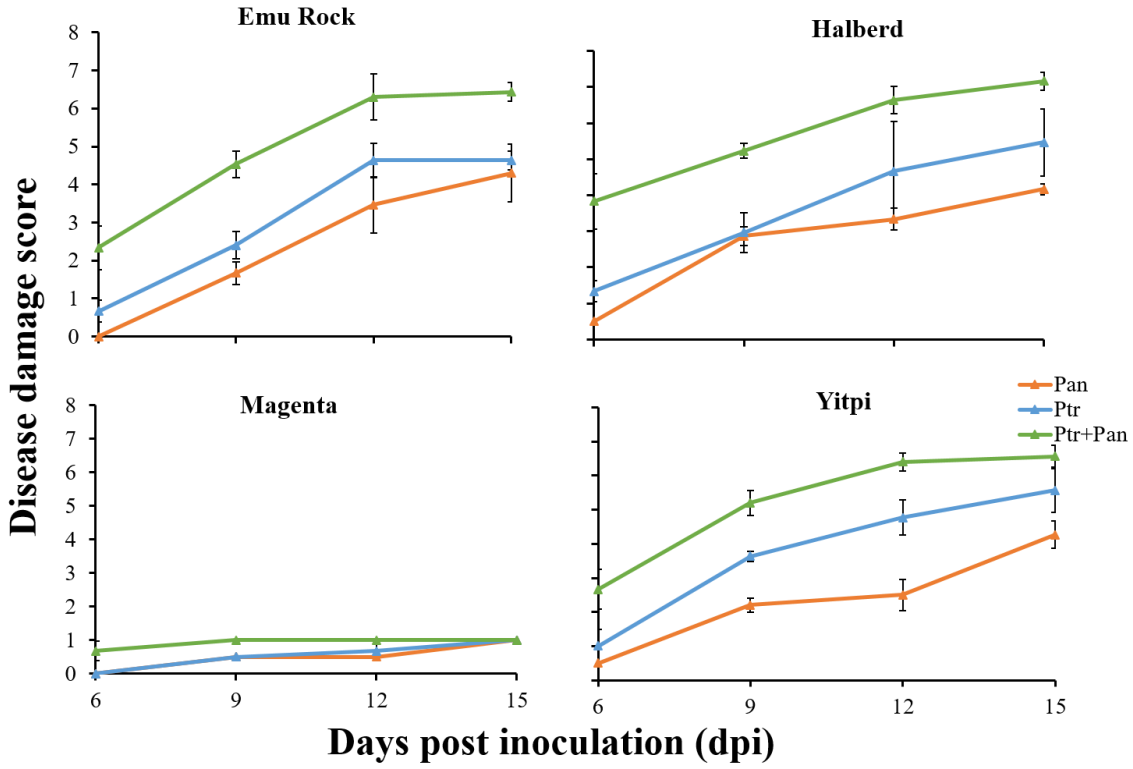

Figure 4.3. Visible disease development on four wheat cultivars following inoculation and synchronous co-inoculation by Ptr and Pan (Experiment 1). Leaves were assessed for diseased leaf area and given a score on a 0 to10 scale. Data are means ± standard deviation (*n*=6).

Ptr benefited from the co-inoculation with Pan and had more abundant fungal DNA in co-inoculated leaves than when Ptr was used alone in all cultivars except Magenta (Figure 4.4). By 6 dpi, the abundance of Ptr DNA in co-inoculated leaves was 2.7-fold greater than that from single Ptr-only inoculations. By 15 dpi, the abundance of Ptr DNA in the co-inoculated leaves reached 4-fold greater than that in single Ptr inoculation (Figure 4.4). In contrast, co-inoculation had a negative impact on Pan and the abundance of Pan was significantly higher in leaves of plants exposed to single inoculation compared to co-

inoculation treatments (Figure 4.4). Although Ptr rapidly outgrew Pan in co-inoculated leaves, Pan remained consistently within/above the LoD of the qPCR assay. No evidence of complete exclusion between Ptr and Pan was observed.

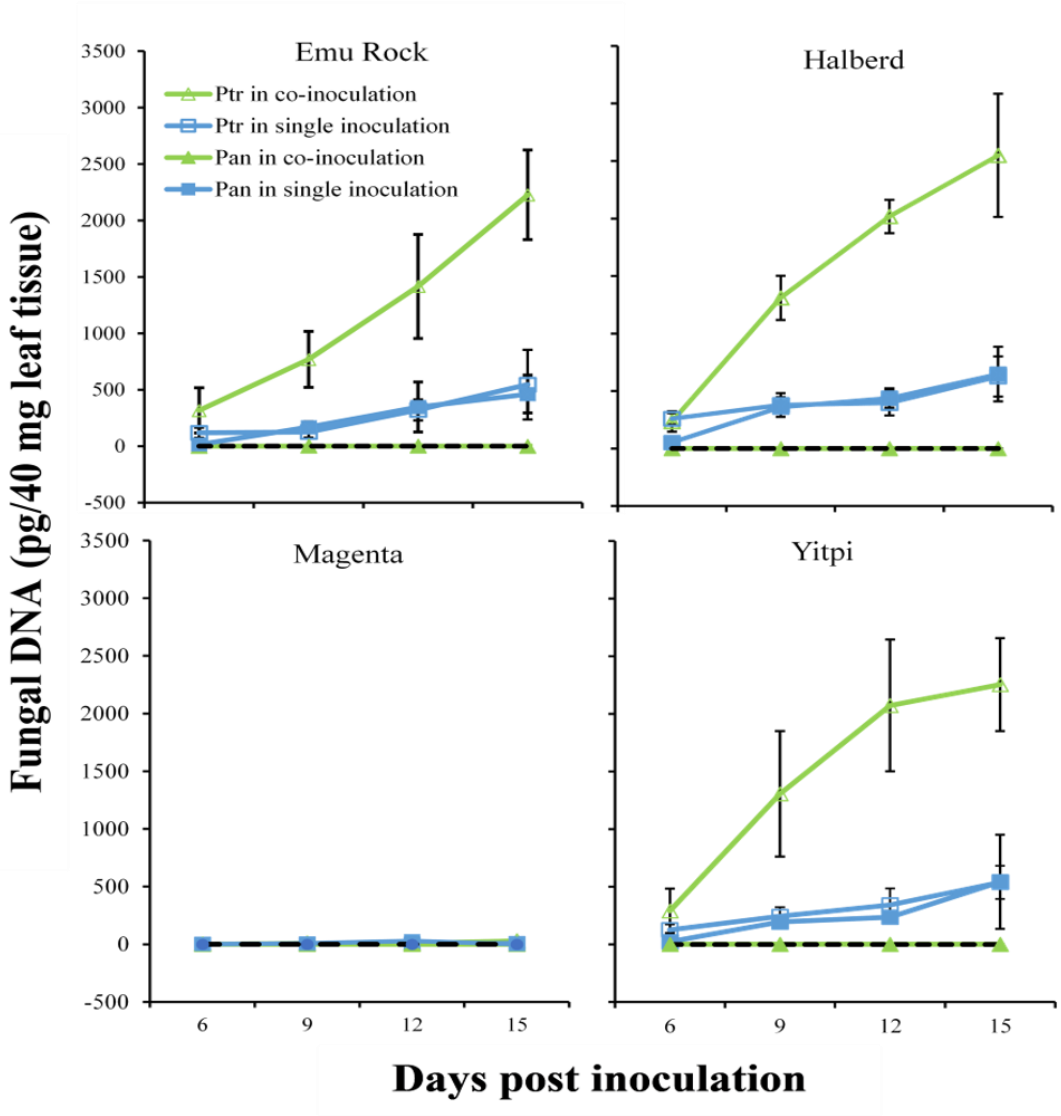

Figure 4.4. Dynamics of Ptr and Pan abundance in leaves of plants exposed to single and co-inoculated treatments on four wheat cultivars (Experiment 1). Single and co-inoculation treatments were done on separate plants but data are co-plotted for comparison. Data are means ± standard deviation (*n*=6). The dotted black line is the zero reference. Fungal DNA was measured using the qPCR assay.

Ptr and Pan coexisted regardless of treatments relating to the inoculation sequence. However, Ptr DNA was often more abundant than Pan DNA (Figure 4.5A). Pan abundance was only more than Ptr in leaves of plants inoculated with Ptr 72 h after inoculation with Pan. Only in this situation was Pan consistently more abundant than Ptr; an effect that occurred independently of the cultivar. No evidence of exclusion was observed and Pan DNA was still detectable despite delayed inoculation and extensive abundance of Ptr DNA (Figure 4.5A). Delaying the inoculation of Pan beyond 24 h resulted in progressively lower disease damage compared to when Pan was inoculated 24 h after Ptr (Figure 4.5B). In contrast, reduced disease damage occurred only when Ptr inoculation was delayed for 72 h after Pan inoculation. Earlier inoculations of Ptr up to 48 h, after Pan inoculation, achieved similar visible disease damage (Figure 4.5B). In order to verify these results, two attempts were made to repeat a shortened version of Experiment 2. However, contaminating infection with unrelated biotrophic pathogens prevented the acquisition of conclusive results (Appendix 2).

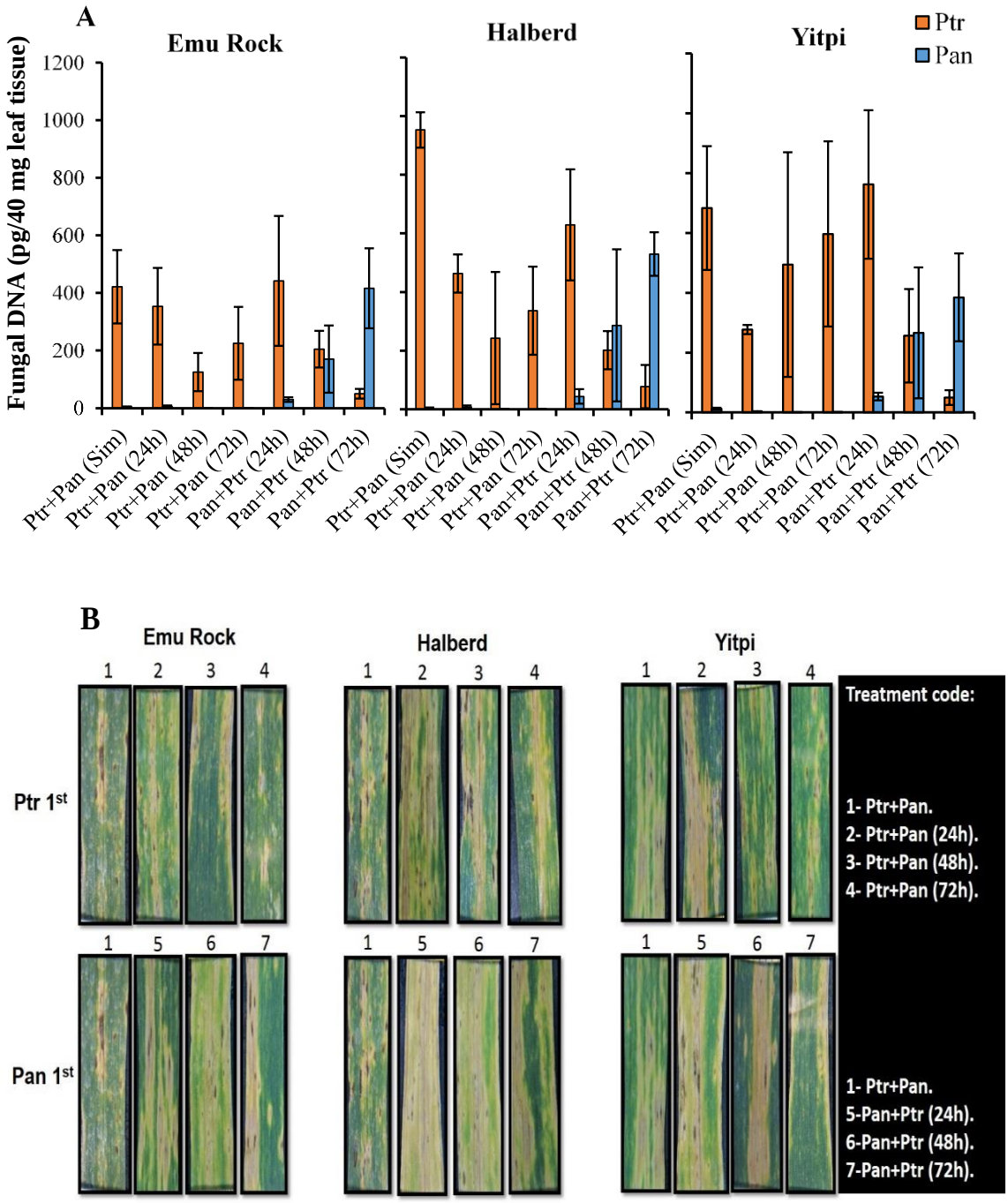

Figure 4.5. Dynamics of Ptr-Pan development in asynchronous co-inoculation (Experiment 2). (A) Fungal DNA (pg/40 mg leaf tissues) of Ptr and Pan in co-inoculated leaves. Leaves were sampled 12 and 15 dpi and pooled together. Pooled samples were assayed for fungal DNA abundance using the qPCR method. Data are means ± standard deviation (*n*=9). (B)

Examples of leaves co-inoculated with Ptr and Pan with various arrival sequences. Leaves were imaged 16 dpi.

4.3.3 Ptr and Pan use different strategies to infect wheat leaves (Experiment 3 and 4)

Transformed Pan, with a gene encoding GFP, was first tested on PDA agar plates for *in vitro* colony characteristics. Colony growth of the GFP-Pan appeared to be similar to wt-Pan (Figure 4.6A). However, GFP-Pan produced fewer conidia on PDA agar than wt-Pan; average conidia were 12.1 ± 6.1 and 18.3 ± 4.8 μl^{-1}, respectively (P<0.05). Nonetheless, GFP-Pan had a comparable growth rate on PDA agar to that of wt-Pan and was successful at causing disease on detached leaves of Halberd (Figure 4.6B). GFP-Pan caused less disease damage on detached Halberd leaves compared with wt-Ptr. Co-inoculation with wt-Ptr and GFP-Pan caused more disease damage than single inoculation with either of the pathogens alone (Figure 4.6B). The co-inoculation caused almost a complete loss of green leaf area by 7 dpi.

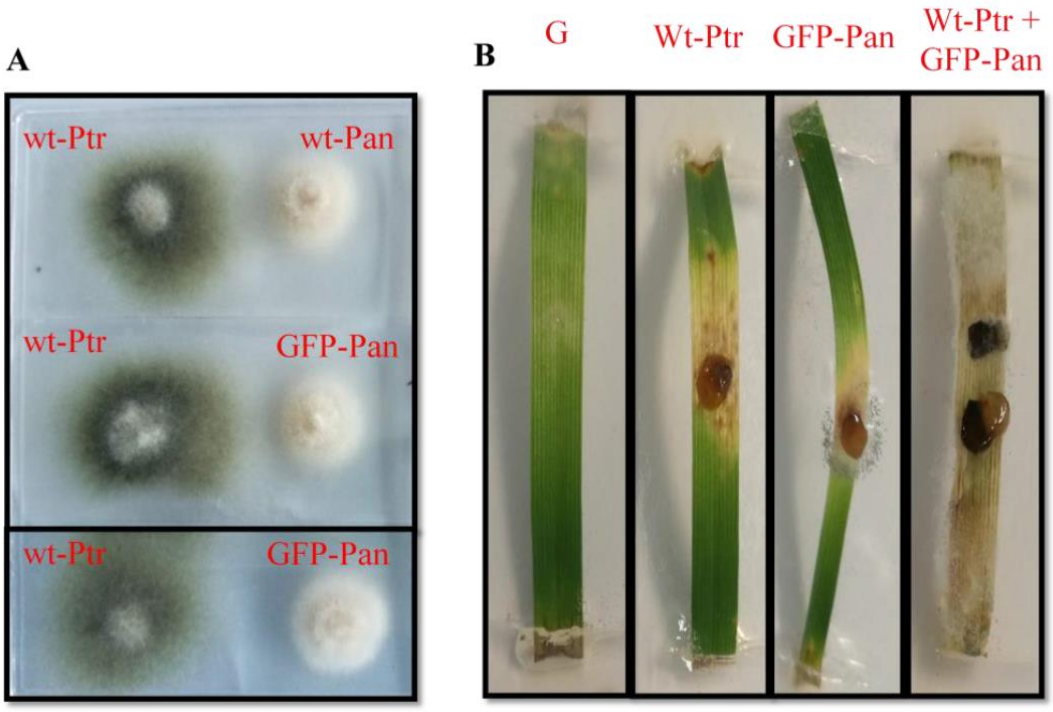

Figure 4.6. Comparative evaluation of the wild type (wt) Ptr and GFP-Pan (Experiment 3). (A) *In vitro* colony characteristics of the GFP-Pan compared with wt-Pan. Images were captured 5 dpi. (B) *In planta* co-inoculation on a detached leaf of the wheat cultivar Halberd. V8-PDA agar plugs with fungal mycelium (2.5 mm) were placed onto four-week-

old leaves with the aid of gelatine (G). Clear PDA agar, without mycelia, was used as a control. The clear PDA agar plugs were removed before image capturing to expose leaf surface beneath the plugs. Images were captured 7 dpi. Wt-Ptr and GFP-Pan were used in this assay.

The interaction between Ptr and Pan was investigated on microscope slides coated with a thin layer of PDA agar (Experiment 4). Two growth zones were identified: Ptr-zone or Pan-zone (Figure 4.7A). The inner ends, where both species share space and resources, is the confrontation-zone (CZ; Figure 4.7H). For visualisation purposes, the wt-Ptr was stained with a chitin-binding dye that fluoresces blue under UV. Pan was visualised with the GFP reporter gene. Slides inoculated with wt-Ptr and wt-Pan were used as controls, and these were visualised in a bright field using an optical microscope. As expected, the Ptr-zone only showed Ptr hyphae (Figure 4.7B, C) and Pan-zone only showed Pan hyphae (Figure 4.7E, F). In the CZ, both species grew towards each other, and their mycelia interacted and curled around each other forming joint non-antagonistic networks (Figure 4.7D, G). No evidence of dead hyphae at the points of contact at the CZ was observed (Figure 4.8).

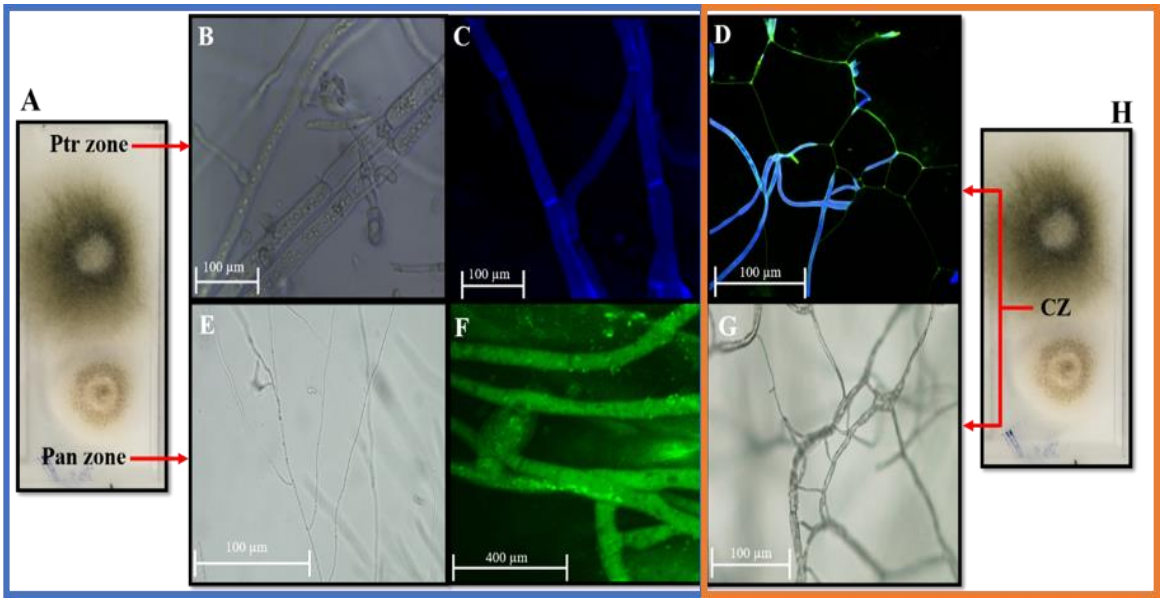

Figure 4.7. Cytological observations of the hyphal interactions between Ptr and Pan *in vitro* (Experiment 4). Both species were grown in the proximity of each other on microscopic slides coated with a thin layer of PDA agar. Fluorescent microscopic images (C, D, and F) were captured using a confocal microscope. Other, non-florescent, images (B, E and G) were captured using an optical view microscope. Scale bars are shown on the images. Blue

box represents the observation at the Ptr or Pan zone (A). Orange box represents the observation at the confrontation zone (H).

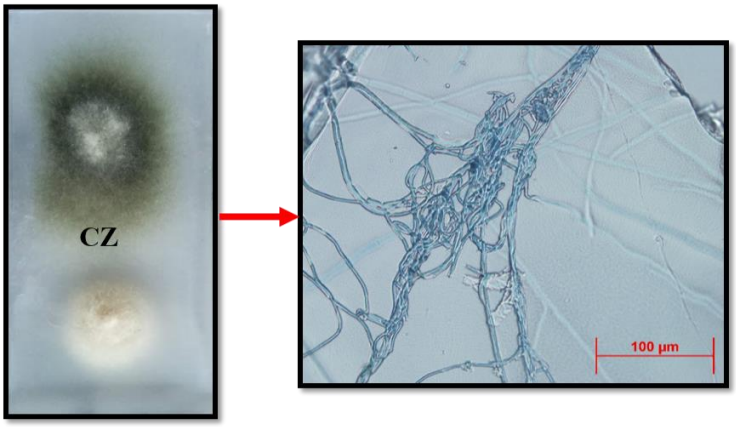

Figure 4.8. Evans blue staining of hyphal interactions between Ptr and Pan at the confrontation zone (CZ). No signs of dead hyphae at the CZ was observed.

To understand the mechanisms by which Ptr and Pan co-exist *in planta*, detached leaves of wheat (Halberd) were co-inoculated with conidia of wt-Ptr and GFP-Pan. The infection process was followed for 9 days using various microscopic techniques. Ptr conidia germinated and within 1 dpi produced hyphae. These made contact with the leaf surface as soon as they germinated. After germination, numerous Ptr hyphae grew along the longitudinal axis of the leaf surface. By 2 dpi, melanised appressoria (AP), that Ptr typically uses for direct leaf invasion, penetrated the leaf indirectly through the stomata (Figure 4.9A-D). Primary hyphae entered the leaf and rapidly differentiated into thick invasion hyphae (IH) with limited hyphal branching. By 4 dpi, IH colonised the leaf and remained visible only in the mesophyll (Figure 4.9E). Infection in an independent detached leaf experiment proceeded similarly with penetration occurring at less than 1 dpi, IH forming at 3 dpi and colonisation of mesophyll tissues occurring at 4 dpi. Development of disease symptoms was not observed until the colonisation of the mesophyll was completed about 4 dpi.

Pan hyphae also grew as soon as it made contact with the leaf surface. Appressoria-like structure were formed from invasion hyphae; these invaded leaf tissues within 3 dpi (Figure 4.9F, G). Penetration of the leaf occurred directly through the cell wall via a thin invasion point (IP) at the tip of the invasion hyphae (Figure 4.9F, G). Secondary hyphae were not

observed on the leaf surface. Instead, these were only visible deep in the leaf vascular buddle about 6 dpi well after an apparent collapse in the host leaf cells (Figure 4.9H). In an independent experiment, leaf tissue penetration occurred 1 dpi, invasion hyphae formed 3 dpi, and the fungi resided within the vascular buddle about 5 dpi.

To determine the primary penetration route taken by co-infecting Ptr and Pan, 20 penetration events were made each with three repeats. These used a detached leaf of Halberd. Leaves were observed 3, 6, and 12 h post-inoculation. When co-inoculated, Ptr entered the leaf 93% of the time through the stomata whilst Pan penetrated directly through the cuticle 95% of the time.

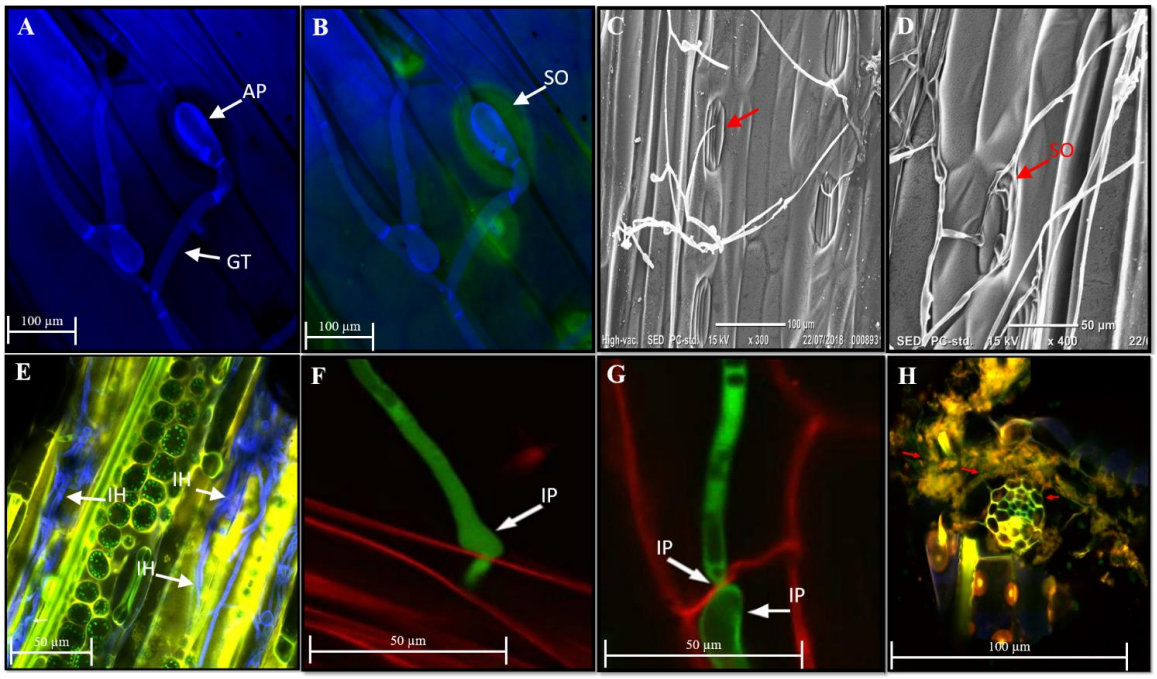

Figure 4.9. Cytological observation of the *in planta* co-inoculation by Ptr and Pan. Fungi were spray-inoculated on detached leaves of the wheat cultivar Halberd. Leaves were sectioned and visualised using a confocal and scanning electron microscopes. (A-D) indirect Ptr penetration of Halberd leaves via stomatal opening (SO). Invasion occurs using invasion point (IP) extended from hyphal germination tube (GT). Images are captured using a confocal microscope (A, B) and scanning electron microscope (C, D). (E) Invasion hyphae (IH) of Ptr residing within Halberd epidermal cells near the leaf surface. Pan invasion point (IP) penetrates Halberd leaf surfaces directly through the cuticle (F, G) and

fungal hyphae reside deep in the vascular bundles (H). Red arrows in H indicating Pan hyphae. Scale bars are shown on the images.

A targeted spot infection assay on detached leaves of Emu Rock was made by adding 20 µl inoculum, using a surgical pipette, in the middle of 9 cm leaves. Leaves were kept in high humidity until the infection was fully established and symptoms were evident. Infected leaves were then inserted into a thinly sliced 10 cm carrot such that the whole leaf was embedded within the carrot. Samples were obtained by slicing transversely through the carrot and the leaf. Leaf sections were labelled according to their distance from the infection spot. Leaf sections were stained and visualised using a confocal microscope. Ptr grew alongside the leaf sections and occupied a greater leaf area than Pan. Ptr was observed up to 3-cm each side of the inoculation spot (Figure 4.10A, C). Pan was only observed in the inoculation spots trapped within dense Ptr mycelium (Figure 4.10B). No evidence of Pan mycelium was observed beyond the inoculation points.

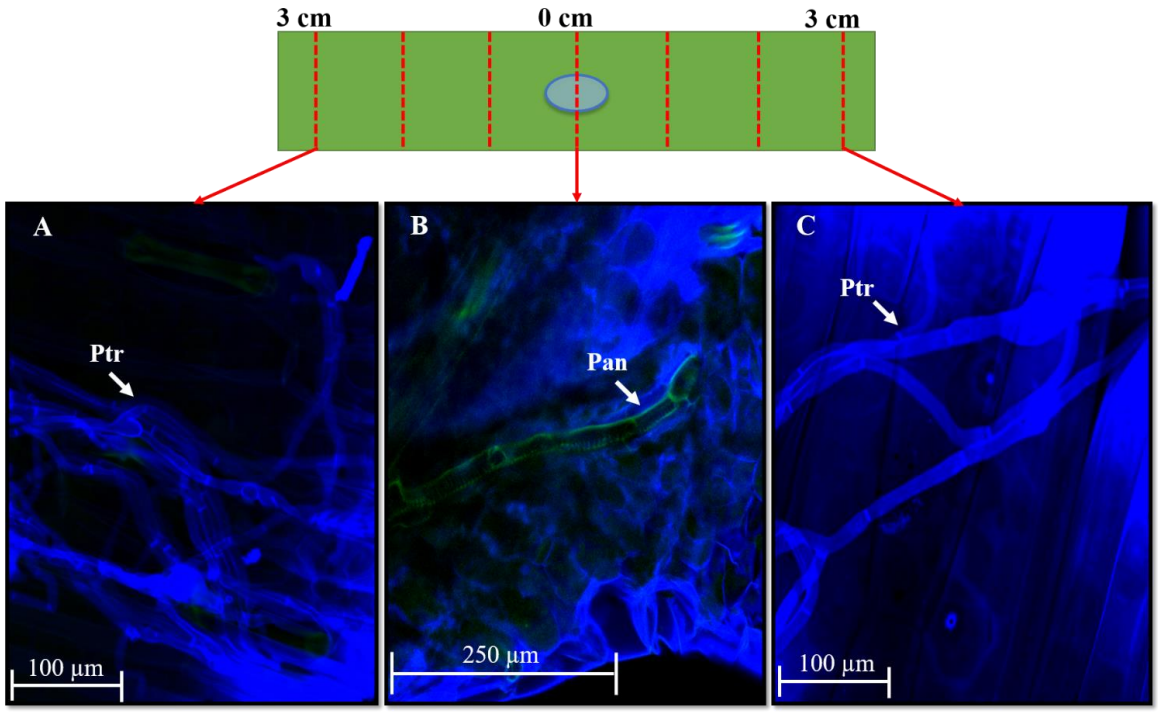

Figure 4.10. Cytological observation of the *in planta* spot infection assay (Experiment 5). Detached Emu Rock leaves (9 cm in length) were used in this experiment. One cm from each end of the leaf was removed to avoid leaf areas that were in direct contact with the benzimidazole agar. The remaining 7 cm of each leaf was sectioned as soon as the infection

was evident. Ptr hyphae grew alongside the leaf cuts and were visible on both ends of the cuts (A, C). Pan hyphae were only visible in the inoculation spot enclosed in thick Ptr mycelium (B). Images were captured using a confocal microscope and scale bars are shown on the images.

4.3.4 Ptr overgrows Pan on agar but does not completely inhibit Pan (Experiment 5)

To examine the interaction between Ptr and Pan, *in vitro* co-plating was achieved by placing two mycelium plugs in the middle of 9 cm PDA agar Petri-dishes. Plugs of Ptr and Pan were placed in direct contact adjacent to one another, and plates inoculated with plugs of only one species were used as controls. The diameter of the colonies was measured over time and was compared between single and co-plated inoculation. By 3 dpi, colony growth in co-plated Petri-dishes exceeded the total growth of Ptr and Pan combined (Figure 4.11A). Much of the observed growth on the co-plated dishes was typical of Ptr (white multinucleate mycelium with light grey centres). No signs of Pan (bright white mycelium) growth were visible on co-plated dishes throughout the experiment. By 6 dpi, colonies of the co-plated dishes reached maximum growth (8.2 ± 0.6 cm) and almost fully occupied the plates, over growing Ptr by 1.8 cm and Pan by 5.9 cm (Figure 4.11B). At this time point, Ptr colonies reached greater diameters than colonies of Pan (Figure 4.11B).

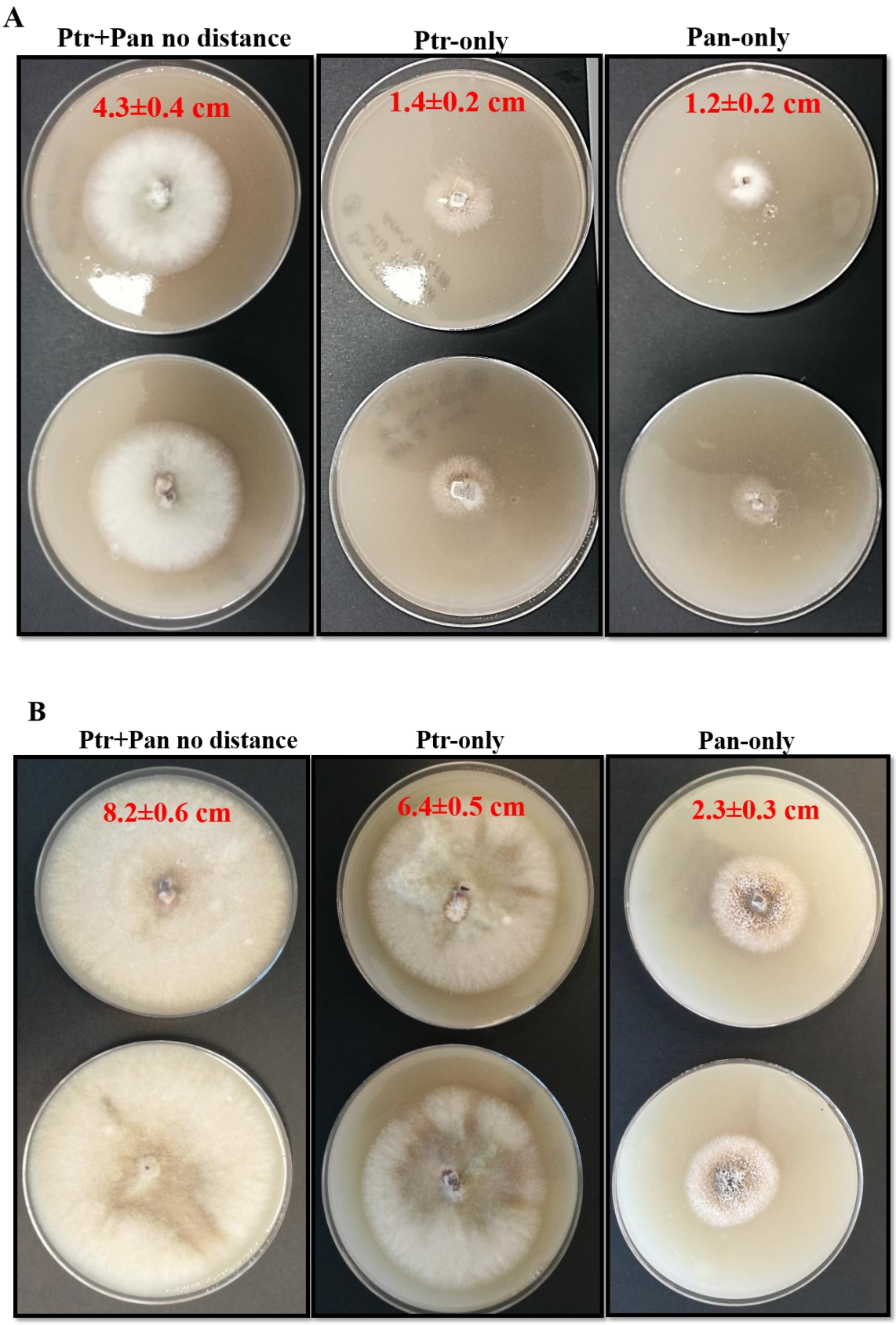
A
Ptr+Pan no distance
Ptr-only
Pan-only
4.3±0.4 cm
1.4±0.2 cm
1.2±0.2 cm
B
Ptr+Pan no distance
Ptr-only
Pan-only
8.2±0.6 cm
6.4±0.5 cm
2.3±0.3 cm

Figure 4.11. Colony of Ptr, Pan and their co-plating on PDA Petri-dishes (Experiment 5). Plates were inoculated by placing mycelium plugs in the centre of 9 cm dishes. Colony size was measured at (A) 3 dpi and (B) 6 dpi. Mean colony size ± standard deviation (*n*=4) are shown on the images. Images are shown in two repeats.

When plugs of Ptr and Pan were placed at distal ends of sides, there was evidence of Ptr-Ptr and Pan-Pan self-recognition. Of these plates, colonies of the same species that were placed at polar ends grew slower than when Ptr and Pan were placed at opposite ends (Figure 4.12). Colonies of both species grow normally with no sign of inhibition when Ptr and Pan were placed at polar ends of the slides (Figure 4.12). By 6 dpi, dishes that were plated by Ptr and Pan at distal ends of sides grew large colonies. Ptr growth on these plates was more than twice that of Pan (Figure 4.12). At the point of contact, where Ptr and Pan colonies met, there was no evidence of exclusion despite apparent signs of separation between the colonies of the two species (Figure 4.12).

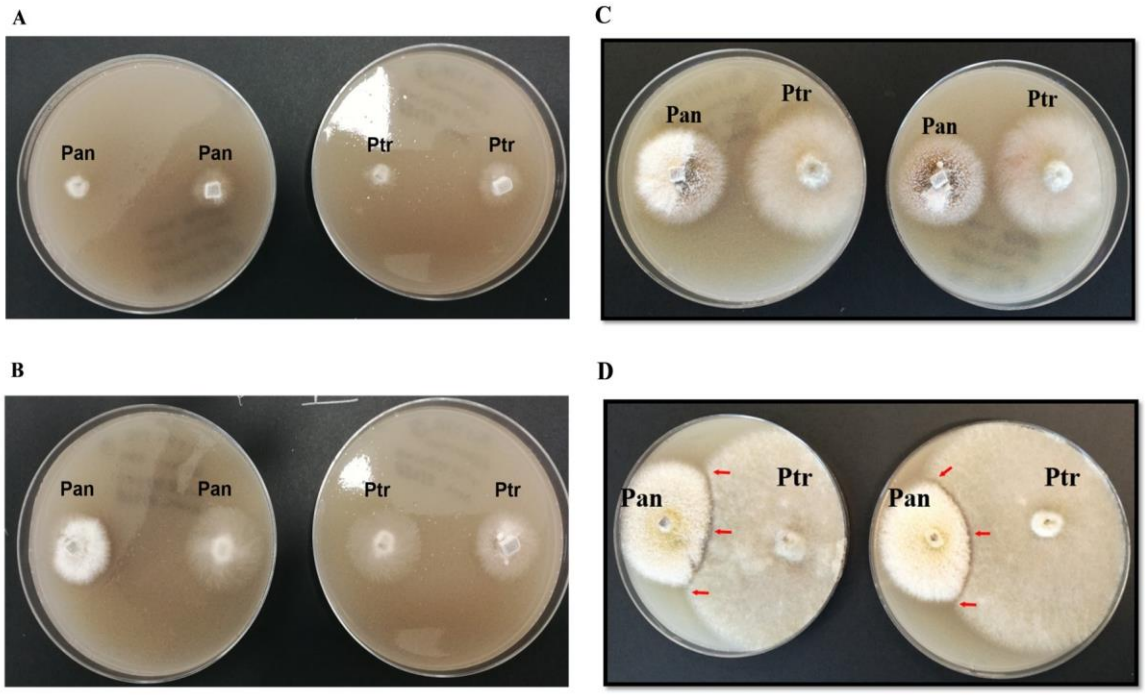

Figure 4.12. Self- and non-self-recognition of Ptr and Pan (Experiment 5). Colonies of the same species were grown on either end of PDA agar plates (A) 3 and (B) 6 dpi. Colony growth of Ptr and Pan plated on either end of agar plates at (C) 3 dpi (D) and 6 dpi. Red arrows indicate interaction front where colonies of Ptr and Pan come into direct contact.

4.4 Discussion

4.4.1 Co-inoculation by Ptr and Pan causes additive disease damage

Infections involving more than one pathogen species have rarely been studied despite their common occurrence and significance. This chapter investigated pathogen interactions in a pathosystem consisting of the host wheat and two foliar fungal pathogens: Ptr and Pan. These fungi are common in many parts of the world, individually causing the diseases tan spot and septoria nodorum blotch, respectively (Bhathal and Loughman, 2001). Together, they cause a leaf spot complex of wheat (Abdullah et al., 2018; Abdullah et al., 2020). Results show that the infection process of Ptr and Pan can be complemented in co-inoculated leaves causing accelerated and significant disease development in wheat seedlings grown under controlled-environment conditions. The underlying mechanisms for this complementation are unclear but it suggests a close co-evolutionary relationship between Ptr and Pan. This relationship is likely to be tripartite when the wheat host is included. Ptr and Pan epidemics occur annually in wheat fields (Oliver et al., 2016). The two species are likely to regularly come into direct contact, facilitating the exchange of genetic materials (Friesen et al., 2006). The potential for complementation between Ptr and Pan may provide an explanation for the success of these two species in causing widespread disease benefiting from a likely reshuffling of pathogenic alleles.

4.4.2 Ptr can rapidly develop and cause disease despite later arrival

Ptr achieved greater abundance under conditions of co-inoculation compared to abundance if inoculated as a single pathogen. This was consistent across almost all co-inoculation sequences with Ptr causing rapid disease development 3 dpi (Figure 4.1 and 4.2). The rapid increase in abundance of Ptr occurred well before any Pan symptoms were visible, suggesting that the effect may involve an interaction that is likely to occur during the latency period of Pan. This interaction may occur directly between Ptr and Pan or may be indirectly mediated by host responses. In contrast, Pan abundance in the co-inoculated leaves was limited and remained restricted throughout the experiment (Figure 4.4). The low abundance of Pan suggests that Ptr inoculation may be antagonistic to the Pan infection process. This potential antagonism between the two species occurred despite differences in the length of the inoculation sequence and was evident in both the *in vitro* and *in planta*

experiments. It is plausible that developing Ptr competes with Pan for growth-limiting resources hindering Pan's ability to obtain nutrients and slowing its growth.

The only situation where Pan dominated leaf infection was when inoculation of Ptr was delayed for 72 h after inoculation with Pan. During this time, Pan established a considerable abundance (Figure 4.2). Fully established Pan may be able to recondition host tissues disadvantaging later arriving Ptr. This is similar to the progression of Ascochyta blight complex in peas where prior inoculation of *Phoma medicaginis* has an antagonistic effect on *Mycosphaerella pinodes* development (Le May et al., 2009). It is also plausible that prior infection by Pan elicits host responses detrimental for later arriving Ptr as found in *Pseudomonas fluorescens* which provoke priming effect in Arabidopsis against subsequent bacterial challenge (Millet et al., 2010). In contrast, the earlier arrival of Ptr had no apparent effect on the outcomes of the infection as the speed of disease symptoms and development of disease were unaffected by the early inoculation of Ptr (Figure 4.3). This may be because early developing Ptr does not induce the infection-promoting plant responses induced by Pan or secret compounds that influence outcomes of the co-infection. Together, these results indicate that the interaction between Ptr and Pan may be influenced by the inoculation sequence and Pan may modulate Ptr virulence towards the host.

4.4.3 Niche differentiation may minimise overlap and enable Ptr-Pan co-infection

Ptr and Pan grew towards each other when plated apart on PDA agar slides forming interlocking mycelial networks (Figure 4.7). At confrontation zones where mycelia of both species met, there were no obvious signs of exclusion between Ptr and Pan. Both species grew actively whilst in contact with each other, despite the appearance of a clear separation zone between both pathogen colonies (Figure 4.11). Nonetheless, when Ptr and Pan were co-plated in the same spot, much of the growth was associated with Ptr (Figure 4.10). In fact, Ptr achieved greater growth from being in direct contact with Pan maintaining larger colonies and more rapid growth than when plated alone. These findings suggest that Ptr and Pan are able to endure each other's presence, and yet to be discovered mechanisms promote their co-infection. It is possible that a cell-to-cell signalling mechanism occurs causing growth complementation of Ptr when co-inoculated with Pan.

Spatial separation in tissues occupied by pathogens is one strategy enabling two species to co-exist (Fitt et al., 2006). Co-inoculated Ptr invaded shallow leaf tissues and remained visible within the epidermal cells of the wheat cultivar Emu Rock. Co-inoculated Pan invaded deeper leaf tissue layers of the same cultivar and remained visible within the vascular bundle (Figure 4.9). This difference in leaf tissue occupied may enable the two species to colonise separate niches within the leaf during the early phases of infection. This anatomical separation may enable co-infecting Ptr and Pan to coexist for at least some time– a strategy not previously identified. Such a niche segregation strategy may lessen competition but a level of contact between Ptr and Pan favours potential exchange of pathogenicity related genetic materials (Friesen et al., 2006). However, it is unclear if such an advantage would remain once necrosis occurs and leaf tissue integrity is lost.

There were also different rates and sites of leaf penetration between Ptr and Pan. Ptr entered detached Emu Rock leaves rapidly and predominately through the stomata (Figure 4.9). In contrast, Pan penetrated leaves at a slower rate and mostly via the cuticle (Figure 4.9). This allows co-infecting Ptr and Pan to follow different penetration routes leading to a minimum within tissue overlap and competition. The possibility of distinct communication signals similar to bacterial quorum sensing (Loh et al., 2002), enabling Ptr and Pan to split-leaf niches cannot be ruled out. When co-inoculated *in planta*, both species responded to each other by unknown mechanisms (Experiment 1 and 2). When co-inoculated in the same spot, Pan growth was restricted to the inoculation spots and Pan was unable to grow substantially beyond the point of inoculation (Experiment 5). This restricted growth of Pan mycelium may reflect Ptr competitive ability to influence hyphal growth of Pan. Whilst there was no evidence of avoidance in Pan vegetative growth or any signs of incompatibility, Pan growth *in vitro* was reduced when grown with Ptr.

4.5 Conclusions and prospects

This chapter investigated the consequences of co-inoculation on pathogen development and disease severity. The chapter uses two major fungal pathogens, Ptr and Pan, and their wheat host. Results suggest that Ptr and Pan can complement disease progress causing rapid and extensive damage of wheat leaves. This complementation is especially evident on susceptible wheat cultivars and is highly influenced by the inoculation order of Ptr and Pan. The link between inoculation order and severity of disease has implications for the onset

and epidemiology of Ptr and Pan in the field. If initial infection by one of these pathogens predisposes the host to further pathogenic attacks, disease control strategies can then be manipulated to account for this. Mechanisms for Ptr-Pan complementation were not studied directly in this chapter, although cytological observations point towards a unique anatomical separation in leaf tissue occupied potentially permitting Ptr-Pan co-infection. Hence, co-infecting Ptr and Pan may be viewed as an organisational complex. The fate of each pathogen in the complex may be influenced by interactions with the other co-infecting pathogen. These results highlight the need for a comprehensive understanding of co-infections on disease progress and pathogen development. Moreover, the effect of co-inoculation in accelerating the development of disease symptoms is consistent with preliminary experiments (Appendix 1). However, attempts to replicate the broader applicability of the results were not possible within the timeframe of this thesis. Further work should seek to replicate the results of this chapter exploring a broader host and pathogen range. Our understanding of the implications of co-infections on disease progress is in its infancy and while the focus of this chapter was Ptr-Pan, a range of other fungal diseases are known to co-infect wheat (Blixt et al., 2010). Future work needs to include a wider range of pathogens and assess their impact on wheat health.

References

Abdullah, A. S., Moffat, C. S., Lopez-Ruiz, F. J., Gibberd, M. R., Hamblin, J., and Zerihun, A. (2017). Host-multi-pathogen warfare: pathogen interactions in co-infected plants. *Frontiers in Plant Science* **8**, 1806.

Abdullah, A. S., Turo, C., Moffat, C. S., Lopez Ruiz, F. J., Gibberd, M. R., Hamblin, J., and Zerihun, A. (2018). Real-time PCR enables diagnosis of co-infection by two globally distributed fungi of wheat. *Frontiers in Plant Science* **9**, 1086.

Abdullah, A. S., Gibberd, M. R., Hamblin, J. 2020. Prevalence of co-infection of wheat by *Pyrenophora tritici-repentis* and *Parastagonospora nodorum* in the wheatbelt of Western Australia. *Crop and Pasture Science* **71**, 119-127.

Adhikari, K., and McIntosh, R. (1998). Susceptibility in oats to stem rust induced by co-infection with leaf rust. *Plant Pathology* **47**, 420-426.

Alizon, S. and Baalen, M. (2008). Multiple infections, immune dynamics, and the evolution of virulence. *The American Naturalist* **172**, E150-E168.

Alizon, S., de Roode, J. C., and Michalakis, Y. (2013). Multiple infections and the evolution of virulence. *Ecology Letters* **16**, 556-567.

Arfi, Y., Levasseur, A., and Record, E. (2013). Differential gene expression in *Pycnoporus coccineus* during interspecific mycelial interactions with different competitors. *Applied and Environmental Microbiology*. **79**, 6626-6636.

Benedikz, P., Mappledoram, C. J., and Scott, P. (1981). A laboratory technique for screening cereals for resistance to Septoria nodorum using detached seedling leaves. *Transactions of the British Mycological Society* **77**, 667-669.

Bhathal, J., and Loughman, R. (2001). Ability of retained stubble to carry-over leaf diseases of wheat in rotation crops. *Australian Journal of Experimental Agriculture* **41**, 649-653.

Bhathal, J., Loughman, R., and Speijers, J. (2003). Yield reduction in wheat in relation to leaf disease from yellow (tan) spot and septoria nodorum blotch. *European Journal of Plant Pathology* **109**, 435-443.

Blixt, E., Olson, A., Lindahl, B., Djurle, A., and Yuen, J. (2010). Spatiotemporal variation in the fungal community associated with wheat leaves showing symptoms similar to stagonospora nodorum blotch. *European Journal of Plant Pathology* **126**, 373-386.

Christensen, N., Nansen, P., Fagbemi, B., and Monrad, J. (1987). Heterologous antagonistic and synergistic interactions between helminths and between helminths and protozoans in concurrent experimental infection of mammalian hosts. *Parasitology Research* **73**, 387-410.

Conrath, U., Beckers, G. J., Flors, V., García-Agustín, P., Jakab, G., Mauch, F., Newman, M.-A., Pieterse, C. M., Poinssot, B., and Pozo, M. J. (2006). Priming: getting ready for battle. *Molecular Plant-Microbe Interactions* **19**, 1062-1071.

Cui, J., Bahrami, A. K., Pringle, E. G., Hernandez-Guzman, G., Bender, C. L., Pierce, N. E., and Ausubel, F. M. (2005). *Pseudomonas syringae* manipulates systemic plant

defenses against pathogens and herbivores. *Proceedings of the National Academy of Sciences* **102**, 1791-1796.

De Vos, M., Van Oosten, V. R., Van Poecke, R. M., Van Pelt, J. A., Pozo, M. J., Mueller, M. J., Buchala, A. J., Metraux, J.-P., Van Loon, L., and Dicke, M. (2005). Signal signature and transcriptome changes of Arabidopsis during pathogen and insect attack. *Molecular Plant-Microbe Interactions* **18**, 923-937.

DPIRD (2018). Wheat disease ratings update for 2018 *In* "Wheat disease ratings", Vol. 2019. Department of Primary Industries and Regional Development, Western Australia, Grains Research and Development Corporation.

Elena, S. F., Bernet, G. P., and Carrasco, J. L. (2014). The games plant viruses play. *Current Opinion in Virology* **8**, 62-67.

Estrada, A. E. R., Jonkers, W., Kistler, H. C., and May, G. (2012). Interactions between *Fusarium verticillioides*, *Ustilago maydis*, and *Zea mays*: an endophyte, a pathogen, and their shared plant host. *Fungal Genetics and Biology* **49**, 578-587.

Fitt, B. D., Huang, Y.-J., van den Bosch, F., and West, J. S. (2006). Coexistence of related pathogen species on arable crops in space and time. *Annual Review of Phytopathology* **44**, 163-182.

Fournier, V., Rosenheim, J. A., Brodeur, J., Diez, J. M., and Johnson, M. W. (2006). Multiple plant exploiters on a shared host: testing for non-additive effects on plant performance. *Ecological Applications* **16**, 2382-2398.

Friesen, T. L., Stukenbrock, E. H., Liu, Z., Meinhardt, S., Ling, H., Faris, J. D., Rasmussen, J. B., Solomon, P. S., McDonald, B. A., and Oliver, R. P. (2006). Emergence of a new disease as a result of interspecific virulence gene transfer. *Nature Genetics* **38**, 953-959.

Giraud, T., Yockteng, R., López-Villavicencio, M., Refrégier, G., and Hood, M. E. (2008). Mating system of the anther smut fungus *Microbotryum violaceum*: selfing under heterothallism. *Eukaryotic Cell* **7**, 765-775.

Glazebrook, J. (2005). Contrasting mechanisms of defense against biotrophic and necrotrophic pathogens. *Annual Review of Phytopathology* **43**, 205-227.

Hamilton, W. D. (1972). Altruism and related phenomena, mainly in social insects. *Annual Review of Ecology and Systematics* **3**, 193-232.

Hardin, G. (1968). The tragedy of the commons. *Science* **162**, 1243-1248.

Hobert, O. (2002). PCR fusion-based approach to create reporter gene constructs for expression analysis in transgenic *C. elegans*. *Biotechniques* **32**, 728-730.

Johnson, K. (1987). Defoliation, disease, and growth: a reply. *Phytopathology* **77**, 393-398.

Lamari, L., and Bernier, C. (1989). Evaluation of wheat lines and cultivars to tan spot [*Pyrenophora tritici-repentis*] based on lesion type. *Canadian Journal of Plant Pathology* **11**, 49-56.

Le May, C., Potage, G., Andrivon, D., Tivoli, B., and Outreman, Y. (2009). Plant disease complex: antagonism and synergism between pathogens of the Ascochyta blight complex on pea. *Journal of Phytopathology* **157**, 715-721.

Liu, Z., El-Basyoni, I., Kariyawasam, G., Zhang, G., Fritz, A., Hansen, J., Marais, F., Friskop, A., Chao, S., and Akhunov, E. (2015). Evaluation and association mapping of resistance to tan spot and Stagonospora nodorum blotch in adapted winter wheat germplasm. *Plant Disease* **99**, 1333-1341.

Loh, J., Pierson, E. A., Pierson III, L. S., Stacey, G., and Chatterjee, A. (2002). Quorum sensing in plant-associated bacteria. *Current Opinion in Plant Biology* **5**, 285-290.

López-Villavicencio, M., Jonot, O., Coantic, A., Hood, M. E., Enjalbert, J., and Giraud, T. (2007). Multiple infections by the anther smut pathogen are frequent and involve related strains. *Plos Pathogens* **3**, e176.

May, R. M., and Nowak, M. A. (1995). Coinfection and the evolution of parasite virulence. *Proceedings of the Royal Society of London. Series B: Biological Sciences* **261**, 209-215.

McGrann, G. R., Stavrinides, A., Russell, J., Corbitt, M. M., Booth, A., Chartrain, L., Thomas, W. T., and Brown, J. K. (2014). A trade off between mlo resistance to powdery mildew and increased susceptibility of barley to a newly important disease, Ramularia leaf spot. *Journal of Experimental Botany* **65**, 1025-1037.

Millet, Y. A., Danna, C. H., Clay, N. K., Songnuan, W., Simon, M. D., Werck-Reichhart, D., and Ausubel, F. M. (2010). Innate immune responses activated in Arabidopsis roots by microbe-associated molecular patterns. *The Plant Cell* **22**, 973-990.

Moffat, C., See, P. T., and Oliver, R. (2015). Leaf yellowing of the wheat cultivar Mace in the absence of yellow spot disease. *Australasian Plant Pathology* **44**, 161-166.

Murray, G. M., and Brennan, J. P. (2009). The current and potential costs from diseases of wheat in Australia," Grains Research and Development Corporation Canberra.

Oliver, R., Tan, K.-C., and Moffat, C. 2016. Necrotrophic pathogens of wheat. In: Wrigkey, C.W., Corke, H., Seetharaman, K. and Faubion, J., (eds) *Encyclopedia of Food Grains*, 2nd Edition, pp. 273-278. Oxford: Academic Press.

Oliver, R., X. Cai, R.-C. Wang, S. S. Xu, and Friesen, T. L. (2008). Resistance to tan spot and stagonospora nodorum blotch in wheat-alien species derivatives. *Plant Disease* **92**, 150-157.

Pedersen, A. B., and Fenton, A. (2007). Emphasizing the ecology in parasite community ecology. *Trends in Ecology and Evolution* **22**, 133-139.

Pijls, C., Shaw, M., and Parker, A. (1994). A rapid test to evaluate *in vitro* sensitivity of *Septoria tritici* to flutriafol, using a microtitre plate reader. *Plant Pathology* **43**, 726-732.

Savary, S., and Zadoks, J. (1992). Analysis of crop loss in the multiple pathosystem groundnut-rust-late leaf spot. III. Correspondence analyses. *Crop Protection* **11**, 229-239.

Seabloom, E. W., Borer, E. T., Gross, K., Kendig, A. E., Lacroix, C., Mitchell, C. E., Mordecai, E. A., and Power, A. G. (2015). The community ecology of pathogens: coinfection, coexistence and community composition. *Ecology Letters* **18**, 401-415.

Sexton, A., and Howlett, B. (2001). Green fluorescent protein as a reporter in the Brassica–*Leptosphaeria maculans* interaction. *Physiological and Molecular Plant Pathology* **58**, 13-21.

Skidmore, A., and Dickinson, C. (1976). Colony interactions and hyphal interference between *Septoria nodorum* and phylloplane fungi. *Transactions of the British Mycological Society* **66**, 57-64.

Solomon, P. S., Wilson, T. G., Rybak, K., Parker, K., Lowe, R. G., and Oliver, R. P. (2006). Structural characterisation of the interaction between *Triticum aestivum* and the dothideomycete pathogen *Stagonospora nodorum*. *European Journal of Plant Pathology* **114**, 275-282.

Susi, H., Barrès, B., Vale, P. F., and Laine, A.-L. (2015). Co-infection alters population dynamics of infectious disease. *Nature Communications* **6**, 5975.

Syller, J. (2012). Facilitative and antagonistic interactions between plant viruses in mixed infections. *Molecular Plant Pathology* **13**, 204-216.

Tack, A. J., Thrall, P. H., Barrett, L. G., Burdon, J. J., and Laine, A. L. (2012). Variation in infectivity and aggressiveness in space and time in wild host–pathogen systems: causes and consequences. *Journal of Evolutionary Biology* **25**, 1918-1936.

Tollenaere, C., Susi, H., and Laine, A.-L. (2016). Evolutionary and epidemiological implications of multiple infection in plants. *Trends in Plant Science* **21**, 80-90.

van Baalen, M., and Sabelis, M. W. (1995). The dynamics of multiple infection and the evolution of virulence. *The American Naturalist* **146**, 881-910.

Yelton, M. M., Hamer, J. E., and Timberlake, W. E. (1984). Transformation of *Aspergillus nidulans* by using a trpC plasmid. *Proceedings of the National Academy of Sciences* **81**, 1470-1474.

5 General Discussion

This thesis investigated pathogen interactions and their consequences for disease development in co-infected plants. Throughout the research chapters, a tripartite pathosystem involving the wheat host and two fungal species: *Pyrenophora tritici-repentis* (Ptr) and *Parastagonospora nodorum* (Pan) was used. These fungi infect the foliar parts of the plant causing yield loss by reducing leaf area available for photosynthesis (Bhathal et al. 2003; Johnson 1987; Salam et al. 2013). Ptr and Pan occur in many wheat regions and are thought to co-occur at times (Blixt et al. 2010). The combined annual yield loss to these fungi is estimated to cost Western Australian wheat growers about $220 million (Murray and Brennan 2009). Despite their importance as diseases, existing diagnostic tools for Ptr and Pan lack specificity and can produce false-negatives (Abdullah et al. 2018). Emerging molecular diagnostic methods have the potential to overcome specificity issues and provide improved accuracy for concurrent quantification for both Ptr and Pan.

In this thesis, a duplex quantitative polymerase chain reaction method (qPCR) was developed (chapter 2). The method enabled simultaneous detection and quantification of both Ptr and Pan in co-infected leaves (Abdullah et al. 2018). Analysis of fungal abundance, using the qPCR method, suggests that Ptr and Pan frequently co-infect wheat in Western Australia. In fact, this co-occurrence was the observed state occurring in 94% of samples (chapter 3). Co-inoculated Ptr and Pan are able to complement their infection process and this was associated with an increase in Ptr's aggressiveness towards the host (chapter 4). Co-inoculated leaves had rapid symptom development and exacerbated disease damage compared to inoculation with either of the pathogens alone. Histological evidence points towards a unique anatomical separation in tissues occupied that is likely to enable Ptr-Pan co-infection. Such anatomical separation of infection within leaf tissues has not been reported previously for these, or any other fungal pathogen complexes.

5.1 qPCR as a tool for detection of co-infecting Ptr and Pan

Detection of fungal pathogens usually relies on distinguishing certain visual features following isolation and culturing on growth media (Lelliott and Stead, 1987). Such methods, although still used for detection of Ptr and Pan, provide information on pathogen

identity but can produce false-negatives when a pathogen is in low abundance or unable to be cultured (Abdullah et al., 2018). Methods using qPCR are well suited for measuring pathogen abundance while providing species specificity (Bates et al., 2001; Holland et al., 1991; Schena et al., 2006). Successful qPCR-based assays have been developed for Ptr and Pan, albeit independently, utilising genomic regions specific to each pathogen (Oliver et al., 2008; See et al., 2016). Due to the cost of labour and resources required to perform separate assays for Ptr and Pan independently, the previously developed methods have been limited to small-scale investigations. Large-scale field studies of co-infection by Ptr and Pan, and other pathogens, require methods that simultaneously detect both species and determine their relative contribution to the overall disease level in a sample. Simultaneous detection also allows greater experimental precision as it inherently incorporates any sources of error that may otherwise occur in isolation during separate assays.

To address the need for simultaneous detection, a duplex qPCR assay was developed that detects and quantifies the presence of Ptr and Pan in wheat leaves. The basis of this assay is the use of two probes that were developed to bind to the middle of selected, unique, genomic sequences of Ptr and Pan. For additional specificity, the probes were also differentially tagged with fluorogenic reporters allowing the simultaneous detection and quantification of Ptr and Pan (Abdullah et al. 2018). This assay enabled the prevalence of Ptr and Pan and their co-infection dynamics to be investigated. Furthermore, the method is able to provide quantitative data on Ptr-Pan relative abundance, equipping researchers with a tool to survey the prevalence of these pathogens in response to various growing conditions and fungicide applications. Although this assay was specifically designed for Ptr and Pan, the framework developed can also be applied to other pathogen species or pathotypes. Further advancement of the assay is required to improve automation, the ability to distinguish between DNA from living and dead cells as well as the number of pathogen targets that can be accommodated in an assay.

5.2 Prevalence of Ptr-Pan co-infection in wheat fields

Results presented in this thesis confirmed that co-infection of Ptr and Pan is widespread in wheat fields of Western Australia. Of this co-infection, Ptr's abundance was greater early in the season while Pan's relative abundance increased during booting and early flowering.

This difference in relative abundance suggests that Ptr-Pan co-infection is dynamic and time is likely to be important when examining their relative contributions to this disease complex. This has important implications for disease management strategies in that targeting only one component of the complex may not necessarily result in successful overall disease management. Due to the stubble borne nature of Ptr and Pan, management of wheat stubble is likely to be equally effective against both pathogens. More research is required to test the efficacy of our current agrochemicals at managing the Ptr-Pan complex.

Despite the difference in abundance, 94% of the surveyed wheat leaves contained DNA of both Ptr and Pan. This suggests that Ptr and Pan are likely to occur as a complex, although this remains to be spatiotemporally tested across a broader range of sites and seasons. Ptr and Pan may play a role in each other's pathogenicity. This is a fertile area for future investigations. Recent work confirmed the existence of a common transcription factor that regulates the expression of ToxA in Ptr and Pan (Rybak et al. 2017). Disruption of this transcription factor strongly reduces Ptr and Pan virulence on wheat (Rybak et al. 2017). Since pathogenicity-related toxins are known to be mainly secreted extracellularly (Geny and Popoff 2006; Pugsley et al. 1990), there is an opportunity for co-infecting Ptr and Pan to modify host environments to their mutual advantage. This hypothesis can be tested by doing parallel co-inoculation experiments with mutants of Ptr and Pan lacking the ability to produce ToxA (Liu et al. 2006; Moffat et al. 2014).

5.3 Impacts of wheat cultivar on the prevalence of Ptr and Pan

One objective of this thesis was to evaluate the impact of wheat cultivar resistance on Ptr-Pan co-infection. Regardless of the resistance of the cultivar, co-infection by Ptr and Pan was very common. In the conditions studied, Ptr was either as or more abundant than Pan despite the reported differences in cultivar resistance. These findings raise questions about the effectiveness of widely-used disease rating systems which consider infection by either Ptr or Pan alone. It is recommended that cultivar assessment for Ptr and Pan should consider that co-infection is likely to be the common state under field conditions. Furthermore, breeding for resistance to the diseases caused by Ptr and Pan simultaneously may provide significantly improved protection for farmers. Recent development in genetic markers for sensitivity to both Ptr and Pan effectors may greatly assist breeders in achieving this

outcome (Oliver et al., 2016). Further studies are required to examine the effects of known sensitivity/resistance QTLs under co-infection conditions. It may be possible that the adoption of certain sensitivity/resistance QTLs may shift the dynamics in favour of one or more of the co-infecting pathogens. For example, certain alleles of the *Mlo* gene are widely used for resistance to powdery mildew in barley. Lines carrying this allele are known to be susceptible to other diseases such as Ramularia leaf spot. Ramularia leaf spot has become a significant barley disease over the period of *Mlo* deployment (McGrann et al. 2014; Wolter et al. 1993).

5.4 Co-inoculated Ptr and Pan complement their infection

Results presented in chapter 4 suggest that Ptr and Pan can complement their infection in co-inoculated wheat leaves causing more rapid development of disease symptoms. The underlying mechanisms for this complementation are unclear but suggest that Ptr and Pan are likely to play a role in accelerating the development of symptoms in co-infected leaves. A broad range of interactions may occur between co-infecting fungi. These can result in changes to mycelial morphology at the interaction points, changes in metabolism and secretion of synergistic enzymes; these are not mutually exclusive (Arfi et al. 2013; Baldrian 2004; Lamichhane and Venturi 2015). Nevertheless, observation from the *in vitro* experiments did not show changes in mycelial morphology at the point of contact between Ptr and Pan when both species were growing in close proximity to each other. In doing so, the rate of growth of Ptr appears to increase in the presence of Pan. Ptr and Pan epidemics occur annually in wheat fields (Oliver et al. 2016), and as shown in chapter 3, Ptr-Pan co-infection is widespread in Western Australia. Thus, the two species regularly come into direct contact with each other which may enable the exchange of genetic material (Friesen et al. 2006). This strongly suggests that in regions where Ptr and Pan co-occur, they should be targeted as a complex for effective disease management efforts.

Regardless of which pathogen was inoculated first, Ptr nearly always reached greater abundance when co-inoculated with Pan. The only exception, where Pan overgrew Ptr, was when Ptr's inoculum was delayed for 72 hrs after inoculation with Pan. Delayed inoculation of Ptr may have provided a window of opportunity for Pan to establish. Established Pan may have re-conditioned host tissues or secreted anti-fungal compounds interfering with

the later arrival of Ptr. It is also possible that prior inoculation by Pan elicits host responses detrimental to later arriving Ptr. If true, this has potential implications for managing the interaction between Ptr and Pan. If prior infection by Pan produces defence signals that protect wheat against later arriving Ptr, treatment of plants by a non-pathogenic Pan isolate may reduce the damage caused by the subsequent arrival of Ptr. Further research is required to test whether early infection by non-pathogenic Pan breaks down Ptr's ability to cause significant disease.

5.5 Mechanisms allowing Ptr-Pan co-infection

Cytological observations presented in chapter 4 demonstrated the existence of an anatomical separation in niches that may enable co-infecting Ptr and Pan to occupy adjacent leaf tissues. Co-inoculated Ptr invaded the upper parts of the leaf and remained visible in the epidermal cells. In contrast, co-inoculated Pan invaded deeper leaf tissues and resided mainly in the vascular bundles. Although Ptr and Pan may invade the same leaf, each species may extract nutrients whilst occupying different spaces, at least during the early stages of infection (i.e. prior to necrosis). This minimises spatial and environmental overlap of the species and reduces the magnitude of direct competition. However, it is also plausible for the tissue separation to be transient, and at later stages of the infection, niches may overlap or merge. Nevertheless, if tissue separation is common between Ptr and Pan, then two types of niches may be realised: (i) Ecological niche (i.e. leaves in which both species co-occur), (ii) functional niches (i.e. tissues in which each pathogen resides). What regulates such separation in niches remains a mystery, but it may indicate the existence of some type of cell-to-cell communication allowing co-infecting Ptr and Pan to invade different tissues. It is also plausible that Ptr may be adapted to invade epidermal cells that are closer to external environments (ambient air and temperature), while Pan may be more adapted to temperature-regulated, less exposed leaf tissues of the vascular bundles. It is possible that as the pathogens enter their necrotrophic phase, the structure of the infected plant tissues collapses. Niches may overlap as a result. However, no attempt was made to separate niches in necrotic vs non-necrotic leaf tissues. Therefore, cytological observation of a whole leaf may have masked the finer detail of interactions within the leaf tissue.

Nonetheless, separation of tissues occupied by Ptr and Pan, assuming it is not transient, represents a barrier that prevents direct gene flow between the two species favouring non-direct exchange of genetic materials. However, given that the experiments presented in chapter 4 were done under controlled-environment conditions, it is not possible to define or rule out that different environmental effects may regulate niche separation. For example, the constant temperature conditions may have favoured the two species to use different penetration strategies and there may have been no necessity for Ptr and Pan to compete. Under field conditions, species are likely to use different adaptation strategies to cope with ever-changing conditions and compete to maximise infection potential. Furthermore, relationships between isolates, although beyond the scope of this thesis, are also known to regulate pathogen interactions in a kin-selective manner (Griffin et al. 2004). Relatives and closely related species can interact altruistically in favour of each other's reproduction (see section 2.5). Although isolates of Ptr and Pan, used in chapter 4, were collected from two separate, widely spaced farm sites in Western Australia, there is no data on their co-occurrence. These isolates may frequently come into close contact facilitating indirect bonds, minimising their competition. Therefore, future works should include a broader range of isolates that better reflect both the local and global distribution of Ptr and Pan.

Preceding the experiments presented in chapter 4, a preliminary co-inoculation experiment was undertaken. This experiment consistently demonstrated the impact of co-infection on accelerating symptom development (Appendix 1). Two further attempts were made to repeat experiments under glasshouse conditions with a focus on the molecular analysis of pathogen growth. However, these attempted-repeats generated inconclusive results as the plants were dominated by a biotroph infection (Appendix 2). Despite the inconclusive repeats, experiments presented in chapter 4 used various infection protocols (whole plant assay, detached leaf assay, and various *in vitro* protocols) and microscopic techniques (optical, confocal and scanning electron microscope). These provided co-supporting results and confidence in the primary observation of chapter 4 that co-infection by Ptr and Pan leads to accelerated disease development in wheat seedlings. When considered in conjunction with the data from the field samples in chapter 3, there is still much to be learned on how various pathogens interact with the host and environment. Mechanisms that allow different pathogens to co-infect a host are an exciting area for future research.

6 General Conclusions and Prospects

In this thesis, plant co-infection by more than one pathogen species was studied. The studies bridge the gap between the heterogeneity of diseases in the field and molecular pathology. A tripartite pathosystem consisted of the wheat host and two fungi: *Pyrenophora tritici-repentis* (Ptr) and *Parastagonospora nodorum* (Pan) was used. These fungi occur annually in many wheat regions and are thought to co-occur at times. Symptoms caused by these fungi are very similar and difficult to distinguish visually (Abdullah et al. 2018). More accurate molecular methods were developed for the detection of Ptr independent of Pan (Oliver et al. 2008; See et al. 2016). Methods to separately detect Ptr and Pan are not efficient for large-scale field investigations. This created a gap for a method that can detect and quantify both pathogens simultaneously.

A molecular method that simultaneously detects and quantifies the presence of Ptr and Pan in a sample was developed and used throughout the thesis. The method provided an opportunity to conduct a field survey to study the prevalence of co-infection by Ptr and Pan across three widely-spaced field sites in Western Australia. Results showed that co-infection by Ptr and Pan is prevalent and likely to be the commonplace. In regions where Ptr and Pan are prevalent, they are likely to form a complex with varying relative contribution depending on sampling time, climatic conditions and wheat cultivar. Management strategies targeting Ptr or Pan alone have not proven very successful in reducing the annual impact of these pathogens on wheat yield (Bhathal et al. 2003). Therefore, targeting these pathogens as a complex may be more effective at reducing Ptr and Pan's joint impacts. Methods that reduce pathogen population densities (e.g. management of stubble) may assist in controlling this complex.

The effect of wheat cultivar resistance on the prevalence of Ptr-Pan co-infection was evaluated. Regardless of the resistance level of the cultivars, Ptr and Pan caused measurable disease damage. Under field conditions, Ptr was either as or more abundant than Pan despite the reported differences in cultivar resistance ratings. Under controlled-environment conditions, Ptr usually dominated the infection. Cultivar resistance ratings under single infection, for Ptr or Pan, may not reflect rating under co-infection. Ratings need to be re-calibrated under conditions of both individual pathogen and joint co-infection. Fortunately,

a method to perform simultaneous assessments of Ptr and Pan is now available (Abdullah et al. 2018). This can be used for more accurate and rapid screening of cultivar responses to these pathogens. Furthermore, the stability of resistance in the wheat cultivar Magenta against Ptr and Pan was evident across studies and under various growing conditions and plant ages. More research is required to understand mechanisms of resistance in this cultivar, to Ptr, Pan and their co-infection. Also, does this resistance have a yield penalty under field conditions?

Whilst the role of co-infection on the evolution of virulence has been widely investigated (Alizon et al. 2013; van Baalen and Sabelis 1995), the impact of co-infection on disease development and severity is less studied (Clement et al. 2012; Fitt et al. 2006). This thesis used a range of molecular, histological and cytological approaches to study disease development and severity of Ptr-Pan co-inoculation. Results suggest that Ptr and Pan can complement the infection of co-inoculated leaves causing more rapid and extensive disease damage. This is most evident in susceptible wheat cultivars and is highly influenced by the inoculation sequence of Ptr and Pan. Mechanisms governing this complementation are unclear, but cytological evidence points towards an anatomical separation in leaf tissue occupied that may enable Ptr-Pan co-existence. This finding opens up new avenues to explore the complexity of co-infections in plant pathosystems. Wheat hosts a large range of microbes and many are known to be pathogenic (Blixt et al. 2010). We are only at the very beginning of addressing the less-studied topic of co-infection. Understanding how Ptr and Pan interact with other pathogens or microbes appears a fertile area for future investigations.

References

Abdullah, A. S., Turo, C., Moffat, C. S., Lopez-Ruiz, F. J., Gibberd, M. R., Hamblin, J., and Zerihun, A. (2018). Real-time PCR for diagnosing and quantifying co-infection by two globally distributed fungal pathogens of wheat. *Frontiers in Plant Science* **9**, 1068.

Alizon, S., de Roode, J. C., and Michalakis, Y. (2013). Multiple infections and the evolution of virulence. *Ecology Letters* **16**, 556-567.

Arfi, Y., Levasseur, A., and Record, E. (2013). Differential gene expression in *Pycnoporus coccineus* during interspecific mycelial interactions with different competitors. *Applied and Environmental Microbiology* **79**, 6626-6636.

Baldrian, P. (2004). Increase of laccase activity during interspecific interactions of white-rot fungi. *FEMS Microbiology Ecology* **50**, 245-253.

Bates, J., Taylor, E., Kenyon, D., and Thomas, J. (2001). The application of real-time PCR to the identification, detection and quantification of *Pyrenophora* species in barley seed. *Molecular Plant Pathology* **2**, 49-57.

Bhathal, J., Loughman, R., and Speijers, J. (2003). Yield reduction in wheat in relation to leaf disease from yellow (tan) spot and septoria nodorum blotch. *European Journal of Plant Pathology* **109**, 435-443.

Blixt, E., Olson, Å., Lindahl, B., Djurle, A., and Yuen, J. (2010). Spatiotemporal variation in the fungal community associated with wheat leaves showing symptoms similar to stagonospora nodorum blotch. *European Journal of Plant Pathology* **126**, 373-386.

Clement, J. A., Magalon, H., Glais, I., Jacquot, E., and Andrivon, D. (2012). To be or not to be solitary: *Phytophthora infestans*' dilemma for optimizing its reproductive fitness in multiple infections. *Plos One* **7**, e37838.

Fitt, B. D., Huang, Y.-J., van den Bosch, F., and West, J. S. (2006). Coexistence of related pathogen species on arable crops in space and time. *Annual Review of Phytopathology* **44**, 163-182.

Friesen, T. L., Stukenbrock, E. H., Liu, Z., Meinhardt, S., Ling, H., Faris, J. D., Rasmussen, J. B., Solomon, P. S., McDonald, B. A., and Oliver, R. P. (2006). Emergence of a new disease as a result of interspecific virulence gene transfer. *Nature Genetics* **38**, 953.

Geny, B., and Popoff, M. R. (2006). Bacterial protein toxins and lipids: pore formation or toxin entry into cells. *Biology of the Cell* **98**, 667-678.

Griffin, A. S., West, S. A., and Buckling, A. 2004. Cooperation and competition in pathogenic bacteria. *Nature* **430**:1024-1030.

Holland, P. M., Abramson, R. D., Watson, R., and Gelfand, D. H. (1991). Detection of specific polymerase chain reaction product by utilizing the 5'----3'exonuclease activity of *Thermus aquaticus* DNA polymerase. *Proceedings of the National Academy of Sciences of the United States of America* **88**, 7276-7280.

Johnson, K. (1987). Defoliation, disease, and growth: a reply. *Phytopathology* **77**, 393-398.

Lamichhane, J. R., and Venturi, V. (2015). Synergisms between microbial pathogens in plant disease complexes: a growing trend. *Frontiers in Plant Science* **6**, 385.

Lelliott, R. A., and Stead, D. E. (1987). Methods for the diagnosis of bacterial diseases of plants, In: Preece TF, ed. *Methods in Plant Pathology* Vol. 2. Oxford, the UK: Blackwell Scientific Publications 215 pp.

Liu, Z., Friesen, T. L., Ling, H., Meinhardt, S. W., Oliver, R. P., Rasmussen, J. B., and Faris, J. D. (2006). The Tsn1–ToxA interaction in the wheat–*Stagonospora nodorum* pathosystem parallels that of the wheat–tan spot system. *Genome* **49**, 1265-1273.

McGrann, G. R., Stavrinides, A., Russell, J., Corbitt, M. M., Booth, A., Chartrain, L., Thomas, W. T., and Brown, J. K. (2014). A trade off between mlo resistance to powdery mildew and increased susceptibility of barley to a newly important disease, Ramularia leaf spot. *Journal of Experimental Botany* **65**, 1025-1037.

Moffat, C. S., See, P. T., and Oliver, R. P. (2014). Generation of a ToxA knockout strain of the wheat tan spot pathogen *Pyrenophora tritici-repentis*. *Molecular Plant Pathology* **15**, 918-926.

Murray, G. M., and Brennan, J. P. 2009. Estimating disease losses to the Australian wheat industry. *Australasian Plant Pathology* **38**, 558-570.

Oliver, R., Tan, K.-C., and Moffat, C. 2016. Necrotrophic pathogens of wheat. In: Wrigkey, C.W., Corke, H., Seetharaman, K. and Faubion, J., (eds) *Encyclopedia of Food Grains*, 2nd Edition, pp. 273-278. Oxford: Academic Press.

Oliver, R. P., Rybak, K., Shankar, M., Loughman, R., Harry, N., and Solomon, P. (2008). Quantitative disease resistance assessment by real-time PCR using the *Stagonospora nodorum*-wheat pathosystem as a model. *Plant Pathology* **57**, 527-532.

Pugsley, A. d., d'Enfert, C., Reyss, I., and Kornacker, M. (1990). Genetics of extracellular protein secretion by gram-negative bacteria. *Annual Review of Genetics* **24**, 67-90.

Rybak, K., See, P. T., Phan, H. T., Syme, R. A., Moffat, C. S., Oliver, R. P., and Tan, K. C. (2017). A functionally conserved Zn2Cys6 binuclear cluster transcription factor class regulates necrotrophic effector gene expression and host-specific virulence of two major *Pleosporales* fungal pathogens of wheat. *Molecular Plant Pathology* **18**, 420-434.

Salam, K. P., Thomas, G. J., Beard, C., Loughman, R., MacLeod, W. J., and Salam, M. U. (2013). Application of meta-analysis in plant pathology: a case study examining the impact of fungicides on wheat yield loss from the yellow spot—septoria nodorum blotch disease complex in Western Australia. *Food Security* **5**, 319-325.

Schena, L., Hughes, K. J., and Cooke, D. E. (2006). Detection and quantification of *Phytophthora ramorum*, *P. kernoviae*, *P. citricola* and *P. quercina* in symptomatic leaves by multiplex real-time PCR. *Molecular Plant Pathology* **7**, 365-379.

See, P. T., Moffat, C. S., Morina, J., and Oliver, R. P. (2016). Evaluation of a multilocus Indel DNA region for the detection of the wheat tan spot pathogen *Pyrenophora tritici-repentis*. *Plant Disease* **100**, 2215-2225.

van Baalen, M., and Sabelis, M. W. (1995). The dynamics of multiple infection and the evolution of virulence. *The American Naturalist* **146**, 881-910.

Wolter, M., Hollricher, K., Salamini, F., and Schulze-Lefert, P. (1993). The mlo resistance alleles to powdery mildew infection in barley trigger a developmentally controlled defence mimic phenotype. *Molecular and General Genetics* **239**, 122-128.

Appendix 1 – Preliminary experiment

Two wheat cultivars were evaluated in this experiment: Calingiri and Janz. These cultivars provide contrasting resistant ratings to the diseases caused by Ptr and Pan (Shackley et al., 2013). Treatment structure was: (1) Ptr only, (2) Pan only, (3) Ptr + Pan simultaneously, (4) Ptr + Pan 24h later, (5) Pan + Ptr 24h later and (6) mock-inoculation control. Plants were grown for 6 weeks and then spray-inoculated as described in section 4.2.3. Leaves were scored for diseased leaf area and sampled as described in section 4.2.3. Synchronous co-inoculation with Ptr and Pan reduced the days required for symptoms to appear, resulting in increased disease damage compared to single inoculation with either Ptr or Pan (Figure S1A, B). Asynchronous inoculation with Pan 24 h prior to Ptr inoculation also reduced the time required for symptom appearance resulting in increased disease damage. The reverse order, Ptr then Pan 24 h later did not lead to the same results (Figure S1A, B).

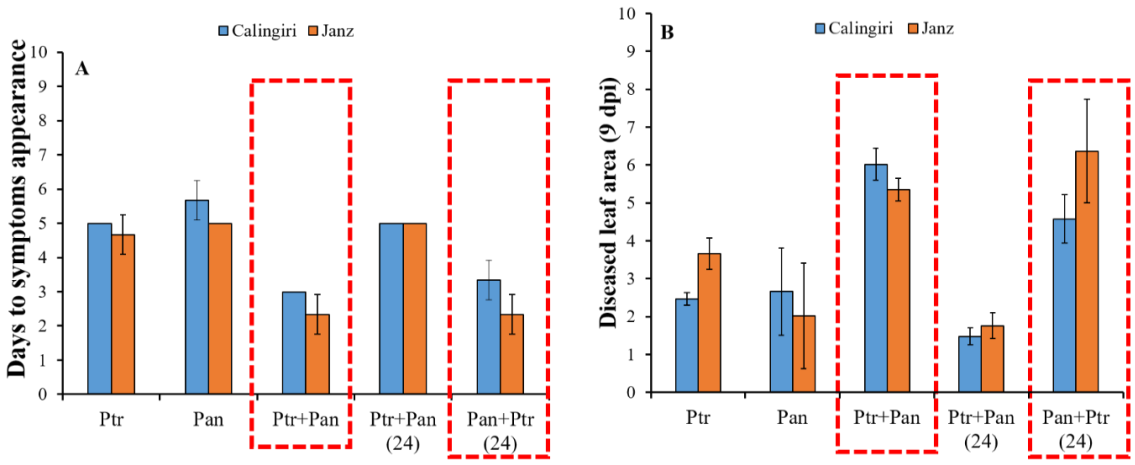

Figure S1. Results of a preliminary co-inoculation experiment using the wheat cultivars Calingiri and Janz. Six-week-old seedlings were used in this experiment. (A) Days from inoculation until 50% of the inoculated plants showed disease symptoms. (B) Disease damage scores (0 to 10 scale) measured 9 days post-inoculation (dpi). Data are means ± standard deviation (*n*=6). Leaf samples were collected but no molecular analysis was done due to failure of laboratory equipment.

Appendix 2 – Reduce set repeat

Two independent co-inoculation experiments were done in the same glasshouse conditions described in section 4.2.3. Four treatments were selected: (1) Ptr + Pan simultaneously, (2) Ptr + Pan 24h later, (3) Pan + Ptr 24h later and (4) mock inoculation – no disease. The main objective of these experiments was to validate (i) whether the more rapid disease development observed following Ptr-Pan co-inoculation, is reproducible and (ii) if the order of the inoculation influences disease outcomes. Plants were grown for four weeks and then spray-inoculated as described in section 4.2.3. The wheat cultivar Emu Rock was used in both experiments (Table 4.1). Results from these experiments are shown in Figure S2. Contaminating infection with non-target biotrophic wheat diseases prevented conclusive results from being acquired. No DNA analysis was carried out as a result. Due to time constraint, no further repeats were made.

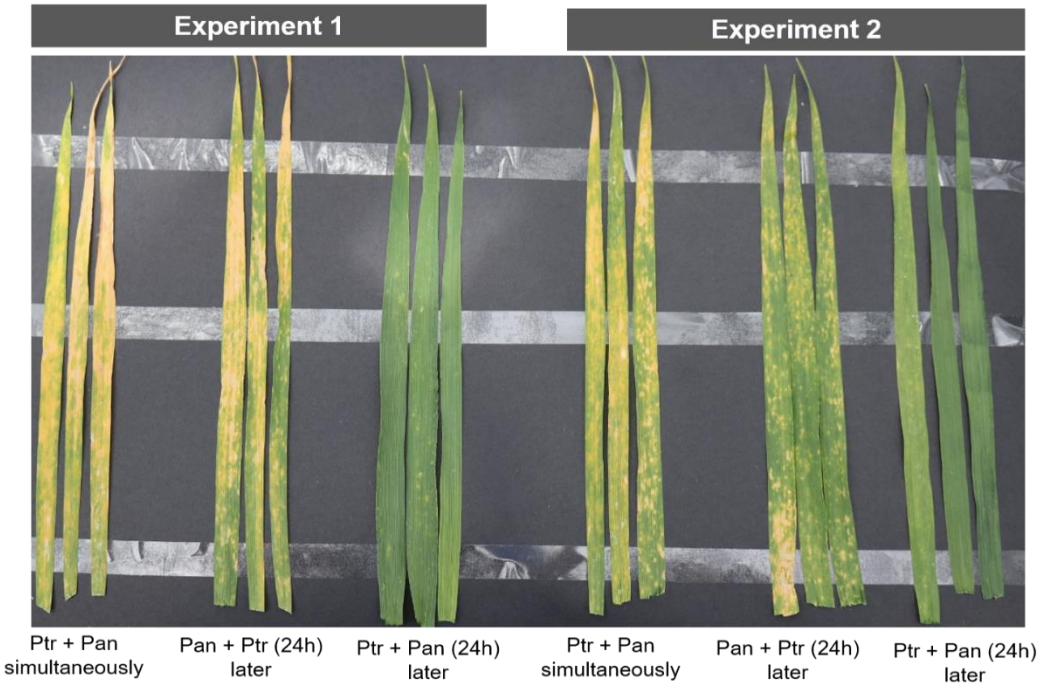

Figure S2. Results of reduced set co-inoculation experiment of the wheat cultivar Emu Rock. Leaves are shown in three repeats. All plants, including mock-inoculated control plants, were contaminated with a biotrophic pathogen. No molecular analysis was conducted on these leaves, as a result.

Reference

Shackley, B., Ellis, S., Zaicou, C., Dhammu, H., and Shankar, M. (2013). Wheat variety guide for Western Australia. (W. A. Department of Agriculture and Food, ed.), Vol. 1, pp. 1-39. Bulletin Perth.

Appendix 3 –Author contribution statement (Chapter 1)

To Whom It May Concern

I, Araz Abdullah, contributed to the conception of the idea, reviewed the relevant literature and drafted the manuscript to the paper entitled "Host–multi-pathogen warfare: pathogen interactions in co-infected plants" published in 2017, Frontiers in Plant Science, Vol 8, issue1806. Reference Abdullah et al. (2017).

[redacted]

Araz Abdullah

I, as a Co-Author, endorse that this level of contribution by the candidate indicated above is appropriate.

1- Caroline Moffat [redacted] 24/05/19

2- Francisco J. Lope[redacted] 16/5/19

3- Mark Gibberd [redacted] 8/2/18

4- John Hamblin [redacted]

5- Ayalsew Zerihun [redacted] 08/2/18

Appendix 4 – Author contribution statement (Chapter 2)

To Whom It May Concern

I, Araz Abdullah, conceived the idea of the project, defined/selected the primers used throughout the study, conducted the experiments, analysed the data, and drafted the manuscript to the paper entitled "Real-time PCR for diagnosing and quantifying co-infection by two globally distributed fungal pathogens of wheat" published in Frontiers in Plant science, Vol 9, issue 1086. Reference Abdullah et al, 2018.

[redacted]

Araz Abdullah

I, as a Co-Author, endorse that this level of contribution by the candidate indicated above is appropriate.

1- Chala Turo

2- Caroline Moffat

3- Francisco J. Lopez-Ruiz

4- Mark Gibberd

5- John Hamblin

6- Ayalsew Zerihun

[redacted]

Appendix 5 – Author contribution statement (Chapter 3)

I, Araz Abdullah, conceived the idea of the research, collected and analysed the samples, performed the data analysis and drafted the manuscript to the paper entitled "Co-infection of wheat by *Pyrenophora tritici-repentis* and *Parastagonospora nodorum* in the wheatbelt of Western Australia" published in 2017, Crop and Pasture Science, Vol 71, issue 2. Reference Abdullah et al. (2020).

Araz Abdullah

I, as a Co-Author, endorse that this level of contribution by the candidate indicated above is appropriate.

1- Mark Gibberd 

I, Araz Abdullah, conceived the idea of the research, collected and analysed the samples, performed the data analysis and drafted the manuscript to the paper entitled "Co-infection of wheat by *Pyrenophora tritici-repentis* and *Parastagonospora nodorum* in the wheatbelt of Western Australia" published in 2017, Crop and Pasture Science, Vol 71, issue 2. Reference Abdullah et al. (2020).

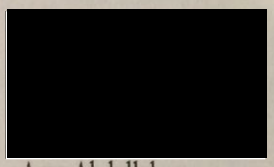

Araz Abdullah

I, as a Co-Author, endorse that this level of contribution by the candidate indicated above is appropriate.

1- Mark Gibberd

2- John Hamblin

Appendix 5 – Copy Right Statements (Frontiers in Plant Science)

Appendix 6 – Copy Right Statements (Crop and Pasture Science)

Copyright statement for Crop and Pasture Science allows non-commercial reuse of published materials.

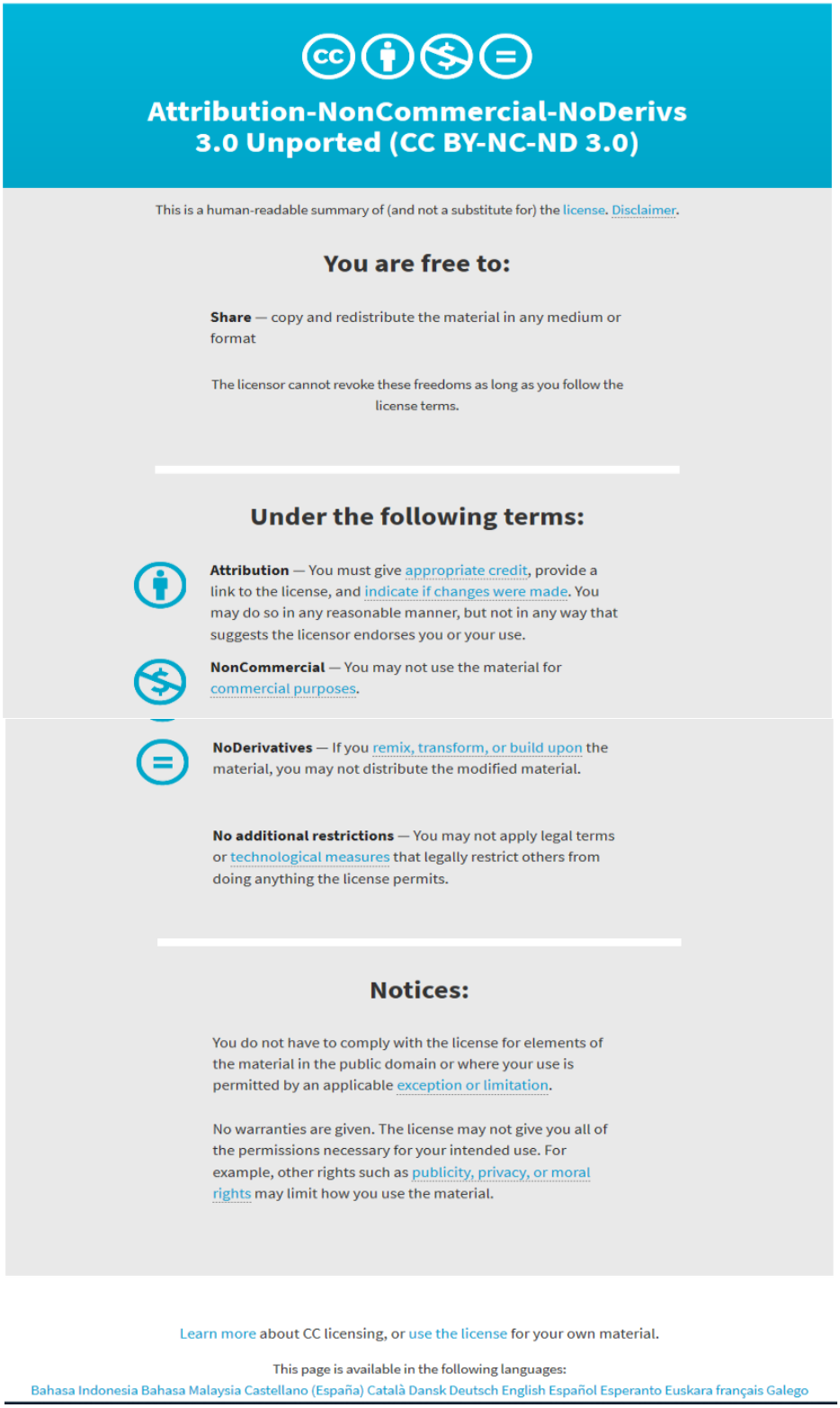

Attribution-NonCommercial-NoDerivs 3.0 Unported (CC BY-NC-ND 3.0)

This is a human-readable summary of (and not a substitute for) the license. Disclaimer.

You are free to:

Share — copy and redistribute the material in any medium or format

The licensor cannot revoke these freedoms as long as you follow the license terms.

Under the following terms:

Attribution — You must give appropriate credit, provide a link to the license, and indicate if changes were made. You may do so in any reasonable manner, but not in any way that suggests the licensor endorses you or your use.

NonCommercial — You may not use the material for commercial purposes.

NoDerivatives — If you remix, transform, or build upon the material, you may not distribute the modified material.

No additional restrictions — You may not apply legal terms or technological measures that legally restrict others from doing anything the license permits.

Notices:

You do not have to comply with the license for elements of the material in the public domain or where your use is permitted by an applicable exception or limitation.

No warranties are given. The license may not give you all of the permissions necessary for your intended use. For example, other rights such as publicity, privacy, or moral rights may limit how you use the material.

Learn more about CC licensing, or use the license for your own material.

This page is available in the following languages:
Bahasa Indonesia Bahasa Malaysia Castellano (España) Català Dansk Deutsch English Español Esperanto Euskara français Galego